MICROSTRUCTURAL UNDERSTANDING OF HYDROCOLLOID AND MIXED HYDROCOLLOID SYSTEMS FOR BIOMEDICAL APPLICATIONS

Abigail Belinda Norton

A thesis submitted to

The University of Birmingham

for the degree of

DOCTOR OF PHILOSOPHY

Department of Chemical Engineering

College of Physical and Engineering Sciences

The University of Birmingham

2016

Abstract

Hydrocolloid materials have been used for some time in the fields of regenerative medicine and drug delivery. Despite a significant body of work, to date the majority of research in the area has focused on relatively simple compositions and microstructures. In comparison, the food industry has long used refined and often subtle methods to structure and thereby tailor the release and handling properties of a vast range of similar materials. In this thesis, a range of processing methodologies has been used to generate novel materials intended for use in the regenerative medicine and drug delivery using gellan and kappa carrageenan. The thesis demonstrates how even small changes in process conditions can result in significant changes in the way a material handles and may deliver therapeutic molecules. It has been demonstrated that gellan, when combined with poly (vinyl alcohol) (PVA) produces a material of enhanced robustness. However, the enhanced robustness was subject to gellan forming the dominant phase.

By imparting a shear force to gelling materials, it was also possible to produce shear thinning fluid materials using similar biopolymers (gellan with kappa carrageenan). These polymers typically phase separate, however, when the concentration of polymers were controlled, simultaneous gelation could be achieved suggesting that a single phase system was formed.

Finally it was demonstrated that it was possible to generate a novel cell

delivery device by the hydration of kappa carrageenan in warm biomedical buffers, with no high temperatures required.

Overall this thesis demonstrates the range and complexity of structures that can be produced using the relatively small number of polymers that can be used in the clinic.

Acknowledgements

I would firstly like to thank my supervisors, Professor Liam Grover and Dr. Fotis Spyropoulos for their invaluable guidance, support and mentorship during my research time and the writing of my thesis. I will be always grateful for your constant motivation and belief.

Special thanks goes to Lynn Draper, who has been so reassuring and helpful throughout my PhD. I would also like to thank the EPSRC for funding this work.

My time in Birmingham has been so gratifying, and I have my friends and colleagues in Chemical Engineering to thank for that. A big thank you also goes to my closest friends outside of the university; you have all been so supportive, and always found ways of taking my mind off the stresses of PhD life.

A massive thank you goes to my family for all their love, support and motivation. My sincerest thanks to my parents, who have been so amazing, especially while I have been writing my thesis. You have supported me in everything I do and I hope I will continue to make you proud.

Finally but most importantly, to Gary, you have been so patient and loving throughout my PhD. I could not have done this without you! Thank you.

Table of Content

List of Figures

List of Tables

Chapter 1.

INTRODUCTION

1.1 Context of the study

Mean life expectancy is consistently increasing (Giacomoni, 2005, Walport, 2014); with governing bodies and agencies describing countries as has having "aging populations" (Cracknell, 2010). This is accompanied by consumers being increasingly more interested in all-natural personal care and cosmetic products (Carvalho et al., 2015). As a result there has been a dramatic increase in the research carried out in the field of natural therapeutics (Lubbe and Verpoorte, 2011).

The human skin is a complex structure (Edwards and Marks, 1995). Its purpose is to protect and regulate the body, to control temperature, prevent water loss, as well as to protect against pathogens or diseases (Bouwstra et al., 2003, Groeber et al., 2011). Whilst the skin is usually able to completely repair with little or no scarring (Percival, 2002), damage over the size of 4 cm in diameter, genetic abnormalities or existing diseases can all result in the human skin being unable to repair itself (MacNeil, 2007, Groeber et al., 2011, Shevchenko et al., 2010). This results in medical treatment being required (MacNeil, 2007). Cartilage also has limited capabilities to repair itself, and therefore trauma to the cartilage would often need medical intervention (Malda et al., 2003).

The gold standard for treating such cases has previously been to harvest tissue or cartilage from elsewhere, and then re-implant them into the patient (known as an autograft (O'Brien, 2011)). The use of autogenous cell or tissue transplantation for cartilage repair has been described as one of the most

promising techniques in biomedical engineering (Hutmacher, 2000, Patrick et al., 1998). However, it also carries high levels of trauma, increased potential of contracting an infection, donor site morbidity and scarring. Alternatively, tissue or cartilage can be harvested from another person and placed in the patient. This is known as allografting (O'Brien, 2011), and carries higher levels of risk of infection as well as rejection from the patient's body. Furthermore, it is said that suitable donors are also limited (Lee and Mooney, 2001).

Wound dressings, such as those applied after any surgical treatment, are primarily designed to protect the affected area of the body, and replace the functions of the skin (Pereira et al., 2013), such as protecting against microorganisms and infections. These dressings can then also have a dose of drugs that can assist in the healing process (Dias et al., 2011, Elsner and Zilberman, 2010, Kim et al., 2008), thus creating a multifunctional dressing. Furthermore, the controlled release of a therapeutic drug from the dressing could reduce the frequency of replacing the dressings (Lisa, 1997). Contrary to previous beliefs (Queen et al., 2004), it has been found that creating a warm and moist environment around the wound can actually increase healing times (Field and Kerstein, 1994, Winter, 1962).

The risks associated with grafting have resulted in an increased interest in the development of new technologies that can advance the treatment of patients, lowering any surgical trauma and speeding up recovery times. Thus, tissue engineering (which involves the fabrication of tissue) has developed (Drury and

Mooney, 2003). Additionally, research into improving the wound dressings for more efficient wound healing treatments has also received interest.

The selection of materials for tissue engineered structures has to be carefully considered (O'Brien, 2011), as the materials must:

- Be biocompatible – meaning cells must adhere to the material, and function normally;
- Degrade allowing for the cells to deposit their own extracellular matrix (ECM) structure, and;
- Have mechanical properties that are consistent with the site which it will be implanted and also have a structural integrity to withstand handling during the implantation process.

Hydrocolloids have been readily used within tissue engineering (Zhu and Marchant, 2011, Radhakrishnan et al., 2014, Hunt and Grover, 2010, Bidarra et al., 2014), as they exhibit many of the characteristics required for a tissue-scaffold material. Hydrocolloids, however, have been previously described as having insufficient mechanical properties, and complexity. This has resulted in research into multicomponent systems, which this thesis will investigate in both the literature review and the experimental chapters.

Hydrocolloid wound dressings are already commercially available (Pereira et al., 2013, Boateng et al., 2008), and has been shown to assist with creating a moist environment around the wound, and also the removal of damaged tissue from

the wound site, hence having a beneficial impact on recovery (Paddle-Ledinek et al., 2006).

1.2 Objectives

Current gold standards within both the pharmaceutical and personal care industries can still be improved upon, in order to give patients the best products, and the best chance of maintaining or improved health.

Considering this, the aim of this thesis was to investigate two hydrocolloids, low acyl gellan and kappa carrageenan, and how they could be utilised to deliver bioactive molecules. This thesis investigated how these materials could be structured to provide a range of structures with differing functions. These include:

- Investigate whether quiescent low acyl gellan/ poly (vinyl alcohol) gels may be used as a structure for auricular replacement.
- Investigate the effect of mixing low acyl gellan and kappa carrageenan during the formation of fluid gels, and how they may be used for wound care.
- Develop structured kappa carrageenan that is compatible for the delivery of hydrophilic drugs or mammalian cells. This involved structuring the hydrocolloid system with minimal heat and shear. These structures were then investigated for the stabilisation of emulsions.

1.3 Thesis Structure

The following chapter reviews the relevant literature of hydrocolloid structuring, including the use of hydrocolloids within emulsion systems.

The first results chapter (Chapter 3) is split into two main parts: Section 3.2 discusses quiescent gelation of low acyl gellan modified with the addition of the synthetic polymer, Poly (vinyl alcohol). Section 3.3 then investigates the development of a staining method to attempt to visualise the resultant microstructure using DTAF.

Chapter 4 investigates the formation and characterisation of low acyl gellan/ kappa carrageenan fluid gels. Processing parameters are investigated for both single polymer fluid gels and mixed fluid gels.

The final results chapter (Chapter 5) discusses the hydration of kappa carrageenan in warm (30 ^{o}C) buffers. These gums are then added to complex emulsions. Both the rheology and stability of the emulsions are analysed.

Chapter 6 concludes the thesis and discusses the possible future work. Chapter 7 then lists the references used for this body of work.

1.4 Publications and Presentations

Results obtained throughout this study have been published as follows:

Publications:

- Norton, A. B., Hancocks, R. D., Grover, L. M., (2014) Poly (vinyl alcohol) modification of low acyl Gellan hydrogels for applications in tissue regeneration, *Food Hydrocolloids*, 42, 373-377.
- Norton, A. B., Hancocks, R. D., Spyropoulos, F., Grover, L. M., (2015) Development of 5-(4,6-dichlorotriazinyl) aminofluorescein (DTAF) staining for the characterisation of low acyl gellan microstructures. *Food Hydrocolloids*, 53, 93-97.
- Norton, A. B., Spyropoulos, F., Grover, L. M., The formation and characterisation of low acyl gellan/ kappa carrageenan mixed fluid gels, Submitted.

Patent:

- Norton, A. B., Spyropoulos, F., Grover, L. M., GB1608595.3.

Oral Presentations (speaker underlined):

- Norton, A. B., Hancocks, R. D., Spyropoulos, F., Grover, L. M., Characterisation of gellan fluid gel microstructures, 12th International Hydrocolloids Conference, Taiwan, 2014.
- Norton, A. B., Hamilton, I. E., Spyropoulos, F., Grover, L. M., Microstructural design of multicomponent hydrocolloid fluid gels for the delivery of model actives, 18th Gums & Stabilisers for the Food Industry Conference, Wrexham, 2015.
- Norton, A. B., Spyropoulos, F., Grover, L. M., Warm hydration of kappa carrageenan and its use to structure and stabilise single and double emulsions, 13th International Conference, Canada, 2016.

Poster Presentations:

- Norton, A. B., Grover, L. M., Mixed Gellan/Poly (vinyl alcohol) Hydrogels for Auricular Replacement, 13th UK Society of Biomaterials (UKSB) Annual Conference, Birmingham 2013.
- Norton, A. B., Grover, L. M., Effect of Poly (vinyl alcohol) on the Structural Properties of Low Acyl Gellan Hydrogels, 1st UK Hydrocolloids Symposium, Huddersfield 2013.

Chapter 2.

LITERATURE REVIEW

2.1 Introduction

Engineering new, sustainable structures to improve everyday products has been a long-standing research field. Improving the quality of life is a big driving force, with research focusing on reducing fat in foods (e.g. “light” versions of mayonnaise and margarine (Norton et al., 2006, Norton et al., 2007)), delivery of pharmaceuticals (Kashyap et al., 2005, Lin and Metters, 2006), and improving personal care products (Ammala, 2013), such as washing detergents and shampoos.

The design of new structures involves consideration of all aspects of the product, including the material properties, their effect on health and sensory qualities, and the possible responses from consumers (a schematic representing these aspects and how they are linked is shown in Figure 2.1 (Norton and Foster, 2002)).

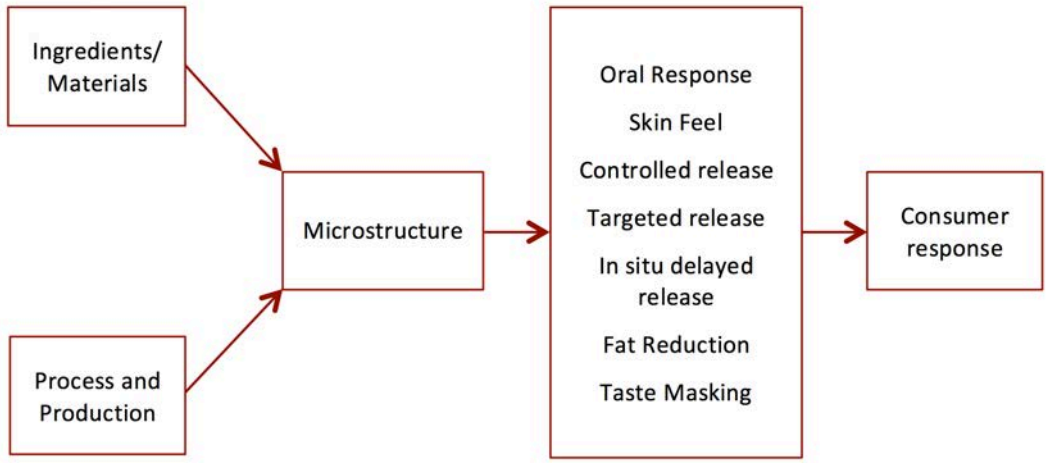

Figure 2.1 – Schematic representation of the microstructural approach, linking the materials and processing parameters with the resultant sensory response. Adapted from Norton and Foster (2002).

Hydrocolloids and emulsions are found in a large proportion of commercial products, in both food and personal care (Dickinson et al., 2009). However, there are areas in both fields which could be further developed (McClements et al., 2009). In addition, there are a number of aspects of both food and personal care which have similar material properties.

For this literature review, hydrocolloids and their capacity to be used in a range of applications will be discussed. This includes hydrocolloids structured to form fluid gel particles, multicomponent gel systems, and the use of hydrocolloids within emulsions.

2.2 Hydrocolloids

Hydrocolloids, which include polysaccharides, proteins and some synthetic polymers such as poly (vinyl alcohol) (PVA), are versatile materials, and thus have received a great deal of attention in food (Tang et al., 1994, Nishinari et al., 1996), pharmaceutical (Osmałek et al., 2014, Guo et al., 1998) and tissue regeneration applications (Birdi et al., 2012, Hunt et al., 2010, Smith et al., 2007).

Polysaccharides (derived from plants, seaweeds, microbial and animal sources) are complex carbohydrates that have repeating monosaccharide units (Rees, 1977). The complex structure, high molecular weight and hygroscopic character of polysaccharides allows for the structuring of free water (Ablett et al., 1978), thus stopping flow so that solid-like structures are produced (Nishinari et al., 2000a, Watase and Nishinari, 1988). Synthetic polymers are often used in tissue regeneration, such as PVA, which are available in a range of molecular weights, all of which have a hygroscopic character and are highly soluble in aqueous media.

Hydrocolloids can be formed from polymers exhibiting a wide range of structures, from random coils to helices, to extended egg box structures, depending on the molecular structure of the polymer backbone (Rees, 1977). This variety of structures and interactions results in a diverse range of rheological and physical properties. These range from hydrocolloids which increase in viscosity, such as guar (Robinson et al., 1982), to those which have suspending properties such as xanthan (Sworn et al., 2010), and to those which form gels,

such as kappa and iota carrageenan, gellan, and agarose (Morris et al., 1980). Of particular interest are the gel properties and how they can be manipulated for use in a wide range of products related to foods, personal care, and pharmaceuticals. The range of gelling profiles (which will be further discussed in Section 2.3), and their resulting mechanical properties, are shown in Figure 2.2 (Phillips and Williams, 2009). Figure 2.2 identifies how the conformation of the polymer backbone, and the presence of side groups, can greatly affect the resultant properties of the gel. For example, xanthan-locust bean gum form a synergistic interaction between the different polymer chains resulting in short ordered sequences (Lundin and Hermansson, 1995), whereas high acyl gellan (containing acyl side groups) form soft and flexible gels, while polymers which form longer and more rigid ordered conformations such as kappa carrageenan (a double helix), agar (a double helix) and low acyl gellan (a double helix) form firmer gels. Within each polymer chain for these hydrocolloids, there are sequences which can adopt the ordered structure and residues or sequences of residues that have a conformation which stops them from interacting (Anderson et al., 1968) (this will be discussed further for the hydrocolloids studied in this thesis in Sections 2.2.1 and 2.2.2). As the length of the sequence which can form an ordered structure increases, the resultant gels become firmer and more brittle (Hermansson et al., 1991, Dunstan et al., 2000). However, if the number of disruptions in the chain decreases too much, the hydrocolloid will become insoluble and precipitate out on cooling, as is the case for starch and cellulose (Parker and Ring, 2001, Jane, 1993). This shows the importance of the molecular

structure of the hydrocolloid backbone, the presence of side groups and the chain conformation, and how the overall rheological and material properties can be affected and manipulated by the careful choice of a hydrocolloid.

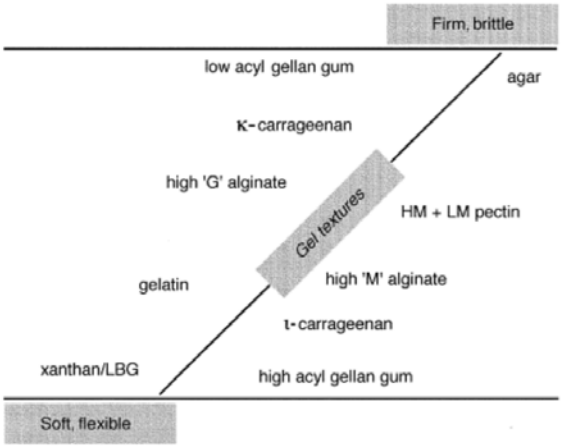

Figure 2.2 – Comparison of the textures, from soft and flexible to firm and brittle, exhibited by a range of hydrocolloids. Image adapted from Phillips and Williams (2009).

The term "dilute hydrocolloid systems" describes when the concentration of polymer is lower than the minimum concentration for gelation, within a solvent such as water (Nickerson et al., 2004). The polymer chains are then able to move independently of each other and the viscosity of the solution increases based on the volume occupied by the independent polymer chains. This results in a gradual increase in viscosity, as shown for the lower concentrations in Figure 2.3 (Phillips and Williams, 2009). The concentration range for this regime varies for different hydrocolloids. Once the polymer concentration is increased, the

polymer chains are forced to occupy less volume and thus overlap. At this point, the viscosity increases more steeply because the polymer chains are unable to move freely due to molecular crowding. This results in chain entanglement which causes a drag when the polymer chains are moved against each other (the more rapid increase shown in Figure 2.3) (Morris et al., 1981). The point of the distinct viscosity change is known as the critical overlap concentration, or C*.

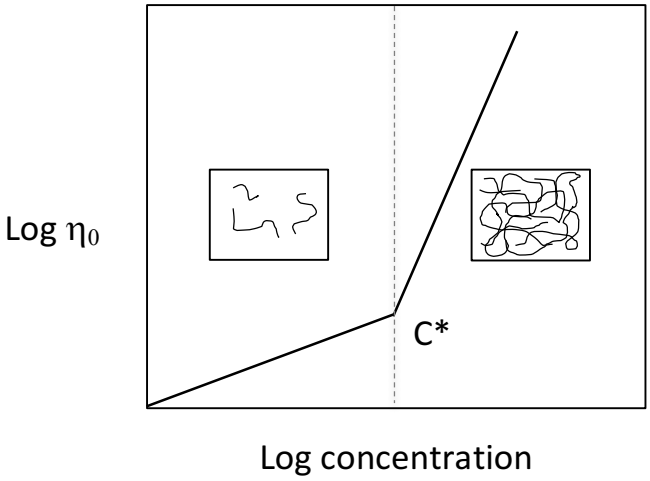

Figure 2.3 – Schematic representation of the viscosity dependence of polysaccharide systems, showing the transition from dilute regions, past the critical concentration (C*) into a concentrated region. Image adapted from Phillips and Williams (2009).

2.2.1 Gellan Gum

Gellan gum is a naturally occurring anionic hydrocolloid containing tetrasaccharide repeating units (1,3-β-D-glucose, 1,4-β-D-glucuronic acid, 1,4-β-D-glucose, 1,4-α-L-rhamnose) (O'Neill et al., 1983, Jansson et al., 1983, Gibson and Sanderson, 1997) (Figure 2.4), which is synthesized from the bacteria

Sphingomonas elodea (formally known as *Pseudomonas elodea*) (Morris et al., 2012, Kang et al., 1982).

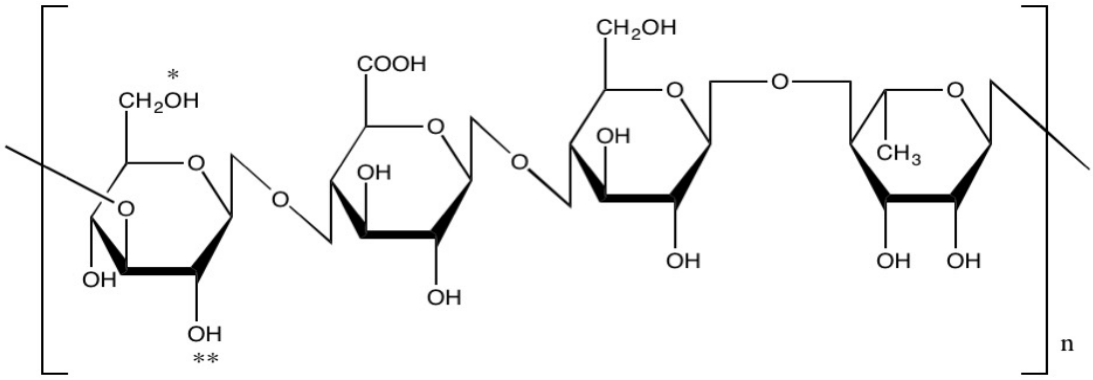

Figure 2.4 – Tetrasaccharide repeating unit of deacylated gellan. The presence of an acetyl (*) and a glyceryl (**) groups are found in native gellan (also known as high acyl gellan). Figure adapted from Mao et al. (2000).

Through alkaline hydrolysis, acyl groups present on the native gellan backbone (otherwise known as high acyl gellan) are removed, to form deacylated gellan (also known as low acyl gellan) (Sworn et al., 2009, Mao et al., 2000, Kang and Veeder, 1982, Kang et al., 1982). The removal of the acyl groups results in the chain being a polyanion due to the carboxyl groups. This results in a salt sensitivity, particularly to divalent ions, and increases the interaction between the polymer chains through an ion bridge, allowing greater aggregation. This results in firmer and more brittle gels, and if only monovalent cations are present, decreases the gelation temperature (from 70 ^{o}C - 80 ^{o}C to 25 ^{o}C - 60 ^{o}C) (Morris et al., 2012). Alternatively, the bridging of the gellan chains can be

achieved using cell culture media for tissue engineering applications (Smith et al., 2007), or bodily fluids such as tears, for medical applications (Rupenthal et al., 2011). Furthermore, low acyl gellan gels are thermoreversible (i.e. they set on cooling and can be remelted by heating) (Morris et al., 2012). The process of deacylation causes a decreased viscosity, probably because the polymer chains are a lower molecular weight due to a small amount of chain cleavage taking place.

High acyl gellan forms weak gels, because the acetyl and glyceryl groups hinder close association of the polymer chains (Mao et al., 2000), while low acyl gellan forms strong gels at very low polymer concentrations (i.e. 0.05% (wt%)) (García et al., 2011, Sworn et al., 2009), which is of economic benefit for using low acyl gellan. Gellan has also been shown to have similar structuring and texture to gelatin, allowing for potential vegetarian alternatives for products (Morrison et al., 1999), such as desserts. Furthermore, gellan has been previously suggested for use in tissue regeneration and cartilage engineering (Oliveira et al., 2010). Gellan has been found to be noncytotoxic, and does not require harsh processing to form gels which are self supporting (Sworn et al., 2009).

As the molecular structure of the high and low acyl gellan are very similar, it may be expected that the two chains could interact or bind together in a mixed network. However, there is no evidence that mixing the two forms of gellan results in helices formed containing both high acyl and low acyl gellan (Matsukawa and Watanabe, 2007), showing that these two forms of the polymer behave as separate polymers (Mao et al., 2000). The two forms of gellan also

exhibit different conformation temperatures (Kasapis et al., 1999) strengthening the indication that they act as individual polymer types.

2.2.2 Kappa Carrageenan

Originating from seaweed (red algae), carrageenan is a high molecular weight linear polysaccharide, consisting of repeating galactose and anhydrogalactose units (Figure 5) (Anderson et al., 1969). Carrageenan is often used within systems for stabilisation, thickening and as a gelling agent.

It has three main molecular forms: iota (ι), kappa (κ) and lambda (λ) (Morris and Chilvers, 1983). One of the major differences between these hydrocolloids is the extent of sulphation of the disaccharide-repeating unit: kappa carrageenan has a single sulphate per disaccharide, iota has two sulphates per disaccharide and lambda has three sulphates per disaccharide (Rochas and Rinaudo, 1984, Nickerson et al., 2004).

Similar gelation mechanisms have been established for kappa carrageenan as for gellan, with molecular ordering into a helix structure followed by aggregation and gelation (Morris et al., 1980). Again, the extent of ordering and gel strength are dependent upon the ionic environment in the aqueous medium (Mangione et al., 2005). This difference in sulphation levels results in kappa carrageenan binding monovalent ions, particularly potassium ions (Austen et al., 1988). As the potassium ions are bound, the random coil conformation of the carrageenan into a double helix; these helices then aggregate to form the gel (Figure 2.6). This

behaviour was first reported by Robinson et al. (1980) and is known as the domain model. The presence of the aggregates in kappa carrageenan gives the structure greater stability, and as a result, a hysteresis exists between the gel setting temperature and the gel melting temperatures which can be separated by approximately 10 ^{o}C (Smidsrød et al., 1980). The strongest and highest melting temperature gels with the greatest extent of aggregation therefore occur for kappa carrageenan in the presence of potassium. However, as the binding of potassium results in extensive aggregation, the gels are cloudy, brittle (i.e. fail at low strains) and show syneresis (Dunstan et al., 2000). Kappa carrageenan has been shown to bind other monovalent ions, resulting in less aggregation, lower melting and more elastic gels and less syneresis. A range of gel properties can thus be obtained with different melting and gelling profiles, potentially valuable in the biomedical area when temperature sensitive molecules need to be delivered.

Iota carrageenan has a greater sensitivity to divalent ions, particularly calcium ions (Morris et al., 1980). At low levels of calcium ions, iota carrageenan forms strong clear elastic gels. It has been argued that iota carrageenan produces clearer, more elastic gels than kappa carrageenan, due to the charge densities and the extent of aggregation being lower for iota than kappa carrageenan (Rees, 1977). The way that the conformation of the carrageenan backbone affects the resultant gel strength, texture and temperature of both melting and setting, and syneresis has been described by Imeson et al. (2000). Lambda carrageenan, which has a highly sulphation level and a lack of anydro bridging,

does not gel even in the presence of high concentrations of ions (Slootmaekers et al., 1991). This shows the importance of the molecular structuring within carrageenan.

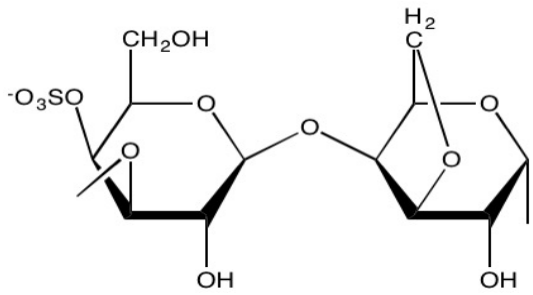

Figure 2.5 – Chemical structure of the kappa carrageenan showing the anydro bridge with a single sulphate group.

Not only do cations have an effect on the ordering and gelation of kappa and iota carrageenan, but so do the anions. This has been shown to follow the lyotropic (Hofmeister) series (Norton et al., 1984), whereby large soft ions such as iodide disrupt the aggregation of the carrageenan, particularly kappa carrageenan. This results in lower gelling and melting temperatures, as well as softer and more elastic gels. Ions from the other end of the series (e.g. hard small ions such as fluoride) cause greater aggregation and stronger, more brittle, gels. Thus if carrageenan is to be used for structuring in complex growth media (such as Dulbecco's Modified Eagle's Medium (DMEM)), the effect of the ions, both cation and anion, need to be considered. This is an area which has received little research, and forms the basis of Chapter 5.

2.2.3 Poly (vinyl alcohol) (PVA)

The use of the synthetic polymer poly (vinyl alcohol) (PVA) has been increasing in recent times, for applications such as biomaterials and drug delivery systems (Bercea et al., 2013, Drury and Mooney, 2003). PVA is formed by the hydrolysis of poly (vinyl acetate) (PVAc), which has been shown to not cause cell death, is flexible in nature, and has the ability to completely degrade (Barbani et al., 2005). Like the natural polymers discussed earlier, PVA requires high temperatures (above 70 ^{o}C) to dissolve, which can potentially decrease the applications that PVA can benefit.

For many pharmaceutical or medical applications PVA is required to be structured. PVA polymer chains can be crosslinked through chemical methods (Drury and Mooney, 2003). Adding glutaraldehyde, acetaldehyde, formaldehyde, or other monoaldehydes, in the presence of an acid (such as sulphuric acid) or methanol, causes acetal bridges to form between the hydroxyl groups of the PVA chains (Hassan and Peppas, 2000a). This chemical method, however, produces residues which are toxic (Baker et al., 2012). This can result in degradation of any bioactives included in the system, such as therapeutic drugs. Therefore, chemically crosslinked PVA gels are often unacceptable for medical applications.

PVA also forms a structured system by hydrogen bonding (ionic bridging) between polymer chains through the process of freezing the PVA, and then defrosting it (Peppas, 1975). This is known as freeze-thaw cycling, resulting in a

structured gel known as a cryogel (Lozinsky et al., 1996). This method overcomes the toxicity drawbacks of chemically crosslinking PVA.

Freeze-thaw cycles result in crystallites forming between the polymer chains. These crystallites force the polymer chains to align, allowing them to hydrogen bond (Gupta et al., 2012, Hassan and Peppas, 2000b). As the concentration of PVA increases, the degree of crystallinity increases (Hassan and Peppas, 2000a), and therefore more structuring occurs within the PVA. It has also been previously shown that as the number of freeze-thaw cycles increases, the gel strength also increases (Bercea et al., 2013). However, while the rate of thawing rate influences gel properties, the rate of freezing rate does not have an effect (Bercea et al., 2013).

If PVA is left untreated from either freeze-thaw cycles, or chemical crosslinkers, then a gel network is not formed. Instead, the PVA is a viscous liquid and has the potential to thicken other systems.

2.3 Gelation

2.3.1 Quiescent gels

Under the right conditions of temperature and salt, the gelation of polysaccharides can occur, whereby the formation of the ordered structure and junction zones between polymer chains are formed (shown in Figure 2.6) (Miyoshi et al., 1996). In natural polysaccharides, these junction zones are often formed through physical interactions (e.g. hydrogen bonding, cation crosslinking

etc.) (Rees, 1977). They are referred to as “physical gels” because the junctions and the gels are transient and can be reversed by changing the conditions (e.g. temperature or salt environment) (Phillips and Williams, 2009). This term is used to distinguish them from hydrocolloids (often proteins and synthetic polymers) which form covalent bonds between chains which are then not reversible (Nishinari et al., 2000b). These gels are termed permanent.

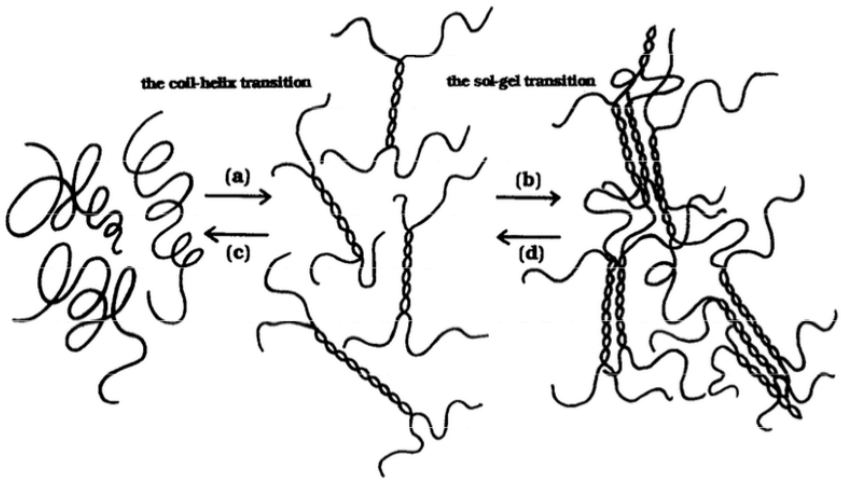

Figure 2.6 – Schematic representation of the coil-helix transition and the sol-gel transition of hydrocolloids (Miyoshi et al., 1996). This highlights how thermo reversible gels behave during the cooling process (a & b) and then transition back through the phases to a random network (d & c) during heating. Temperatures of the transitions are dependent on the hydrocolloid.

Major attractions to using hydrocolloids that form physical gels are that gelation and gel melting may be manipulated to suit a given application. Hydrocolloid systems, formed under quiescent conditions, are beneficial as they are self

supporting (shown in Figure 2.7), allowing a range of tissue engineering applications to use hydrocolloids as the scaffold systems (Hunt et al., 2009, Hunt and Grover, 2010).

Hydrocolloids are also highly hydrated in nature, enabling the diffusion of a range of molecules through their matrix. This allows structures to be designed for delivery of bioactives. Furthermore, with the wider range of hydrocolloids available, with a variety of gelation pathways and mechanical properties as discussed above, there is potential for producing structures with the desired rheological and mechanical properties.

For physical gels there are two further subdivisions that need to be considered: those hydrocolloids which can form thermo reversible gels such as gellan, iota and kappa carrageenan and xanthan; and hydrocolloids that form thermo irreversible gels such as alginate. Thermo reversible gel systems have been widely used for drug delivery as a method of controlling and modulating the drug release due to their swelling behaviour (Roy et al., 2010, Lee and Mooney, 2012). Whereas, thermo irreversible gels are widely used in food products which are subjected to a high temperature process (e.g. pasteurisation or sterilization) after formation. In the study carried out here, the target was to obtain structures that can be used in skin applications and deliver a range of bioactives, hence the major interest is on thermo reversible systems (Boateng et al., 2008).

Although the gelation and gel properties can be tailored by the selection of the hydrocolloid and ionic environment, there are still occasions when the properties

of the final application require further modification/manipulation. For example, in fat replacement for food products (Norton et al., 2006, Lundin and Golding, 2009), where a single gelling systems causes textural defects in use, or in mouth sensory defects, or in skin application where spreadability and easy of application are not satisfied by application of a three dimensional gel or highly viscous liquids. For this reason, two approaches have more recently been investigated: 1) fluid gels (Gabriele et al., 2009, Mahdi et al., 2014a, Norton et al., 1999) and 2) mixed hydrocolloid systems (Morris, 1986, Wolf et al., 2000). These will now be further discussed in the next two sections.

2.3.2 Fluid gels

Fluid are produced by applying a shear during gelation of hydrocolloids such as kappa-carrageenan (Gabriele et al., 2009, Garrec et al., 2013), agarose (Norton et al., 1999) or gellan (Sworn et al., 1995, Mahdi et al., 2014b). By applying shear as the hydrocolloids undergo conformational ordering and gelation, the gelation is forced to occur over a limited length scale so that discrete particles are produced (Brown et al., 1996). These studies have shown that shear needs to be applied throughout the majority of the ordering and gelation process. This results in a system of gel particles suspended in a non-gelled continuous medium, which are a pourable and spreadable (as shown in Figure 2.7). This allowed for a wider range of applications to have the inclusion of hydrocolloids, such as dressings (Sworn et al., 1995), shampoos and skin creams.

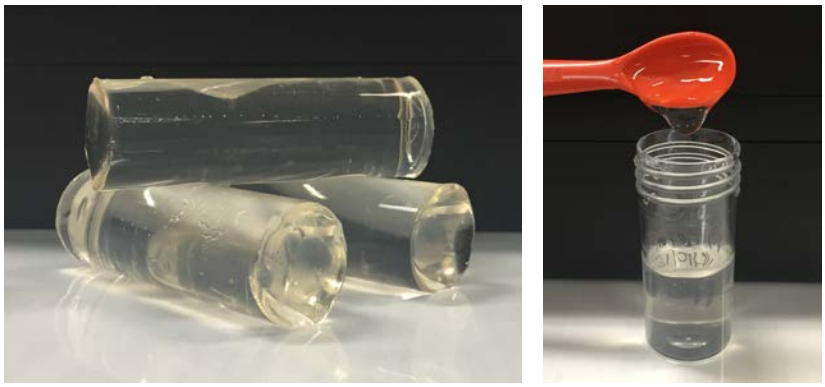

Figure 2.7 – Low acyl gellan formed under quiescent conditions (a) and sheared cooling to form a fluid gel (b) of low acyl gellan.

However, if the shear is stopped before complete ordering, then some of the chains remain in the disorder state and will then order and aggregate quiescently (Garrec and Norton, 2012). This leads to bridging between particles and gives the fluid gel a yield stress when subsequent shear is applied.

For thermally set gels, the bulk properties of the fluid gel can be directly influenced by the polymer concentration, cations added, level of shear applied, and the temperature profiling throughout the gelation process (Norton et al., 1999).

Researchers have shown that the properties of the hydrocolloid within the gel particle are the same as those measured for the bulk quiescent gel. A paper from Garrec and Norton (2012) did identify a small decrease in the enthalpy of melting of kappa carrageenan fluid gels when compared with quiescent gels. They argued that this was a consequence of less helix formation in the chains that were close to the surface of the particle. The difference measured was small and

could well be due to some disruption of molecular ordering at the surface. Other papers have not reported this effect and have shown that the melting enthalpies are the same for the fluid gel as for the quiescent gel. Thus it would seem that the difference observed by Garrec and Norton (2012) was down to the particular process used (e.g. cooling rate). Data reported in this thesis has shown that for the particles produced here, there is no difference in the melting enthalpies (data shown in Chapter 4).

In addition to the formulation controlling the final rheology of the fluid gels, it has also been shown that processing parameters have a major effect. By increasing the shear rate applied during gelation, the resultant particles are reduced in size. This includes the gel particle conformation, which can be greatly changed and tailored to the end application requirements. This flexibility allows the systems to closely mimic emulsion properties (Nishinari et al., 2000b, Wolf et al., 2000). This has been shown to be ideal for reduced fat products. These suspensions can be “disguised” in a product to avoid a possible negative sensory response, whilst still achieving the desired microstructure. Furthermore, these can be used as a protective layer to environment sensitive actives, such as flaxseed (Carneiro et al., 2013).

As will be discussed in the next section, mixed hydrocolloids are often used to obtain the desired rheological and thermal properties of gels. There is the opportunity to further control and manipulate the properties of fluid gels by producing fluid gels from mixed hydrocolloid systems. This was initially reported by Wolf et al. (2000) who studied the formation of a fluid gel produced with a

gelling hydrocolloid in the presence of a non gelling hydrocolloid. They showed that the gelling hydrocolloid was an included phase for all their experiments and that the gelling hydrocolloid phase could be spherical or could develop asymmetric particles, depending on the flow pattern applied during gelation. Attempts to produce a fluid gel particle containing two gelling hydrocolloids have not been reported before the work carried out in this thesis (Chapter 3).

Within the literature, systems known as sheared gels have been reported. The term sheared gels is normally used to describe a material which has been gelled quiescently and subsequently sheared. This results in the formation of gel particles which can flow; however, the particles tend to be much larger than those produced via the fluid gel approach. Sheared gel particles are irregularly shaped and tend to show high levels of syneresis. These systems have been used in applications such as piping gels for pastries and cakes. However, they will not be discussed further here as the large gel particles and synerisis would cause problems in skin cream type applications.

2.4 Mixed hydrocolloid systems

There is a desire for a wide range of applications, but particularly tissue engineering, to have systems which have both good mechanical properties, and good biocompatibility (Barbani et al., 2005). As a consequence, for many end applications, a single phase hydrocolloid system does not have the appropriate properties such as gel strength, ability to self support, plasticity or stability

(Norton and Frith, 2001a). More complex structures are required for many tissue regeneration applications, as they are seen to better mimic the complex nature of cartilage, ligaments and bone. Furthermore, for drug delivery systems, it has been shown that by mixing polymers, such as alginate and chitosan, a controlled and sustained release of drugs can be administered, both topically (Lira et al., 2009) and orally (Wang et al., 2010, Wang et al., 2011).

Therefore, mixed systems, and for this body of work, mixed hydrocolloid systems, are of interest and potentially of great importance. Within bioengineering and biomaterials, there is also a significant interest in the combination of natural and synthetic macromolecules, as these have been found to have the potential to closely relate to the structures that are being mimicked (Barbani et al., 2005).

When two hydrocolloids (either natural or synthetic) are in the same system, three resultant networks can be formed: interpenetrating (Morris, 1986); coupled (Fernandes, 1995) or phase separated (Butler and Heppenstall-Butler, 2003).

Interpenetrating networks involve two polymers (*A* and *B*) that are only physically entangled (Figure 2.7a). This system involves no chemical interactions between the two polymers, and both networks span the entire sample (Kasapis et al., 1993).

Within a coupled network, there are interactions between the two polymers (*A* and *B*), which favour the formation of a single *A*-*B* network (Figure 2.7b).

Optimum levels for a coupled network are related to the number of junction zones on each polymer chain. A coupled network can also be the binding of two separate polymer chains via anion to cation association, or through covalent bonding (Kasapis et al., 1993).

Finally, phase separated gels involve a polymer matrix where *polymer A* and *polymer B* do not interact. Instead, in this system, one of the polymers usually forms a continuous network, e.g. *A* forms the continuous and therefore dominant phase, with *polymer B* as an included phase, or "filler" phase (Zasypkin et al., 1997). When the two phase volumes of the polymers are approximately 50%, a bi-continuous structure forms (both polymers form continuous, intermingled structures) (Figure 2.7c). Literature shows that for some phase separated systems, there can be a sharp change in bulk modulus, as the dominant phase changes (Çakır and Foegeding, 2011).

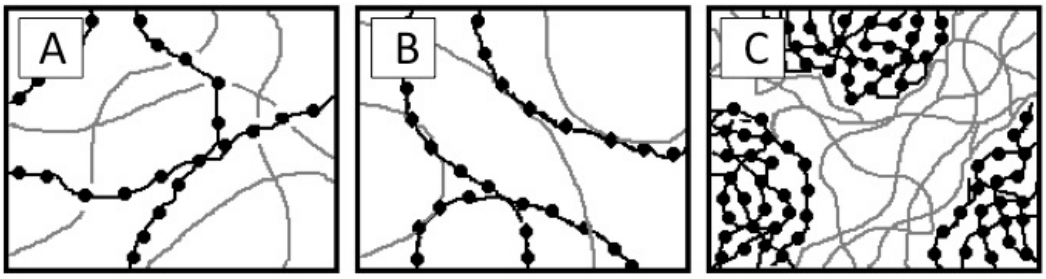

Figure 2.8 - Examples of possible structures for double polymer networks: interpenetrating networks (a), coupled networks (b) and phase separated networks (c).

By the addition of a secondary network, the mechanical properties of a hydrocolloid gel system can be manipulated and, in some cases, enhanced. An advantage of mixed systems is that the blends can have superior material properties compared with polymers which are in individual systems (Nautiyal, 2012), resulting in stronger gels. Mixed systems may also result in more stable gels. Alternatively, the equivalent gel strength can be achieved at lower polymer concentrations (Morris, 1990) which is beneficial industrially.

However, while some mixed hydrocolloid systems enhance mechanical properties, some mixtures behave in an inferior manner to the individual systems (Morris, 1990). This can often be explained by the phase separation of the hydrocolloids into their own discrete phases (this is shown in the micrographs in Figure 2.9). At low concentrations of the hydrocolloids, there is miscibility. However, as the concentration of either or both hydrocolloids is increased, the system reaches the bimodal line and phase separation occurs. Mixtures that are made up with concentrations of the hydrocolloids within the bimodal region phase separate; one region which is rich in polymer A (gelatin for instance in Figure 2.9) and the other region rich in polymer B (maltodextrin is the polymer B in the Figure 2.9). The concentrations of each of the two hydrocolloids in each of the phases are those that are shown by the point at which the tie line meets the binodal.

When two polymers phase separate, the system then contains an included polymer phase within a continuous polymer phase (this is shown in Figure 2.9). This is often dictated by the concentrations of each of the polymers within the

system, whereby the polymer that is a higher concentration becomes the continuous phase. This is also often seen in oil and water emulsions, where the phase that is above 50% phase volume will dominate. However, when polymers are in a 50:50 phase volume, then a bicontinuous system is formed. Phase inversion describes when the polymer goes from being the continuous polymer, to the included polymer, and vice versa. Phase inversion in relationship to overlap concentration of PVA will be discussed in Chapter 3 and has been published by Norton et al. (2014).

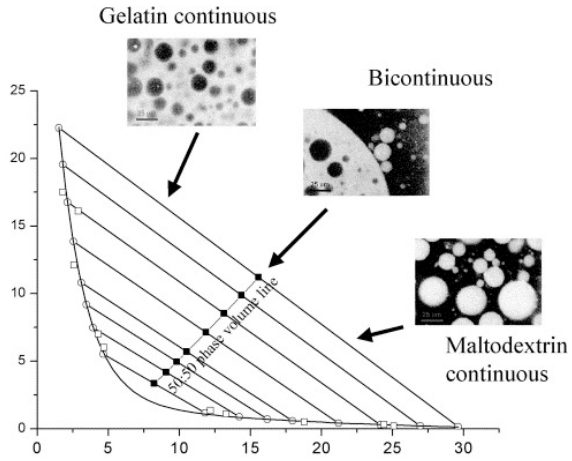

Figure 2.9 – Phase diagram for gelatin and maltodextrin mixed systems (Norton and Frith, 2001b). Norton & Frith show the bimodal, phase inversion concentration line and photomicrographs of the microstructure along a tie line. (Gelatin is the light phase in the micrographs).

The resultant network can also be influenced by gelation profiles of the individual polymers. For example, if the gelation temperatures and gelation rates are similar for both polymers and happen on the same timescale as phase

separation, there is a greater chance of forming an interpenetrating network or interpenetrating phases, as the polymers will be structuring the water simultaneously and thus could be forced to entangle or trapped in an early stage of phase separation. This idea is further developed in Chapter 4. However, testing these ideas is hampered by the ability to measure/visualise the microstructures formed as there is little or no contrast between the phases as they are constituted mainly by the aqueous medium. Attempts to overcome this visualization problem are further discussed in Chapter 3 and have been published by Norton et al. (2014).

2.5 Hydrocolloids in emulsions

One of the major uses of hydrocolloids is to increase the stability of water continuous emulsions such as dressings or skin creams. The hydrocolloid increases the viscosity of the continuous phase and thus causes the droplets to collide less frequently and with lower force, thus slowing down or stopping coalescence. In more recent times hydrocolloids have also been used for increasing the stability and in use sensory properties of oil continuous emulsions, such as low fat spreads.

2.5.1 Emulsion formation

An emulsion is the dispersion of two immiscible liquid phases, into a continuous and a dispersed phase (Aguilera, 1999), stabilised using a surface-active agent

(Figure 2.8). These are either direct emulsions (O/W) or inversed emulsions (W/O).

While emulsions are extensively used in the food and cosmetic industries, the bulk of emulsions formed are thermodynamically unstable, with the dispersed phase eventually coalescing and separating out into the component phases. The period of stability is largely dependent upon the characteristics of the interface between the two phases, the frequency of collisions between droplets (dependent on the dispersed phase volume and the viscosity/structuring of the continuous phase) and force of the collisions which is dependent on either the kinetic energy or the forces applied externally such as shear.

The ability to deliver bio actives and flavours in a controlled fashion has been a popular interest for many years. Although this can be achieved using simple emulsions (for example for the delivery of oil soluble bio actives from an oil in water emulsion) there is also an interest in delivering water-soluble actives from a water continuous system. This requires more complex structures (e.g. a double or duplex emulsion), which have a secondary water phase, included in the system. This is achieved by emulsifying the primary emulsion into a water phase to create the double, or duplex, emulsion (shown in Figure 2.8). This is also known as an “emulsion-of-emulsion”. Since their discovery, duplex emulsions have been of interest and widely researched as ways to encapsulate ingredients (for instance, as actives for pharmaceuticals, nutritional compounds and flavours), as well as to reduce fat content in food products (Muschiolik, 2007). However, duplex emulsions are more unstable than primary emulsions. This is

due to, in part, the presence of two interfaces so that two surface-active molecules are required in order to stabilise the water in oil interface and the oil in water interface. The two interfaces have different curvatures, and two different surface active molecules are required. These molecules tend to migrate between the interfaces over time. This results in less stabilisation of the interface, with a greater tendency for coelescence, thus causing instability of the duplex emulsion and a collapse to a single emulsion or even total phase separation with an oil and water layer.

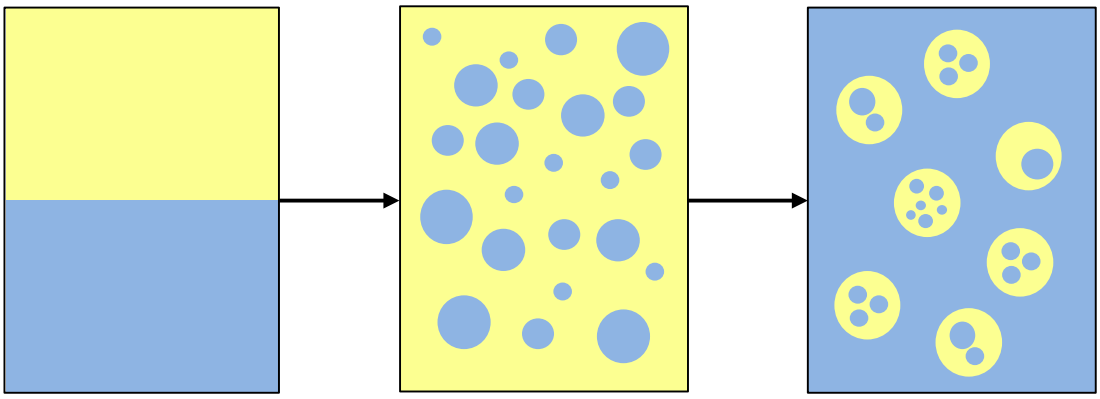

Figure 2.9 – Schematic representation of the formation of a primary emulsion and then a double (or duplex) emulsion from two immiscible liquids (water and oil).

The surface-active molecules required for emulsion formation are amphiphilic molecules which absorb at the water-oil interface, thus forming droplets in a continuous phase. The surface-active molecule used dictates whether oil or water are the continuous phase, with this being the phase when the molecule is more soluble. The role of the molecule is to reduce the interfacial tension during

the emulsification stage, and therefore reduces the required mechanical energy. The surface-active molecules also stabilise the interface and prevent newly formed droplets from coalescing (McClements, 2005) in the process and then stabilize the interface on storage.

There are two types of surface-active molecules which can stabilise the water-oil interface (Wilde, 2000):

- Surfactants: detergents, emulsifiers and lipids. These can be either water or oil soluble and usually create a compact absorbed layer, with a low interfacial tension.
- Polymers: amphiphilic macromolecules, usually proteins. Polymers form an 'irreversible absorbed layer' due to having multiple contacts points onto the interface. As the concentration of low molecular weight emulsifier is added to an emulsion already stabilisied by a protein, a mixed interfacial layer is formed and the protein occupies smaller and smaller areas of the interface, but never becomes totally displaced (Wilde, 2000, Gunning et al., 2004). This makes polymeric emulsifiers of interest in duplex emulsions as transfer from one interface to the second interface is slowed or stopped. Hence, most of the studies have used the emulsifier PGPR which has shown high levels of stability and which has been used in the studies carried out in this work, as reported in Chapter 5.

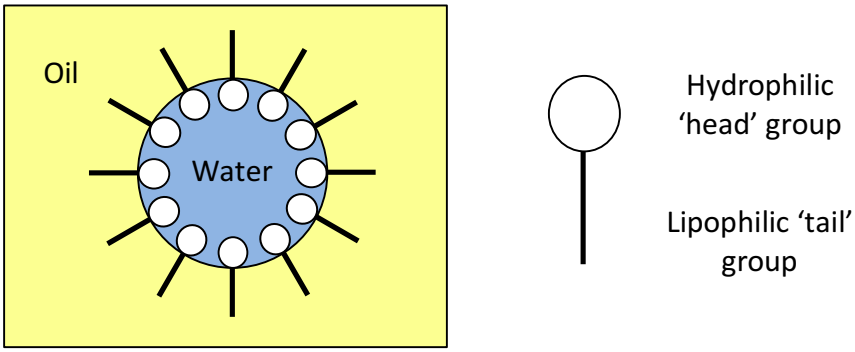

Figure 2.10 – Schematic representation of an amphiphilic molecule stabilising a water-in-oil (W/O) emulsion.

2.5.2 Role of Hydrocolloids

There has been significant research into the use of polysaccharides in emulsions, as these have been extensively shown to stabilise the emulsion interface (Surh et al., 2006, Dickinson, 2003). There has also been extensive research into the use of hydrocolloids to stabilise oil in water emulsions, as mentioned above. The hydrocolloids increase the viscosity and structuring of the continuous phase and can reduce the interaction of the droplets, leading to less coalescence on storage and in use. However, the use of a hydrocolloid within the aqueous phase of a water in oil emulsion has received less attention in the scientific literature, with the majority of this research surrounding the use of a hydrocolloid in the aqueous phase in low fat spreads (Alexa et al., 2010, Cheng et al., 2008), and cocoa-butter emulsions (Sullo et al., 2014).

The use of hydrocolloids within the aqueous phases of water in oil emulsions has been shown to enhance the consumer sensory perception of the low fat product, including spreadability. However, the increased concentrations of a hydrocolloid, such as kappa carrageenan, can disrupt the breakup of the aqueous phase during the emulsification process, particularly if gelation occurs prior to, or in tandem with, the emulsion formation. This problem has been reported at concentrations as low as 1.88% κC in the aqueous phase with a significant change in the microstructure (Alexa et al. (2010)). This is an important consideration for the work reported here: Chapter 5 looks at how structuring of the inner water phase of a duplex emulsion could give enhanced stability and potential for cell inclusion.

Chapter 3.

FORMATION AND CHARACTERISATION OF QUIESCENT GELLAN GELS AND MIXED GELLAN/PVA GELS

3.1 Background

Gels are often used in biomedical engineering: as replacement structures (e.g. for cartilage); materials applied for wounds to enhance healing; or as three-dimensional scaffolding structures for housing mammalian cells. Within these medical fields, there is a growing desire to use natural materials. However, for many naturally occurring biopolymers, such as hydrocolloids, there are mechanical issues that need to be addressed, such as hydrocolloid gel structures typically not having the required gel strength for implantation into the body.

The aim of this chapter is to investigate the effect of the synthetic polymer poly (vinyl alcohol) (PVA) on the properties of gellan gels produced under quiescent conditions, with the aim of achieving improved gel strength and functionality. It is hoped that these structures would be able to be used as cartilage replacements. A range of both gellan and PVA concentrations were investigated, with characterisation determined by compressive testing and rheology. Finally, a method of visualising the mixed gel microstructure was investigated by the use of stains, in an attempt to further understand the behaviour of the mixtures.

3.2 Materials and methods

3.2.1 Materials

Low acyl gellan (CP Kelco, UK) and poly (vinyl alcohol) (PVA) (Sigma-Aldrich Company Ltd., UK) were used for gel systems. Distilled water was used as the solvent with no added ions.

5-(4,6-Dichlorotriazinyl) Aminofluorescein (DTAF) powder was stored at -20 °C; once dissolved into the correct concentrations, solutions were stored at 5 °C until required. Ammonium hydroxide (6.42 M) (Sigma-Aldrich Company Ltd., UK) and hydrochloric acid (5 M) (Sigma-Aldrich Company Ltd., UK) were used to adjust the pH of the gellan solution.

All concentrations were calculated by weight to weight (w/w) in distilled water, unless stated otherwise. All materials were used with no further purification.

3.2.2 Methods

3.2.2.1 Preparation of gellan PVA gels

Aqueous solutions of gellan were produced, at concentrations of 1% or 2%, and at a temperature of approximately 80 °C in order to avoid gelation. Once fully dissolved, varied amounts of PVA were added (0 – 30%). Samples were poured into 30 ml cylindrical sample pots (diameter 21 mm, height 80 mm), and left to gel at room temperature for a minimum of 24 h. Mechanical testing of all gel samples was carried out between 24 h and 48 h after production.

3.2.2.2 Gellan stained with 5-(4,6-Dichlorotriazinyl) Aminofluorescein (DTAF)

The natural pH of the gellan solutions was measured and recorded at pH 5.4. The pH was increased to pH 9 - 10, through the dropwise addition of ammonium hydroxide prior to staining. 10 ml of DTAF solution (400 μM) was then added, and left to react for 5 hours. The pH was then reduced to natural pH of gellan, by the dropwise addition of hydrochloric acid.

PVA was added to the system once the gellan's natural pH had been re-established. Approximately 5 ml of each sample was poured into petri dishes, and wrapped in foil, until analysed using confocal microscopy (method described in a later section) between 24 h and 48 h after production.

3.2.2.3 Mechanical Testing

The mechanical properties of the gellan PVA gels, and stained gellan PVA gels, were assessed by performing compressive testing (5848 MicroTester, Instron, UK), using a 2 kN load cell, and 50 mm diameter stainless steel plate covered with parafilm. Samples were cut into 20 mm length cylinders, with a diameter of 21 mm. Compression rate of 20 mm/min was applied. Data shown is a mean of six or more replicates.

Compression force and change in sample height were then used to determine the stress (eq. 3.1) and strain (eq. 3.2), true stress (eq. 3.3), true strain (eq. 3.4), and then the Young's modulus (eq. 3.5), of each sample.

$$\delta_E = \frac{F}{A_\circ} \quad \text{Eq 3.1.}$$

$$\varepsilon_E = \frac{H_0 - h}{H_0} \quad \text{Eq 3.2.}$$

$$\delta_T = \delta_E(1 - \varepsilon_E) \quad \text{Eq 3.3.}$$

$$\varepsilon_H = -\ln(1 - \varepsilon_E) \quad \text{Eq 3.4.}$$

$$E = \frac{\delta_T}{\varepsilon_H} \quad \text{Eq 3.5.}$$

where δ_E is Stress, F is compression force, A_o is original area, ε_E is strain, h is compressed length of sample, H_o is original length of sample, δ_T and ε_H are true stress and true strain respectively, and E is Young's modulus.

From the obtained true stress/true strain curves, the slope of the second linear region (strains over 0.1), leading to the subsequent failure of the structure, were used to calculate the bulk modulus of each sample (Norton et al., 2011 and Nussinovitch, 2004).

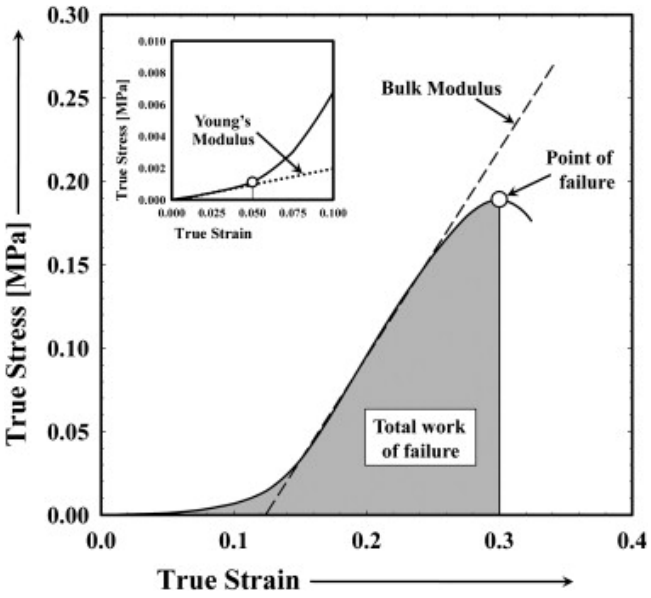

Figure 3.1 – Schematic representation of a typical true stress/ true strain curve during compression of a quiescent gellan gel. The figure shows how both Young's modulus and bulk modulus are interpreted. (Image from (Norton et al., 2011))

3.2.2.4 Rheological Analysis

For determination of PVA specific viscosity, and the polymer overlap concentration, PVA stock solutions were prepared (3%, 5%, 7.5%, 10%, 14%, 15%, 17%, 20% and 25% (w/w) in distilled water).

Solutions were analysed at a range of shear rates (0.01 – 1000 s^{-1}), with readings taken when steady state was achieved. Cup and double gap geometry was used for dilute solutions, and cone (40°, 40 mm) and plate (65 mm) geometry used for higher viscosity solutions. Viscosity measurements were taken in a controlled 25 °C environment.

The "zero shear" or "Newtonian" viscosity (η_0) of the sample and distilled water data were used to calculate the specific viscosity (η_{sp}) of the samples using the below equation (eq. 3.6) (Morris et al., 1981).

$$\eta_{sp} = \frac{\eta_0\,(sol) - \eta_0\,(H_2O)}{\eta_0\,(H_2O)} \qquad \text{Eq 3.6.}$$

3.2.2.5 Confocal Scanning Laser Microscopy (CSLM)

Confocal scanning laser microscopy (CSLM) (Lecia TCS-SPE, Lecia Microsystems Ltd., UK) was used for DTAF gellan samples. Images were taken on a best focus plane, using an argon laser, and 10x magnification lens. Images were all processed using Image J.

3.3 Results and Discussion

3.3.1 Understanding poly (vinyl alcohol) (PVA) modification of gellan gels

In order to replace structural biological materials, it is important to understand large deformation properties, both in terms of the Young's modulus and the failure strength and strain. Thus, as a starting position, the properties of 1% gellan alone, with no added ions, were investigated under compression. Figure 3.2 shows the true stress verses true strain as measured using the Instron MicroTester. As was expected for gellan with no added salt (open squares in Figure 3.2), low stress at all strains was observed and no clear failure was observed, showing that no gel structure was present.

It is known that the addition of a second polymer can enhance the material properties by forming a mixed gel network (Nautiyal, 2012) (e.g. by causing molecular binding); producing a bicontinuous gel structure (in which both polymers form a continuous three dimensional structure throughout the sample); or phase separating, thus causing the effective concentration of both polymers to increase (Morris, 1986).

To investigate the effect of a secondary polymer on gellan, varying concentrations of the synthetic polymer poly (vinyl alcohol) (PVA) were added to 1% gellan. Gels formed under quiescent conditions were investigated using compression testing. Figure 3.2 shows the true stress verses true strain of each sample tested on the Instron MicroTester. On addition of 1% PVA, there was little change in the true stress/true strain curve observed compared with gellan alone; on further addition of PVA, the force required to deform the material increased and the failure stress decreased, from strain values of 0.5 for 1% PVA, to 0.24 for 15% PVA. This indicated that the material was developing gel properties and that the gels were becoming stronger and more brittle. As expected, the deviation between repeats became larger once sample failure had occurred due to the presence of a broken gel. As the concentration of PVA was increased above 20%, the stress at all strains decreased and the failure strains increased (from strain values of 0.24 for 20% PVA, to 0.38% for 30% PVA), so that at 30% PVA the behaviour was similar to that observed for 7.5% PVA.

Acetal linkages were not formed, as neither formaldehyde nor glutaraldehyde were added, nor was a physical gelation of PVA performed (e.g. freeze-thaw

cycles) (Nuttelman et al., 2002). PVA is therefore classed in this system as a non-gelling component. Thus, the change in moduli is either due to the PVA causing the gellan to interact with itself more strongly in a phase separated system by reducing the available water, or because a network involving both polymers is being formed.

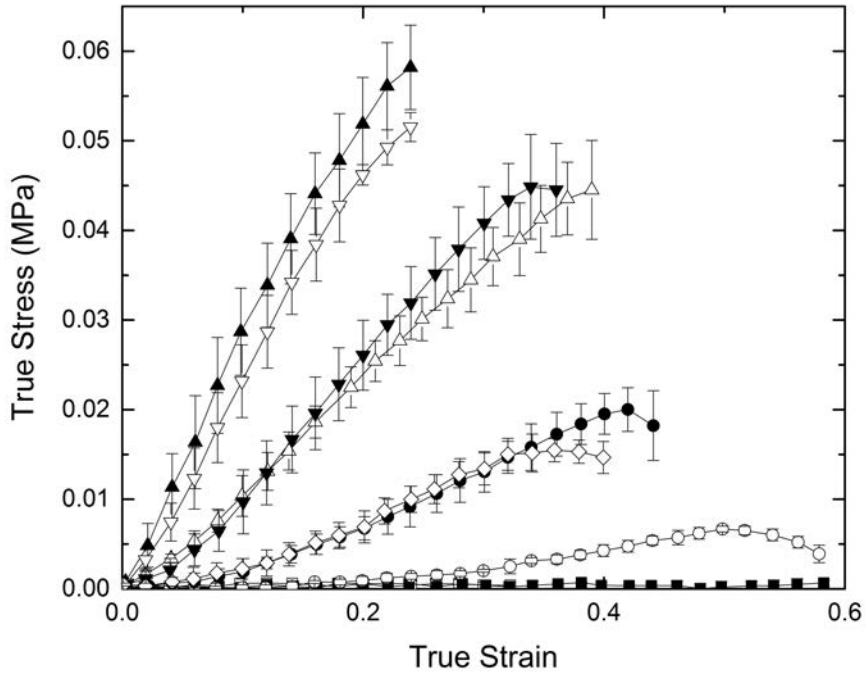

Figure 3.2 - True stress/true strain curves for 1% gellan gels formed with 0% (□), 1% (■), 5% (○), 7.5% (●), 10% (△), 15% (▲), 20% (▽), 25% (▼), and 30% (◇) PVA. Gelation occurred with temperature decrease. No external cross-linking agents were used. Error bars represent a single standard deviation.

In order to investigate which of these two mechanisms of interaction was occurring, the gellan concentration was increased to 2% and studies were carried out with addition of PVA, up to 20%. Further addition of PVA was not possible as

inhomogeneous samples were produced, possibly as a consequence of reaching the solubility limit of PVA in the presence of gellan. Figure 3.3 shows the true stress versus true strain of 2% gellan gels, with added PVA. As was observed for 1% gellan, the 2% gellan in the absence of added salt results in a weak gel with a failure strain of 0.5 (open squares in Figure 3.3). On addition of PVA, the stress for failure increased and the strain of failure decreased (from strain values of 0.44 for 1% PVA, to 0.32 for 10% and 15% PVA) with increased concentration of PVA. The fracture stress is higher than that observed with 1% gellan. As can be seen in Figure 3.3, 2% gellan, 10% PVA gels exhibited the maximum stress and lowest failure strain. On further increasing the PVA concentration, the gels became weaker again and the failure strain increased. This behaviour is a very similar to the results shown previously in Figure 3.2 for 1% gellan and again the variation in stress between samples was highest after failure has occurred so the data is not shown.

By comparing Figure 3.2 and 3.3, it can be seen that the maximum stress of failure occurs at about the same PVA concentration, suggesting that this behaviour is unlikely to be due to a binding of the two polymers into a coupled network; if this was the mechanism, maximum network formation would be expected to occur at a higher concentration of PVA when the concentration of gellan is increased as the potential for interaction is higher with higher gellan concentration.

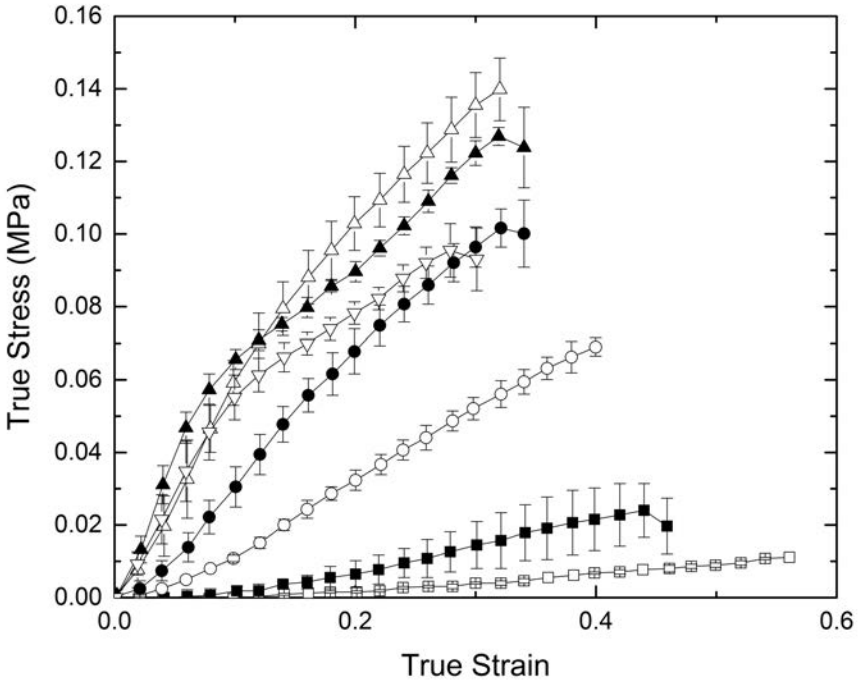

Figure 3.3 -True stress/true strain curves for 2% gellan gels formed with 0% (□), 1% (■), 5% (○), 7.5% (●), 10% (△), 15% (▲), 20% (▽) PVA. Gelation occurred with temperature decrease. No external cross-linking agents were used. Error bars represent a single standard deviation.

When designing systems for tissue engineering, the Young's modulus and the compressive strength of the gels are important. Figure 3.4 shows the Young's modulus of both gellan concentrations (1% and 2%), as a function of addition of PVA calculated from Figure 3.2 and 3.3. The Young's modulus for the 2% gellan was higher than that measured for the 1% gellan samples. Although this would be expected, the magnitude of increase (about 4 to 5 times for a doubling of the gellan concentration) would not be expected for a coupled or bi-continuous network, but it is in the range expected for phase separation, as a C^2 relationship

is expected (Baines and Morris, 1987). For both gellan concentrations, the stiffness of the gels increased with PVA concentration up to 10 to 15% PVA. On further addition of PVA, the Young's modulus decreased. This behaviour has been reported for other hydrocolloid mixtures in which phase separation occurs, and the concentration with the highest stiffness has been described as the phase inversion point. This would suggest that between 0 – 10% PVA, gellan is the continuous phase, and thus is the polymer that dominates the overall material properties (Morris, 1986). Above a PVA concentration of 10%, the system then becomes bi-continuous (10% and 15% PVA), before PVA becomes the continuous phase with gellan as the included phase at higher concentrations. As PVA is a non-gelling polymer, under the conditions used, it would be expected that once it forms the continuous phase, there would be no gel like properties to the composite. The fact that a Young's modulus is observed suggests that phase volume of the gellan included phase is high enough to cause close packing of the included droplets. On increasing the PVA concentration further (i.e. to 30%), the phase volume of the gellan particles decreases as the PVA forces the gellan into more concentrated and smaller particles and a lowering of the Young's modulus.

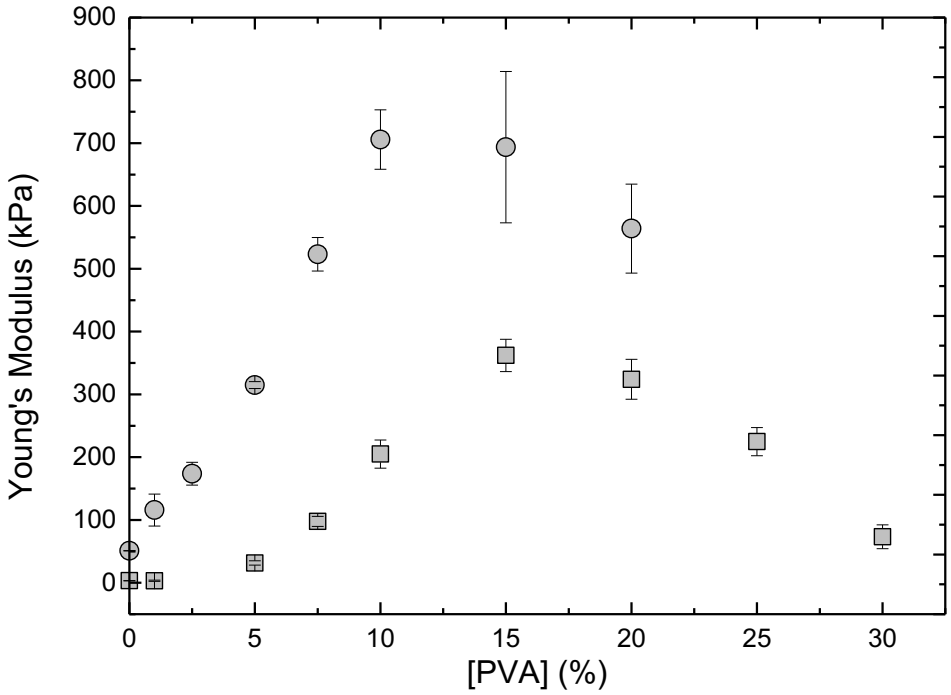

Figure 3.4 - Effect of PVA concentrations on the Young's modulus of gellan gels. Gels were made with 1% (□), and 2% (○) gellan. Error bars represent a single standard deviation; where not seen, error bars are smaller than the symbol.

The force which a material can withstand before failure occurs is important for the understanding of gel systems. Compressive strength was determined from Figure 3.2 and 3.3 (Figure 3.5). Similar to the trends shown in Figure 3.4, the mixed gels reach maximum strength when PVA is between 10% and 15%. The larger errors observed once the gellan is an included phase are consistent with the phase volume argument discussed earlier i.e. at these concentrations large variations between the nine samples tested suggested that within the quiescent gel, there are regions of higher amounts of gellan phase, and therefore regions of higher amounts of PVA phases. As the PVA is non-gelling, this heterogeneity in

microstructure results in a wide variability of the mechanical behaviour. However when gellan is the continuous phase, with an included PVA phase, the PVA is trapped within the structure at the gelation stage. This creates a more homogenous structure and more consistent mechanical behaviour.

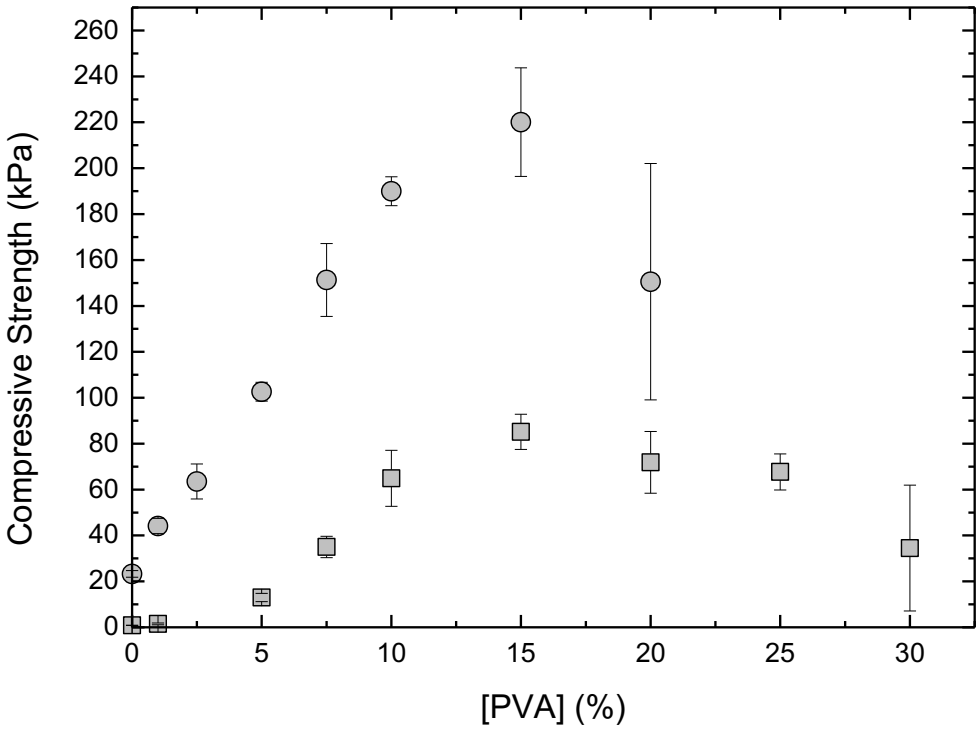

Figure 3.5 - Effect of PVA concentrations on the Compressive Strength of gellan gels. Gels were made with 1% (□), and 2% (○) gellan. Error bars represent a single standard deviation; where not seen, error bars are smaller than the symbol.

The data obtained indicates that the gellan and PVA phase separate, and that the phase inversion point is independent of the gellan concentration, occurring at a concentration of ~ 15% for both concentrations of gellan.

Having established that the mechanical behaviour in the system is a consequence of phase separation, the results could be dependent on the way

the samples were prepared. In order to investigate this, the order of polymer addition was varied. Gels were prepared with gellan dissolved first (standard practice), PVA dissolved first, and the two polymers dissolved simultaneously. The results obtained for Young's modulus and compressive strength for the three sample preparation methods are shown in Figure 3.6. As can be seen, the material properties are independent of the order in which the polymers were dissolved and as such it appears that the microstructure produced is the same for all three methods. Therefore, order of addition has no influence on polymer interactions, and cannot be used to induce either a coupled or interpenetrating network, rather than phase separation.

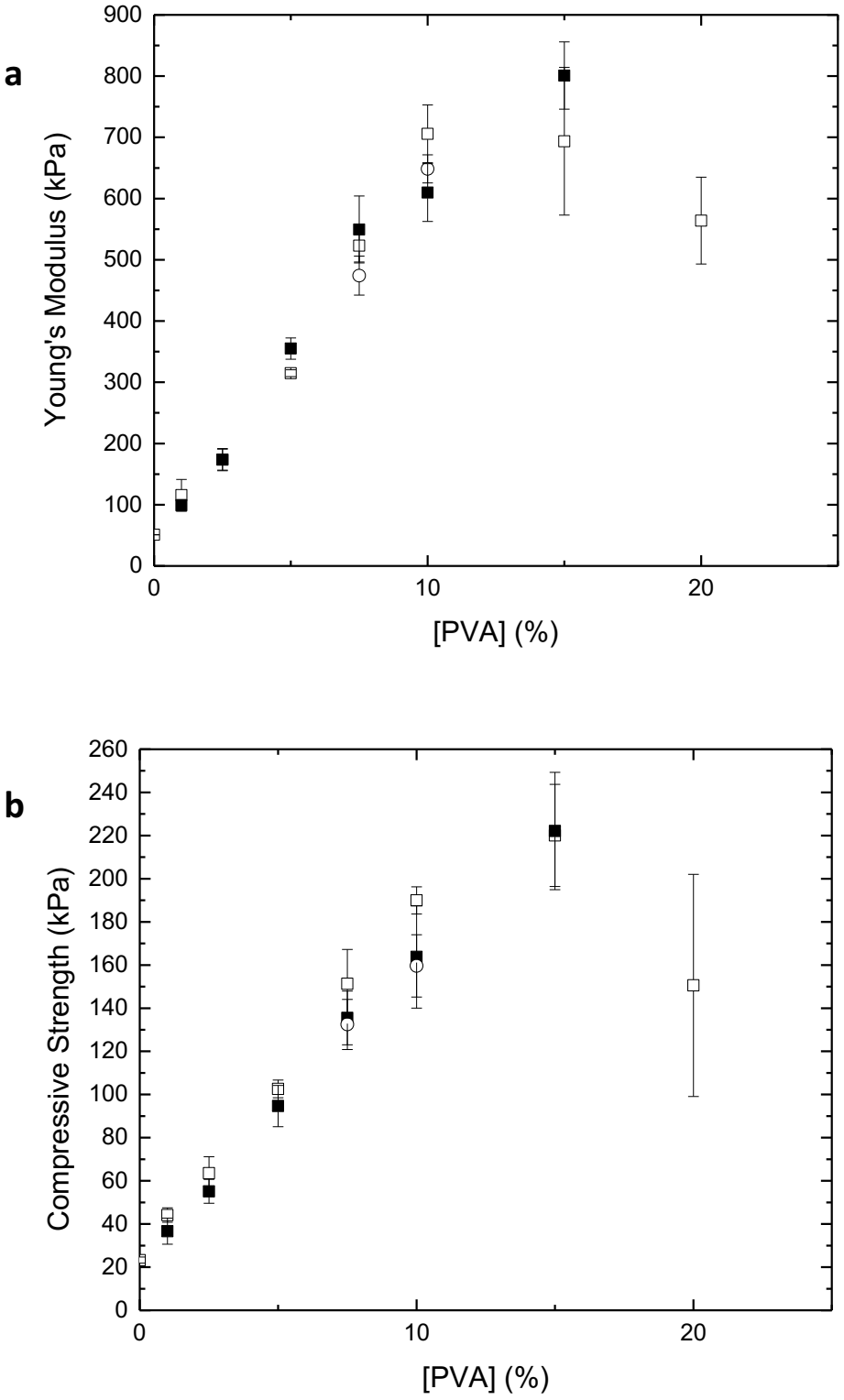

Figure 3.6 - Effect of order of polymer addition on Young's modulus and Compressive strength of the gellan-PVA gels, formed by gellan dissolved first (□), PVA dissolved first (■), or by dissolving simultaneously (○). Error bars represent a single standard deviation; where not seen, error bars are smaller than the symbol.

The data presented so far suggests that the disruption of the gellan network could be a result of increasing concentrations of PVA occupying a larger volume of the sample, which would cause the gellan to be forced into an included phase. If this is happening, then the effect would be expected to occur above the PVA concentration that hydrodynamically occupies the whole volume. This is the concentration at which the PVA chains overlap in solution. To investigate this, the polymer overlap concentration (C*) of PVA was determined.

This was determined by measuring the viscosity as a function of shear rate for a range of polymer concentrations (Figure 3.7). This data shows that at low concentrations of PVA (3 to 7.5%), the samples behaved as Newtonian fluids with the viscosity showing no dependency on shear rate, as expected for a low molecular weight random coil polymer. When the concentrations of PVA were increased, the viscosity of the samples increased, and started to show a shear thinning behaviour at 17 and 20%.

In order to determine the overlap concentration, specific viscosities need to be calculated for each concentration of PVA polymer solution. Specific viscosity is obtained by extrapolating the viscosity back to zero shear. The data obtained for PVA is plotted in Figure 3.8. As can be seen at low PVA concentrations, there is a linear dependency on the log/log scale for specific viscosity versus concentration. Then at higher PVA concentrations (above 15%), there is a linear dependency with higher slope. When these two linear behaviours are extrapolated to the point where they intercept, this is the overlap concentration. As can be seen, this

occurs for PVA at a concentration of ~ 14%. Hence it seems that the PVA overlap concentration, the concentration at which the PVA polymer occupies the majority of the space, and the concentration at which mixtures of gellan and PVA become PVA continuous, are the same. This implies that at this concentration the gellan polymer is forced into an included phase, or filler phase before gelation. This has not been demonstrated before and in the future this needs to be checked with PVAs of different molecular weight which have different C* values. If this hypothesis is proved, it should allow a method of controlling the properties of phase separated gellan/PVA mixtures with the potential to closely mimic the properties of native tissue for applications in regenerative medicine.

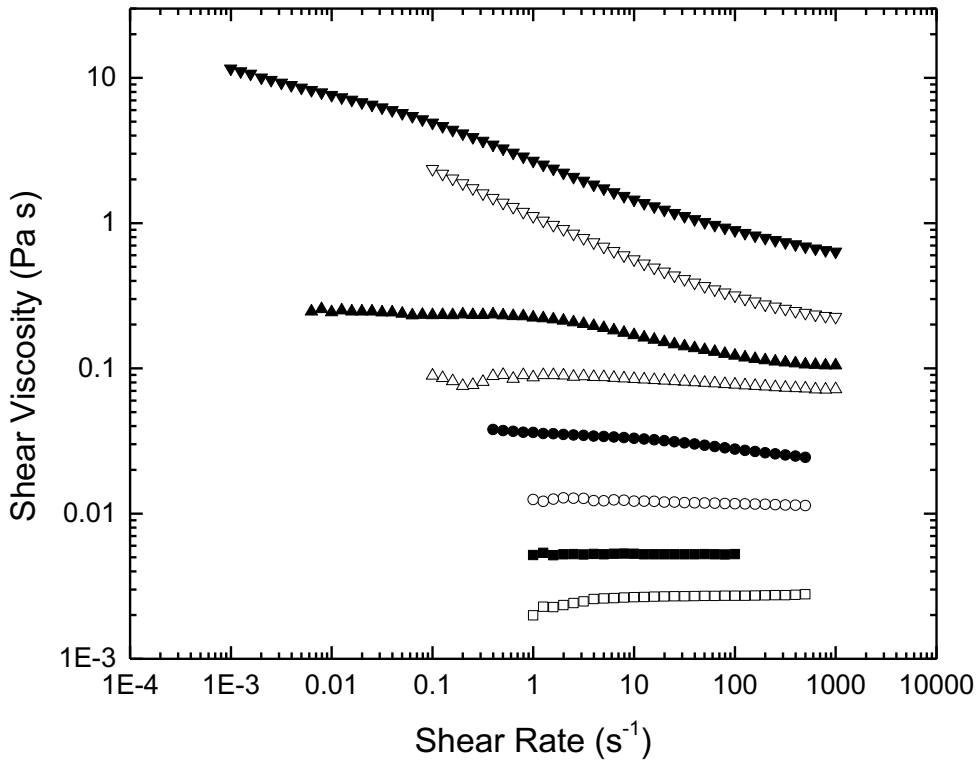

Figure 3.7 - Flow curves for poly (vinyl alcohol) at 3% (□), 5% (■), 7.5% (○), 10% (●), 14% (△), 15% (▲), 17% (▽), and 20% (▼).

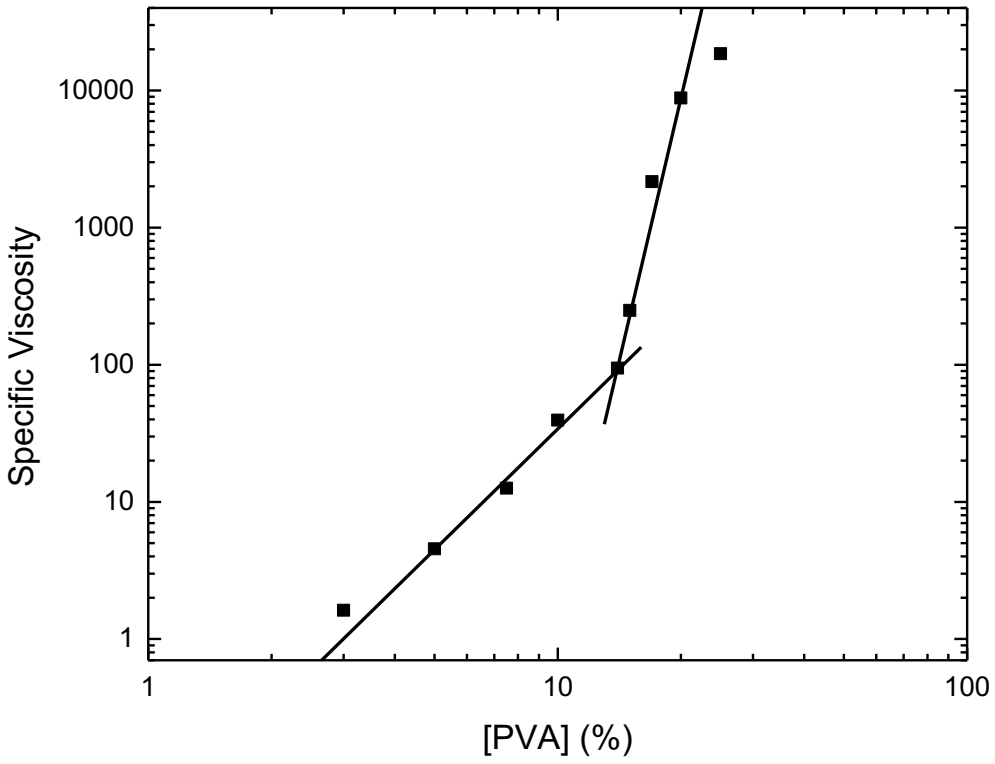

Figure 3.8 - Viscosity *vs*. poly (vinyl alcohol) concentration showing the C* for PVA at 14%, in distilled water.

The success of these mixed polymer gels is related to their ability to create self-supporting, three dimensional structures, which can potentially be implanted. A model of auricular cartilage was provided (Figure 3.9), after being sculpted to match a paediatric patient. From this, a mould was made, and the gellan-PVA mixes were gelled within the auricular mould.

At 2% gellan/ 10% PVA (Figure 3.9a), the moulding of a structure for an ear was unsuccessful, with failure occurring when the gel was removed from the mould. When the concentration of PVA was increase to 15% (Figure 3.9b), the gel network withstood the forces of being removed from the mould, and remained

intact. Above 15% PVA, failure to form a gel in the mould was observed. This further indicates that the addition of PVA in the gellan structure has initially enhanced the gel network, but above 15% has weakened it. For these studies it was the mixture where the PVA is at the polymer overlap concentration (~ 15%), which gave the successful 3D structure. It appears as if the entanglement of the PVA is therefore assisting the structure, rather than hindering it. This would be interesting to study more fully in the future.

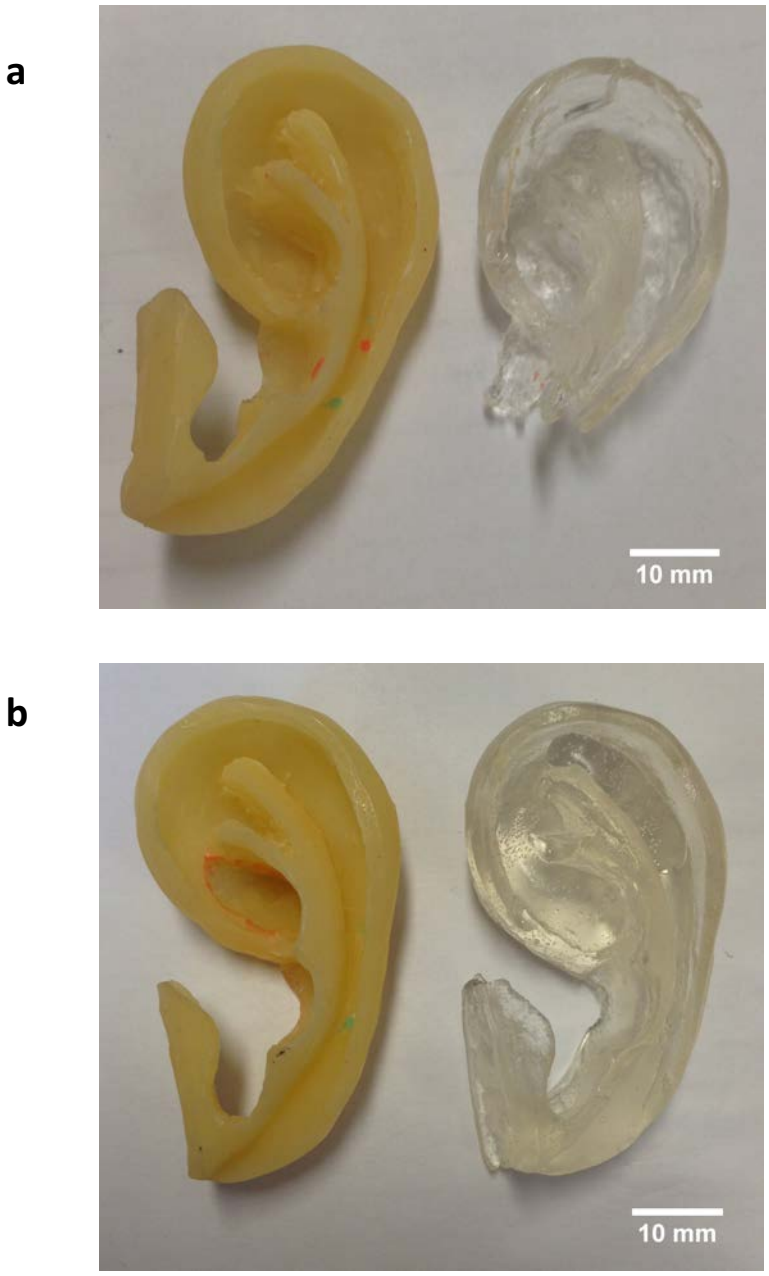

Figure 3.9 - Photographs of 2% gellan, 10% PVA (a) and 2% gellan, 15% PVA (b) moulded into three dimensional paediatric auricular cartilage. Removal of the sample from the mould caused damage to the 2% gellan, 10% PVA structure. There was successful removal from the mould, with no damage caused, for the 2% gellan, 15% PVA.

3.3.2 Visualisation of gellan/PVA microstructures

As many of the observations and material properties of gellan/PVA mixtures can be explained by a phase separation mechanism, visualisation of the structures could give a better understanding of the behaviour of the microstructures developed. However, due to a lack of contrast between the phases, microscopic visualisation of the mixtures indicated that some structure had been formed, but the pictures were not of a good enough quality to interpret. This was the case when using both simple transmission and cross polar methods. The use of simple dyes proved inconclusive, as they were not preferentially bound to either polymer, or just stained the water in which the polymers were structure. Therefore, a stain was required which would preferentially stain just one of the polymers, preferably through covalent binding.

5-(4,6-dichlorotriazinyl) aminofluorescein (DTAF) has been used to successfully stain a range of proteins, carbohydrates and polysaccharides (Russ et al., 2013, Li et al., 2003). It is reactive at pH levels of 9 and above (Li et al., 2003) and binds via carboxyl groups; it was therefore hypothesised that this could be used to bind to gellan which could then be used in the double polymer system, providing the second polymer was added at a pH below 9.

Gellan solutions were prepared in water, to result in the required final concentrations when PVA was later added. The gellan solutions were increased in pH from pH 5.4, to above pH 9, using ammonium hydroxide. DTAF was then added and left to react for 5 hours. The pH of the solution was then decreased to pH 5.4, and the PVA was added to the solutions, to form the final concentrations.

For this part of the research, 5%, 10% and 15% PVA were investigated, as these should represent the three stages of the gel microstructure: gellan continuous, bicontinuous, and then PVA continuous.

Figure 3.10 shows confocal microscopy of the DTAF labelled gellan and PVA mixtures. The confocal microscope was programmed to so that the DTAF appeared in green, due to the fluorescence. Anything not excited at these wavelengths is black. Therefore, due to the sample preparation, gellan should appear green, and PVA should be black. A range of DTAF concentrations were investigated; however, for this chapter, only 400 μM will be discussed.

The images in Figure 3.10 clearly show an increase in black regions when the concentration of PVA was increased. This indicated that the PVA was left unstained, and the addition of the PVA into the system when the pH had been reduced resulted in the PVA remaining unstained.

Figure 3.10a shows that at low concentrations of PVA, the continuous structure is green, and therefore is the gellan. Darker regions are visible within the gellan, indicating that the PVA is in distinct regions, with the dimensions of approximately 10 microns or smaller. On increasing the PVA concentration to 10% (Figure 3.10b), the confocal images showed large (100 micron sized) areas of gellan and PVA co-existing. This is what would be expected for a bicontinuous structure. On increasing the PVA to 15% (Figure 3.10c), the image shows a dark structure in which faint green droplets are visible in the background showing that the system is now PVA continuous with gellan as an included phase.

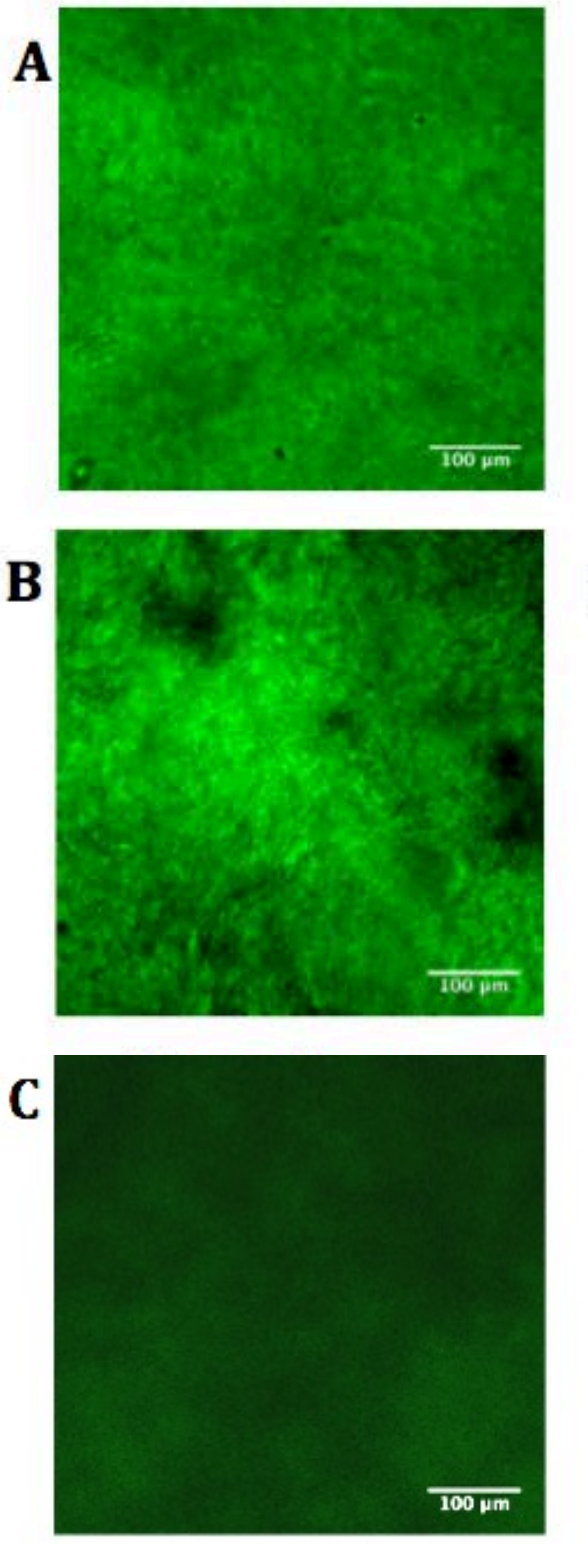

Figure 3.10 - Confocal microscopy images show quiescently set 2% gellan system with the addition of PVA, of varying concentrations ((A) 5% PVA, (B) 10% PVA, and (C) 15% PVA) in the presence of DTAF. Images show successful staining of the gellan polymer (shown in green), with PVA left unstained (black).

In order to understand the effect that the presence of the DTAF stain had on the gellan structure, mechanical testing was carried out on 2% gellan with DTAF in comparison with unstained 2% gellan. Figure 3.11 shows the true stress verses true strain of 2% gellan gels, with and without DTAF, and then mixed systems of unstained and stained gellan. As can be seen, the addition of the DTAF stain affected the strength and stiffness of the resultant gel, with DTAF gellan being stronger, and more brittle than the control (i.e. lower failure strains). This suggests that the addition of the DTAF in the gellan structure has affected the side-by-side aggregation of the gellan, as a consequence of the molecular size of the stain. However, the DTAF causes a stronger interaction between gellan chains than that observed for the unstained gellan, hence exhibiting behaviour similar to that shown when gellan is crosslinked with ions. This is probably as a consequence of DTAF/DTAF interactions between chains.

If the DTAF is interacting with itself leading to junction zones and increased gel strength, it was then hypothesised that mixing stained gellan with unstained gellan should reduce these interactions and reduce the mechanical changes seen with DTAF gellan. Different ratios of unstained and stained gellan, with an overall gellan concentration of 2%, were produced and stress/strain measurements performed (Figure 3.11). The unstained gellan gave the lowest gel strength and as the ratio of stained gellan was increased to 40% higher moduli, higher failure stresses and smaller failure strains were observed (Figure 3.11) showing that the DTAF cross linking of the gellan is having a significant effect. As the ratio of stained gellan was increased to 60%, the stress/strain behaviour and failure

stress decreased to similar levels observed for 20% stained sample. A further decrease in stress/strain was observed for 80% stained gellan.

It appears that the addition of the stained gellan to the unstained gellan structure initially increased the gel strength, until further addition of stained gellan then disrupted the gellan microstructure. This indicates that phase separation is occurring between the unstained gellan, and the gellan chains containing the DTAF molecule. As discussed earlier in this chapter, this behaviour is typical for multicomponent gel systems, where the presence of a second incompatible polymer at high enough concentration causes the two polymers to gain more enthalpy by associating with polymers of similar structure, than the loss in entropy caused by the phase separation.

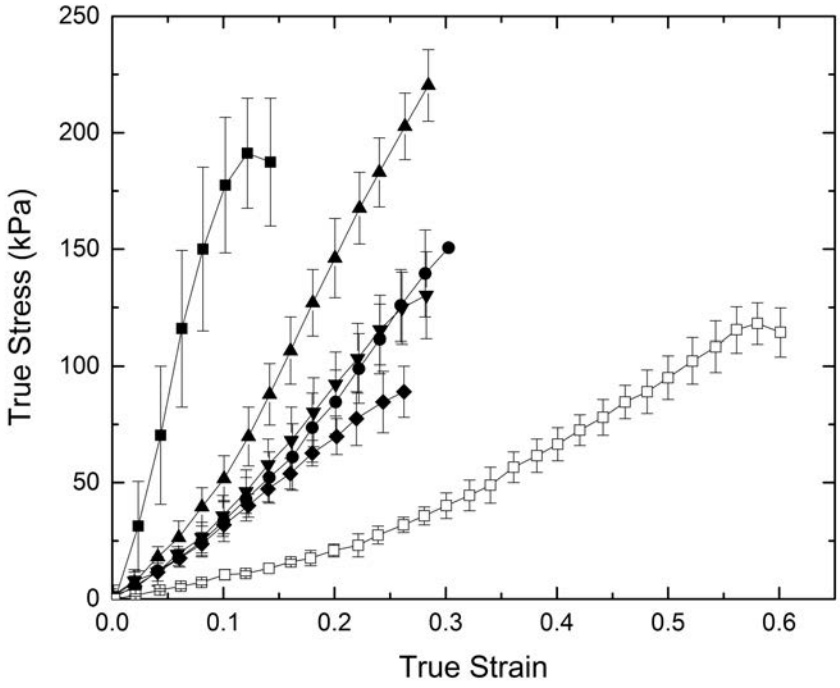

Figure 3.11 - True stress/true strain curves for DTAF gellan (at 2%) (■) and the control (unstained gellan) (at 2%) (□) and 2% low acyl with ratios of unstained to stained gellan present: 80:20 (●), 60:40 (▲), 40:60 (▼), and 20:80 (◆).Error bars represent a single standard deviation from 9 repeats.

It would not be expected that phase separation would occur between stained and unstained gellan as the majority of the polymer structures are identical. It would, however, be predicted that the modulus would increase linearly with increasing ratios of stained gellan, due to the stain appearing to cause more aggregation. This would occur in a mixture where the polymers form a joint network or even for a bi-continuous system. The bulk modulus of the different ratios of stained and unstained gellan were calculated from Figure 3.11 and are plotted in Figure 3.12. Initially, a linear relationship was observed on addition of

stained gellan, with the modulus being a simple summation of the ratio of the gellan and stained gellan moduli (as highlighted by the dashed line). This indicates that, at values below 40% stained gellan, the system is either forming a single network of chains or is bi-continuous. When the level of staining is increased to 60% and 80%, the modulus drops well below the predicted value for a single network (i.e. the dashed line) suggesting that phase-separation occurs, with the stained gellan as the included phase. This hypothesis is further supported because the modulus for 80% stained gellan is close to that of the 100% unstained gellan. The trend shown in Figure 3.12 is similar to that expected for a mixed polymer system (two component composites) obeying polymer blending laws in which an isostress/isostrain fit can be applied (Clark et al., 1983 and McEvoy et al., 1985).

Although it would not be unexpected that covalently binding a dye to gellan would result in phase separation, the sensitivity of gellan to slight changes in structure has previously been demonstrated. Phase separation was observed when low acyl gellan was mixed with high acyl gellan (Bradbeer, Hancocks, Spyropoulos, & Norton, 2014). This indicates that a difference in branching on the polymer backbone results in the low acyl gellan and high acyl gellan phase separate so they behave and should be considered as two completely different polymers, similarly to low acyl gellan and low acyl gellan bound to DTAF.

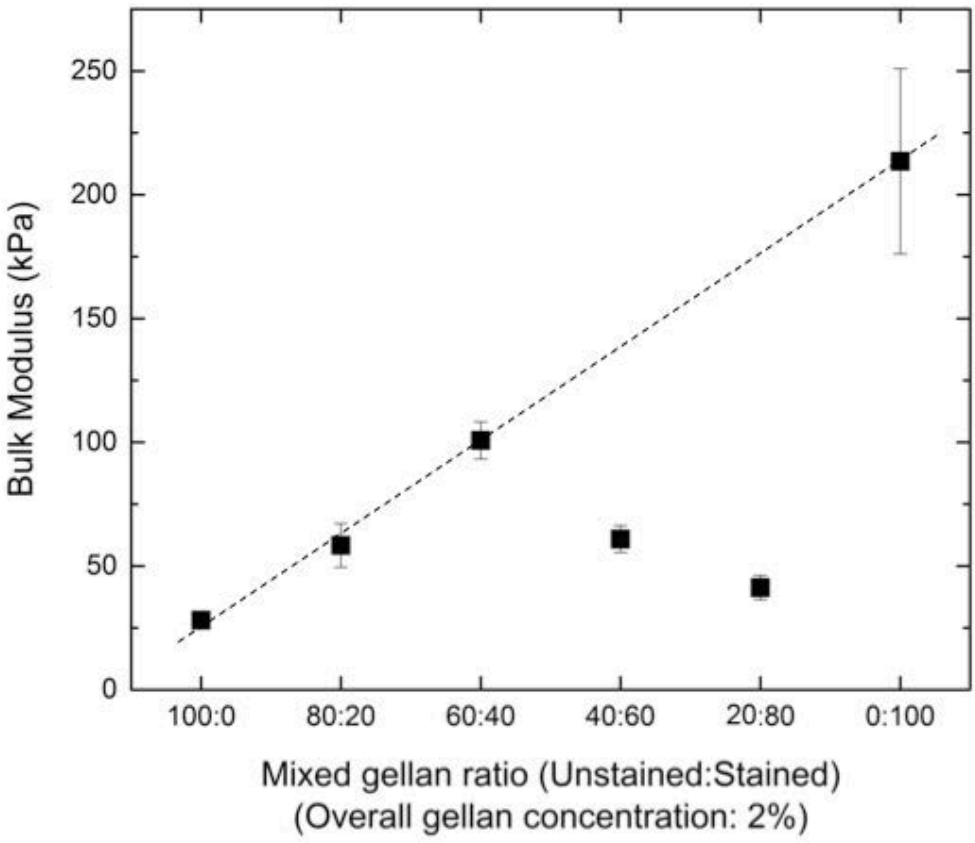

Figure 3.12 – Bulk modulus of 2% low acyl gellan, with ratios of unstained and DTAF stained gellan. Dotted line represents the hypothesised result of a linear change as ratios were changed. Gelation occurred with temperature decrease. Error bars represent a single standard deviation.

3.4 Conclusions

This research has shown the potential for developing a material that can mimic the structural properties and complexity of native tissue as described by Boschetti et al. (2004).

The inclusion of poly (vinyl alcohol) in gellan systems has been shown to increase the gel strength up to a critical concentration, after which the gel strength

decreases again. The same trend is present at higher gellan concentrations, although overall gel strength is increased, and the critical concentration of PVA has been shown to be independent of the gellan concentration between 1% and 2%. As the PVA modified gellan forms a phase separated system, the point of maximum gel strength and stiffness corresponds with the phase inversion point, and the polymer forming the continuous phase determines the material properties. Additionally, the research has shown that the dissolution order has no effect on gel strength or stiffness, indicating that the structure formed is not affected.

Viscosity of PVA solutions increased with polymer concentration. At low concentrations of PVA, there is a linear dependency, with a separate linear dependency at higher concentrations of PVA. This two-stage viscosity shows that the polymer becomes entangled at the point of interception. Therefore, the decrease in gel strength of PVA modified gellan appears to be due to the polymer entanglement of the PVA, rather than as a result of the increased viscosity caused by the addition of PVA.

5-(4,6-dichlorotriazinyl) aminofluorescein (DTAF) has been shown to successfully stain low acyl gellan, and can be processed to ensure that a secondary polymer remains unstained. However, the addition of the DTAF within a gellan quiescent gel affects the mechanical properties of the bulk gel. Using ratios of unstained gellan and stained gellan results in phase separation of the polymers. Therefore, it is suggested that staining should only be used as a visualisation of an investigated microstructure, and be one of many analytical methods.

Furthermore, 100% staining should be used for visualisation so that it is known that a second phase separation is not occurring within the system. Future work could investigate the processing (i.e. time to stain, concentration of stain), and how this affects the change in mechanical properties. This study left the stain to react for a 5 hour period; however, if this time period was reduced, fewer mechanical property changes should be seen.

This research has successfully shown that gellan hydrogels can be modified and gel strength can be increased through the addition of a secondary polymer, poly (vinyl alcohol). Therefore, gel properties can be enhanced and controlled in order to closely mimic the properties of human tissue, with the potential to replace current painful and traumatic tissue regenerative procedures.

Chapter 4.

THE FORMATION AND CHARACTERISATION OF LOW ACYL GELLAN/ KAPPA CARRAGEENAN MIXED FLUID GELS

4.1 Background

By processing hydrocolloid gel systems during the gelation process, gel particles can be formed, rather than to form a block of gel. This then potentially widens the application relevance because fluid gels can flow and are spreadable, allowing their use in products such as skin creams (as discussed in Chapter 2, Section 3.2).

There is an increased amount of knowledge in fluid gels; however, understanding of the effect of two polymers on the fluid gel production is more limited. The aim of this chapter, therefore, is to investigate the effect of the secondary polymer on the fluid gel production, and to determine if particles of both polymers could be formed.

4.2 Materials and Methods

4.2.1 Materials

Low acyl gellan (Kelcogel F, CP Kelco, UK) and kappa carrageenan (Sigma-Aldrich Company Ltd., UK) were used for this research, without further purification. No external cross-linking agents were used to produce the fluid gels. The water used for all solutions was passed through a reverse osmosis unit, and then a milli-Q water system. All sample concentrations are weight percentage.

Salt analysis, using Inductively Coupled Plasma Mass Spectrometry (ICP-MS), was carried out on both low acyl gellan and kappa carrageenan powders, straight

from the respective companies. Salt concentrations for both powders are listed in Table 4.1. The cations present in the powders will have an effect on the gelation of each polymer, as the calcium divalent cation is said to form true ionic bonds between gellan chains (Nickerson et al., 2003), while kappa carrageenan has a higher affinity to the potassium cations (Morris et al., 1980).

Table 4.1 - Concentrations of salts (wt %) present in gellan and kappa carrageenan powders. Concentrations determined by ICP-MS

	Potassium	Sodium	Calcium
Gellan	2.16%	0.52%	0.35%
κ Carrageenan	3.63%	0.49%	0.05%

4.2.2 Fluid gel preparation

Low acyl gellan and kappa carrageenan were dissolved in deionised water at approximately 80 ^{o}C whilst stirring to ensure fully dissolved. Fluid gels were produced using a vane geometry on a rheometer (Kinexus, Malvern, UK). The rheometer was set to 80 ^{o}C before the sample was added, to avoid any gelation occurring prior to the application of shear. Once the sample had been added to the rheometer cup, the temperature was allowed to equilibrate for 5 min before the sequence was started. The cup temperature was decreased from 80 ^{o}C to 5 ^{o}C, at 2 ^{o}C/min. A range of shears was investigated while gelation was occurring.

Fluid gels were produced between 0.5% and 2% with different ratios of the two polymers.

4.2.3 Fluid gel characterisation

4.2.3.1 Rheological characterisation

Rheological characterisation of the fluid gels was carried out 24 hours after fluid gel production, to allow any possible aggregation of particles to occur. Fluid gels were characterised using a cone, with an angle of 4^{o}, diameter of 40 mm, and plate on a rheometer (Kinexus, Malvern, UK). Viscosity tests and frequency sweeps were carried out on each sample, between 0.001 and 100 s^{-1}. All rheological characterisation was carried out at 25 ^{o}C.

Particle interactions were investigated for the 12 hours immediately after fluid gel formation. Once a fluid gel sample was made, the temperature of the vane was slowly increased to 25 ^{o}C (at 1 ^{o}C/min). Once the temperature had equilibrated for 5 min, a single frequency oscillation test was carried out (with frequency of 1 Hz, and strain kept at a constant of 0.5%).

4.2.3.2 Differential scanning calorimetry (DSC)

A μDSC evo Dynamic Scanning Calorimeter (DSC) (Setaram Instrumentation, France) was used to measure enthalpies and thermal transitions of the gel systems. Screw-top ‘closed batch cells’ were used, and filled with 650 +/- 5 mg of a fluid gel. Reference cells were filled with an equal mass of deionised water.

The samples were held isothermally at 5 °C for the first 30 mins, followed by heating to 90 °C (step 1) and then cooling to 5 °C (step 2). The sample was held isothermally for 30 mins at 5 °C, to ensure sample uniformity, followed by heating to 90 °C (step 3) and then cooling to 5 °C (step 4) (schematic representation shown in Figure 4.1). All temperature transitions were at a rate of 1.2 °C/ min. Transitions and enthalpies are calculated from an average of three repeats.

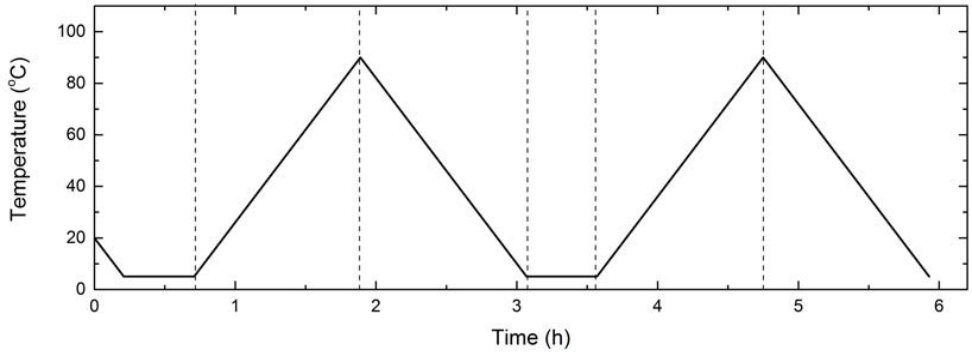

Figure 4.1 – Schematic representation of the Differential Scanning Calorimetry (DSC) temperature profile used. Temperature ramps were conducted at 1.2 °C/min.

4.3 Results and discussion

4.3.1 Single polymer fluid gels

Initially, the formation mechanism and rheological properties of low acyl gellan and kappa carrageenan fluid gels were investigated. Figure 4.2 shows the viscosity profiles on cooling through the ordering and gelation transitions for 1% low acyl gellan and 1% kappa carrageenan at three different shear rates (200 s^{-1}, 300 s^{-1} and 500 s^{-1}). As the temperature is decreased (at all shear rates), both

gellan and kappa carrageenan show a small increase in shear viscosity, until a rapid ordering process occurs, resulting in a sharp increase in shear viscosity. The onset is known as the temperature of ordering (T_{ord}). As the shear rate was increased, the final shear viscosity (as measured at 5 ^{o}C) of the fluid gel decreased. Higher shear rate for production suggests that more discrete particles were produced, as particles are unable to aggregate. It was previously suggested that an applied shear rate affects the particle shape and size (Garrec and Norton, 2012), and not the internal structure of the fluid gel particles. The observed T_{ord} appears unaffected by the applied shear rate (Figure 4.2a and 4.2b), suggesting that the internal nature of both the gellan and the kappa carrageenan particles are unaffected by shear.

As can be seen in Figure 4.2b, the increase in viscosity peaked at 17 ^{o}C and then decreased as the temperature was lowered further. The decrease in viscosity below 17 ^{o}C was probably a consequence of the larger gel particles breaking up due to the applied shear forces. The subsequent increase in viscosity at about 5 ^{o}C occurred as the strength of particles became sufficiently high to resist further breakup at the applied forces.

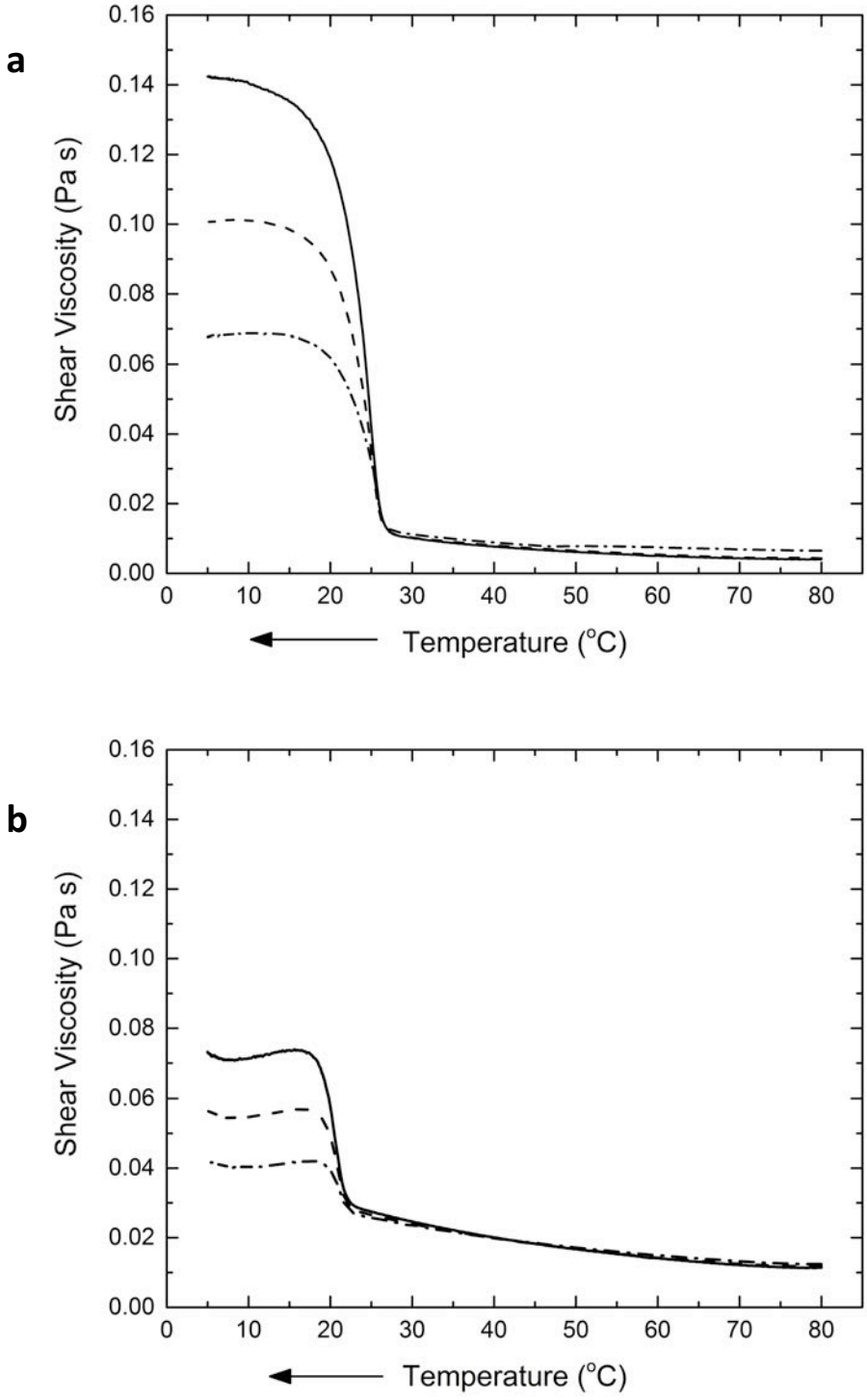

Figure 4.2 – Fluid gel production: viscosity profiles of 1% low acyl gellan (a) and 1% κC (b) during sheared cooling at 2 °C/min. Data is shown as a function of shear rate: 200 s^{-1} (——), 300 s^{-1} (- -) and 500 s^{-1} (–·–).

The influence of hydrocolloid concentration on gellan and kappa carrageenan fluid gels was investigated at a shear rate of 500 s^{-1} (Figure 4.3). As expected, the end viscosity of the fluid gel increased as the concentration of the polymer system increased. Additionally, as the concentration of gellan and kappa carrageenan increased, the onset of gelation also increased. This could be explained either by the increase in polymer concentration, or by increased salt concentration as a consequence of the ions present in the hydrocolloid powders used (Table 4.1 in Materials section).

It is well known that the addition of salt induces the ordering of carrageenan chains and their subsequent aggregation, resulting in a higher onset temperature than when no salts are added (Dai et al., 2010). As no extra ions (bridging/cross-linking agents) had been added for the studies here, the fluid gels produced exhibited lower viscosities and were weaker gels than previously described (Garrec and Norton, 2012). Additionally, the onset of gelation is salt dependent (Garrec and Norton, 2012) and as such onset was noted at a relatively low temperature, which was in line with the expected temperature for the ion content present.

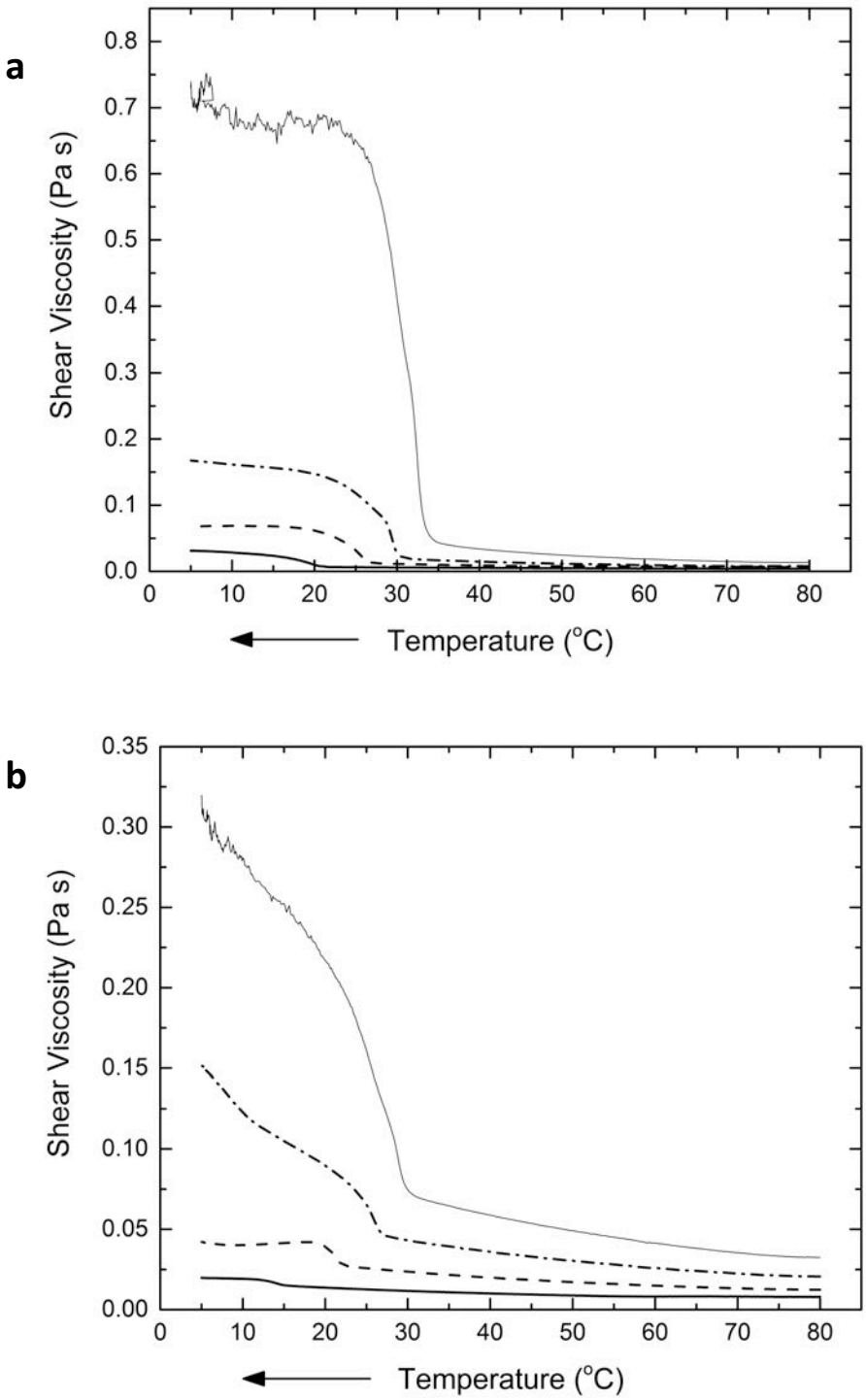

Figure 4.3 - Fluid gel production: viscosity profiles of low acyl gellan (a) and κC (b) during sheared cooling at 2 °C/min, at 500 s^{-1}. Data is shown as a function of concentration: 0.5% (—), 1% (- -), 1.5% (-·-) and 2% (—).

In order to understand how the fluid gel properties changed on storage, the viscosity of the fluid gels produced with gellan and kappa carrageenan was measured after 24 hours storage post production (Figure 4.4). The samples were stored and measured at room temperature (25 ^{o}C). As can be seen, the samples were all highly shear thinning as would be expected for a particulate system, and the viscosities of both the gellan and kappa carrageenan fluid gels increased after 24 hours compared with the final viscosity during production. Furthermore, all the fluid gels exhibited similar viscosity profiles after 24 hours, irrespective of the shear rate during production. This suggests that further particle/particle interaction, or particle hardening, had occurred during the 24 hours between production and testing. As can be seen from Figure 4.4, the viscosity profiles of both gellan and kappa carrageenan fluid gels were very similar, suggesting that the gel strength of the individual particles and phase volume of the fluid gels are similar.

The yield stress for all the fluid gels after 24 hours have the same shear viscosity (Figure 4.5), within the error bounds. Therefore, the bridging, or stickiness, of the particles is the same on storage, regardless of the shear rate used for production (between 200 s^{-1} and 500 s^{-1}). Error bars are larger for samples made at 200 s^{-1} than the higher shear rates of production, suggesting that while the bridging between the particles may be similar, lower shear rate for production results in larger and more irregular shaped particles than particles produced at higher shear rates.

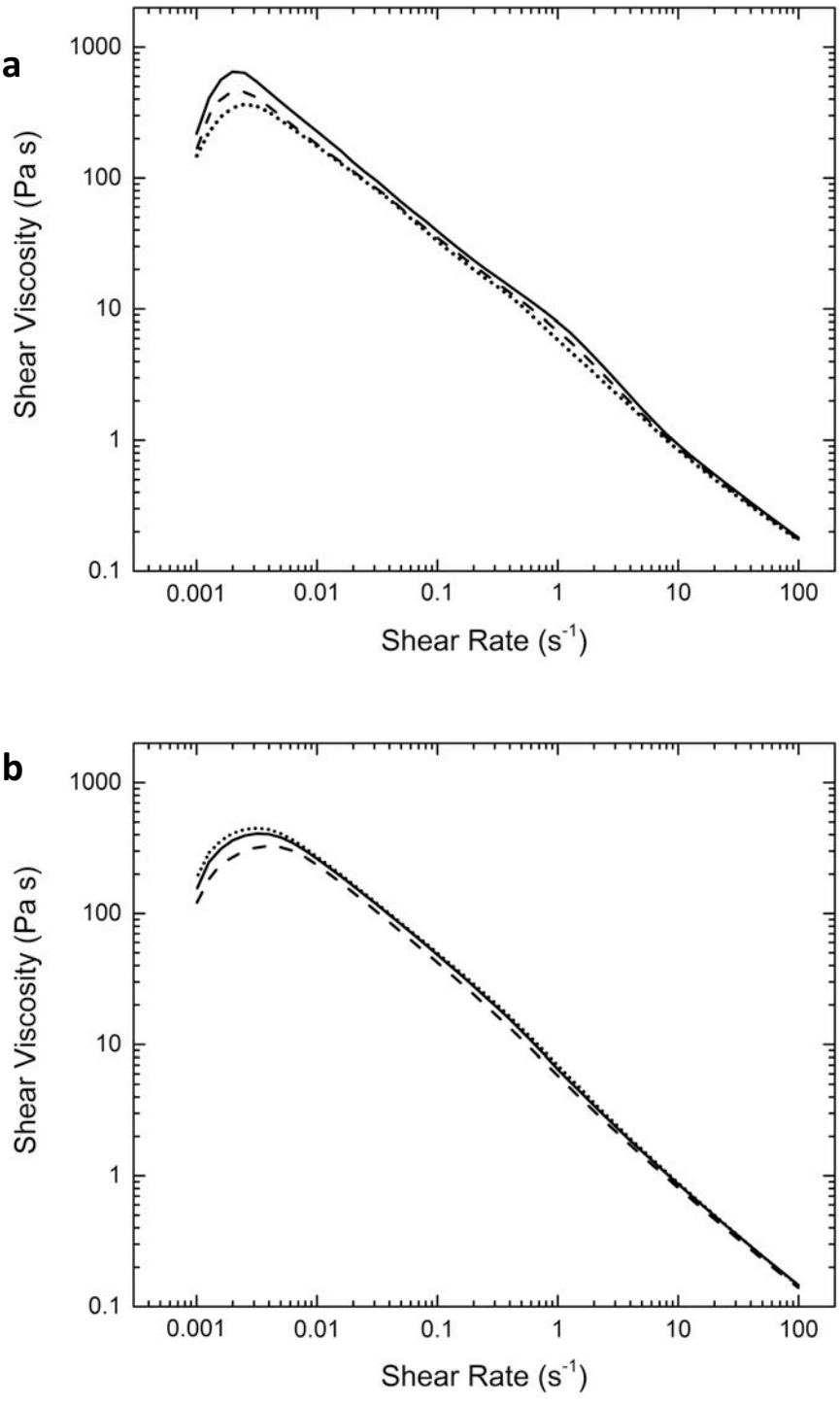

Figure 4.4 - Viscosity profiles of low acyl gellan (a) and κC (b) fluid gels, 24 hours after production. Data is shown as a function of shear rate: 200 s^{-1} (——), 300 s^{-1} (- -) and 500 s^{-1} (–·–).

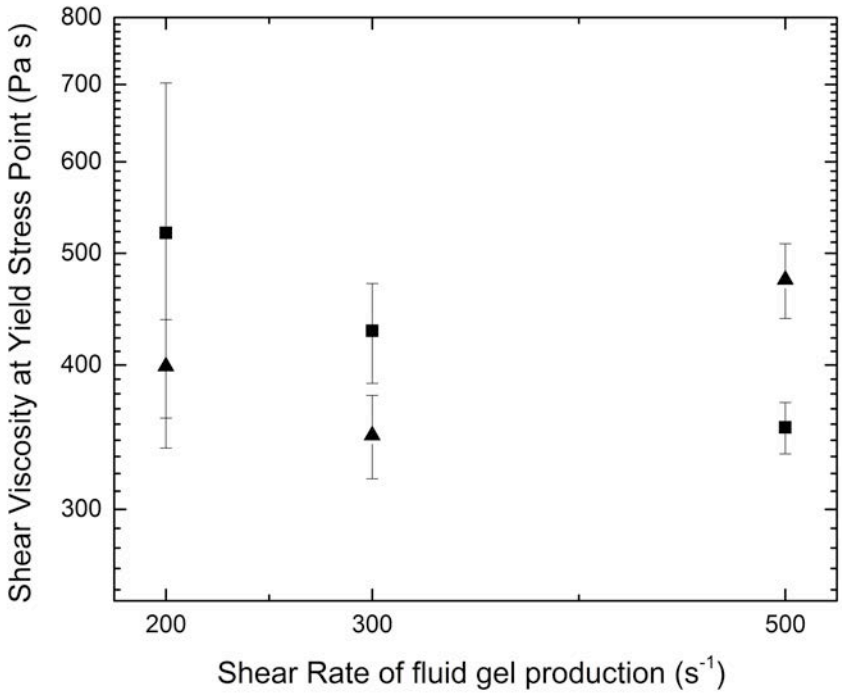

Figure 4.5 – shear viscosity of gellan (■) and kappa carrageenan (▲) fluid gels at the yield point (24 hours after production).

In order to test whether particle/particle interaction was occurring on storage, oscillatory studies were carried out for the 12 hours immediately after fluid gel production for the 1% kappa carrageenan and 1% gellan samples produced at a shear rate of 200 s^{-1} (Figure 4.6). As can be seen, the gellan elastic modulus increases (G' increasing from ~8 to almost 30 Pa), but no increase was observed for kappa carrageenan. As G' was above G'' for both samples, the materials were weak gels. The weak gel behaviour was further demonstrated at low shear rates (see Figure 4.4), as initially there appeared to be shear thickening. As the shear was increased, however, the samples yielded and then showed shear thinning

behaviour. These results suggested that there was particle bridging in the samples and that this occurred to a greater extent for the gellan sample. Gabriele *et al*. (2009) showed an increase in storage modulus (G') in the two hour period after fluid gel production for kappa carrageenan, which they explained as a result of helix annealing and further aggregation. This was not seen in this study, suggesting that the samples produced here were sheared to temperatures well below the coil to helix transition such that almost complete ordering occurred during the shearing process. Thus there is no further ordering possible between particles.

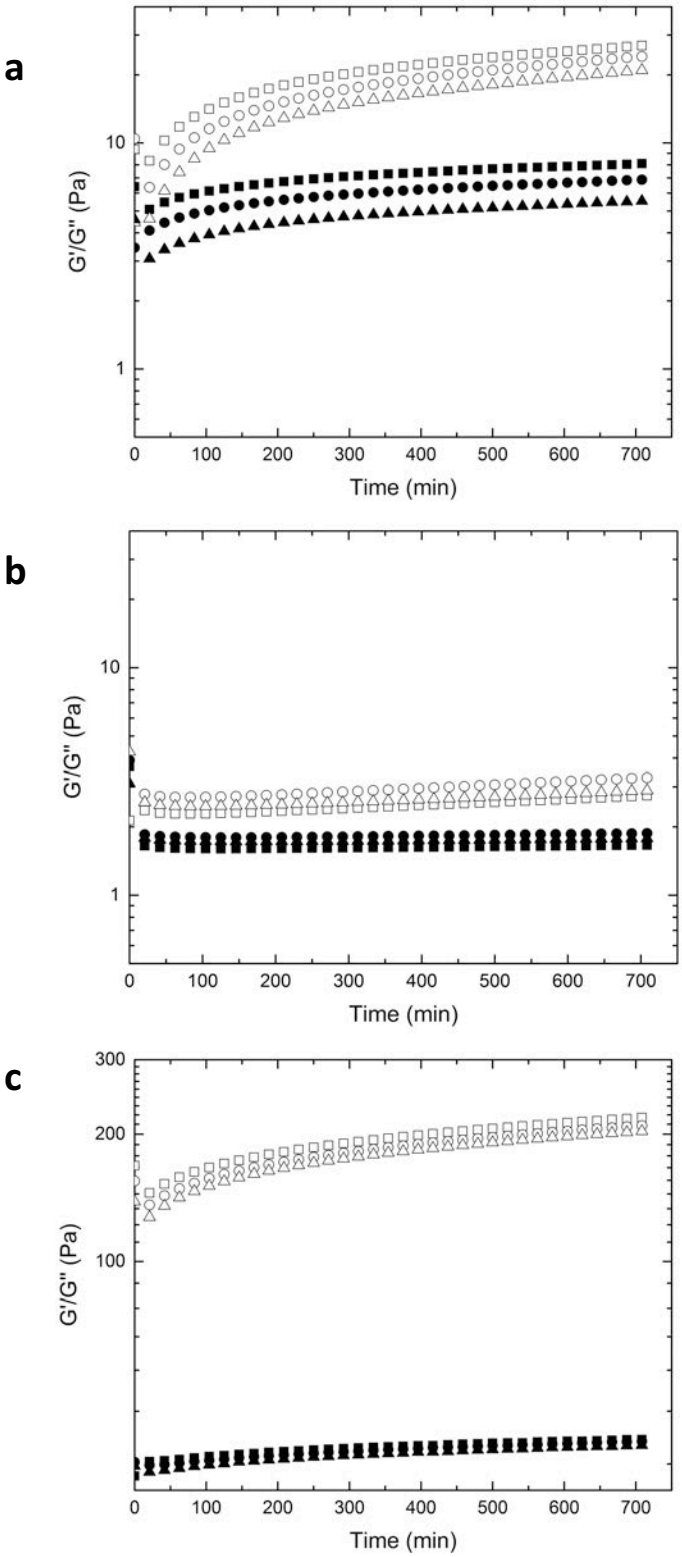

Figure 4.6 – 12 hour oscillation immediately after fluid gel production of 1% gellan (a), 1% kappa carrageenan (b) and 1% gellan, 1% kappa carrageenan (c). Fluid gels were produced at 200 s^{-1} (□/■), 300 s^{-1} (○/●) and 500 s^{-1} (△/ ▲). Open symbols are G', and filled symbols are G''.

4.3.2 Mixed polymer fluid gels

The formation mechanism and rheological properties of mixed low acyl gellan and kappa carrageenan fluid gels were investigated. Figure 4.7 shows the viscosity profile on cooling 0.5% gellan on its own and then in the presence of 0.5, 1.0 and 1.5% kappa carrageenan. As can be seen, the addition of kappa carrageenan increased the overall viscosity of the fluid gel and increased the onset temperature for the viscosity increase (from about 21 ^{o}C to about 34 ^{o}C).

At kappa carrageenan concentrations of 1% and 1.5%, the profile exhibited a two-step process with the onset temperature at 34 ^{o}C and a second step (a shoulder) at 30 ^{o}C. The presence of the shoulder suggested that there was separate gelation occurring within the mixed system, and it was unlikely that the two polymers formed a combined network. As the onset of gelation of gellan occurred before kappa carrageenan when in single polymer systems, it would suggest that the initial step was the gelation of gellan and the shoulder was due to the gelation of kappa carrageenan. This was investigated by DSC and will be discussed more fully in the next section.

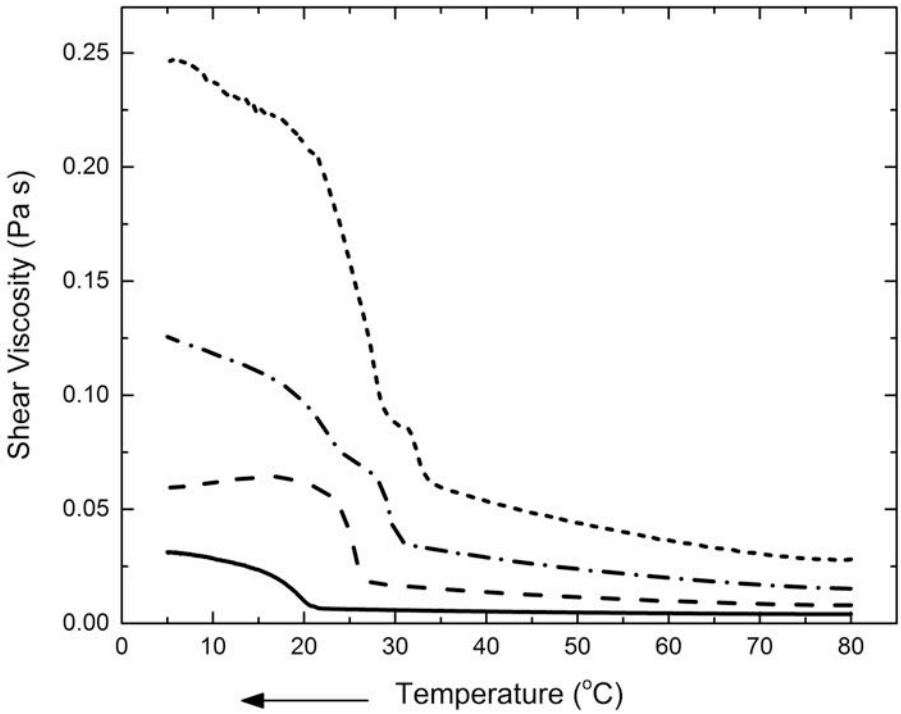

Figure 4.7 - Fluid gel production: viscosity profiles of 0.5% low acyl gellan (——), and 0.5% low acyl gellan with increasing concentrations of κC (0.5% (– –), 1% (–·–), and 1.5% (----)) during sheared cooling at 2 °C/min. Fluid gels produced at 500 s^{-1}.

On increasing the concentration of gellan to 1% (Figure 4.8), the addition of kappa carrageenan resulted in the fluid gel having a higher final viscosity (at 5 °C) and at 1% kappa carrageenan the process had two steps with the onset temperature and temperature of the shoulder being very similar to those observed at 0.5% gellan (Figure 4.7). A small shoulder was seen when the kappa carrageenan concentration was 0.5% (Figure 4.8); however, this was not defined enough to establish if this is due to separate gelation occurring, or if this is a degree of noise on the data.

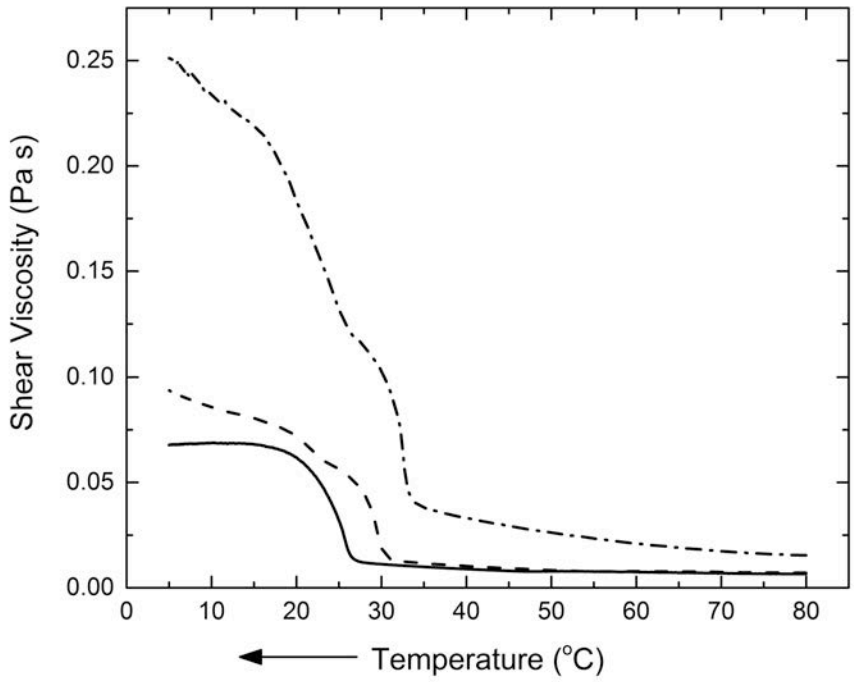

Figure 4.8 - Fluid gel production: viscosity profiles of 1% low acyl gellan (—), and 1% low acyl gellan with increasing concentrations of κC (0.5% (– –) and 1% (– · –)) during sheared cooling at 2 °C/min.

On increasing the gellan concentration to 1.5% (Figure 4.9), with 0.5% kappa carrageenan, no shoulder was observed in the viscosity during cooling. This could be due to the gelation of the two polymers occurring simultaneously. Considering the temperature profile obtained for the single component systems, the shearing process was started at temperatures well above the gelation of either component, and probably above the phase separation temperature, so at lower gellan concentrations the gellan forms fluid gel particles first, with kappa carrageenan being forced to form fluid gel particles within the gellan structure or within any remaining unstructured water which existed between the gellan fluid

gel particles. An alternative theory is that phase separation occurred on cooling before gelation and fluid gel formation. If this was the case, then a mixture of gellan fluid gel particles and kappa carrageenan fluid gel particles would be formed. However, when the gelation occurs at very similar temperatures, it is likely that phase separation and fluid gel formation are occurring at the same time, meaning that there is a possibility of being able to produce fluid gel particles which contain both polymers.

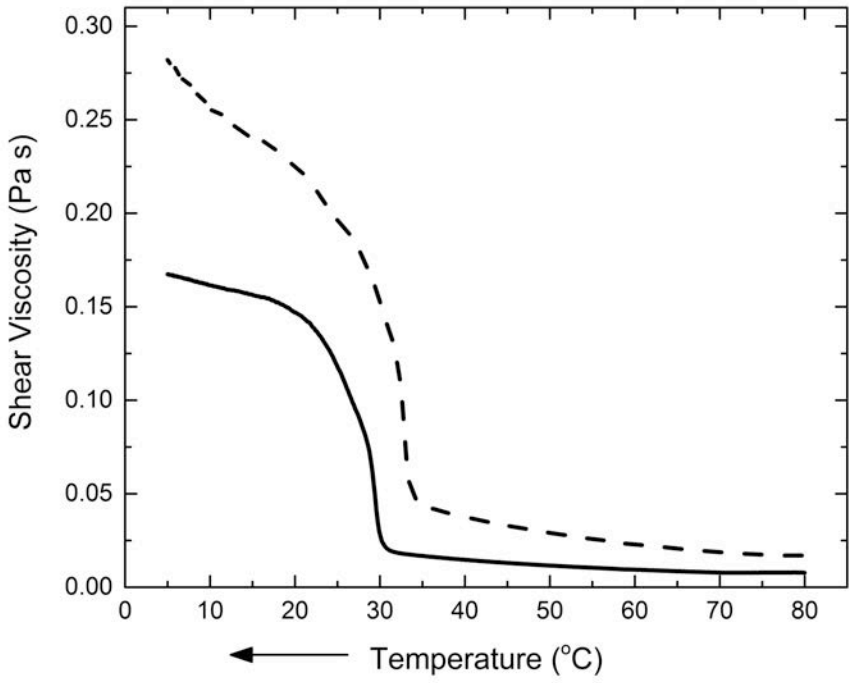

Figure 4.9 - Fluid gel production: viscosity profiles of 1.5% low acyl gellan (—), and 1.5% low acyl gellan with 0.5% κC (– –), during sheared cooling at 2 °C/min.

It was observed that when the overall concentration of the system was kept at 2%, with different ratios of each polymer, that the final viscosity of production

was approximately 0.25 Pa s (Figures 4.7, 4.8 and 4.9). This suggests that the bulk properties of the fluid gel at this stage were dependent on phase volume of the particles regardless of internal morphology of the particles. It is also interesting to note that this end viscosity is in the same region as 2% kappa carrageenan in a single system, but lower than observed for the 2% gellan i.e. 0.7 Pa s. Therefore, further examination was needed to determine why it appears that the end viscosities were dictated by phase volume, and more closely match the behaviour of kappa carrageenan than the gellan. Viscosities of the fluid gels were examined after 24 hours, giving time for any particle aggregation to occur (Figure 4.10). All mixed polymer concentrations show similar viscosity profiles to the single polymer systems; however, these do align more with the kappa carrageenan behaviour. It was previously hypothesised that gellan was forming gel particles first, with kappa carrageenan particles forming in the remaining unstructured water. As the viscosities of mixtures (after 24 hours) were more similar to kappa carrageenan, this suggested that the bulk properties were more influenced by how the remaining water is structured in the secondary gelation, rather than the internal morphology of the particles.

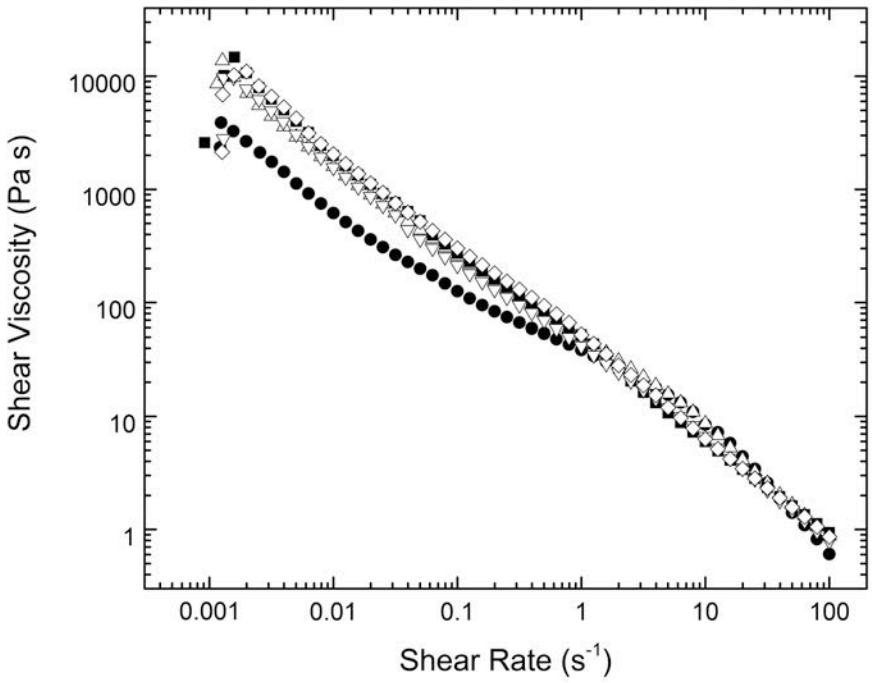

Figure 4.10 - Viscosity profiles of 2% low acyl gellan (●) and 2% κC (■) fluid gels, compared with fluid gels with different ratios of the two polymers, with concentrations remaining at 2% (0.5% gellan with 1.5% κC (△), 1% gellan with 1% κC (▽), 1.5% gellan with 0.5% κC (◇)).

Differential scanning calorimetry was used to determine the melting and setting temperatures of the gellan and kappa carrageenan on their own, and when mixed. Figure 4.11a shows the heating endotherm and Figure 4.11b shows the cooling exotherm obtained for gellan. The sample loaded into the cell was a fluid gel, thus the first heating cycle temperature and enthalpy are for the fluid gel with subsequent heating cycles and all cooling cycles are for quiescent gels. As can be seen, there was a single endotherm for all heating cycles and the peak area was, within experimental error, the same for both the quiescent gel and the fluid gel. The melting and setting temperatures were both approximately 27 ^{o}C, showing that there was no hysteresis in the gellan ordering process. However, the endotherm and exotherm peaks for low acyl gellan should be equal, which is not the case (Table 4.2). The heating enthalpy obtained from integrating the area under the peak is 3.4 J/g of gellan, whilst the cooling peak gives an enthalpy of 9.9 J/g. This discrepancy was a consequence the melting temperature being close to the starting temperature of the scan 5 ^{o}C, so that the start-up transient in the calorimeter was overlaying the start of melting peak. This means we can use the data to obtain the melting temperature, but we cannot use the heating curve to determine the enthalpy of melting. The cooling curve doesn't suffer from this problem so the enthalpy of the transition can be determined from the peak.

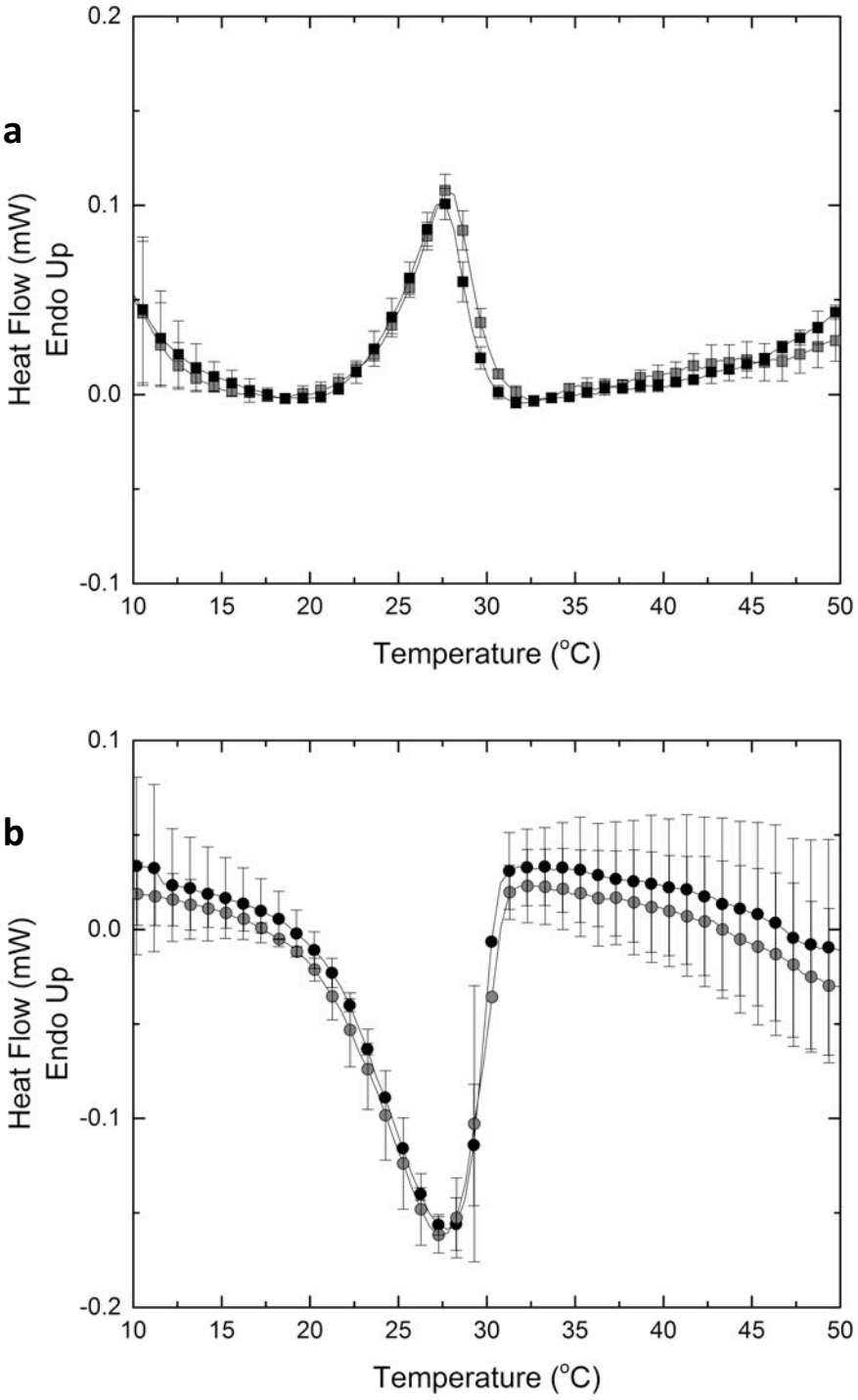

Figure 4.11 - DSC heating (a) and cooling (b) profiles of 1% low acyl gellan. The first heating scan (step 1(■)) shows melting of a fluid gel; the second heating scan (step 3 (▣)) shows the melting of a quiescent gel; step 3 (●) and step 4 (◉) show formation of a quiescent gel and any hysteresis affects.

Figure 4.12a shows the heating endotherm and Figure 4.12b shows the cooling exotherm obtained for 1% kappa carrageenan. Again, the sample loaded into the cell was fluid gel, so the first heating cycle temperature and enthalpy are for the fluid gel, while subsequent heating cycles and all cooling cycles were for quiescent gels. As can be seen in Figure 4.12a, the first scan (heating of the fluid gel) gives an endothermic peak with a melting temperature of approximately 33 ^{o}C and a very small peak at about 20 ^{o}C. Subsequent heating curves (melting of the quiescent gel) show a major peak at approximately 32 ^{o}C and a smaller peak (shoulder) at approximately 23 ^{o}C, which was not present in the melting of a fluid gel. The ratio of peak area for the shoulder in relation to the major peak is proportional to the quantity of iota carrageenan, present in commercial kappa carrageenan powders. Therefore, it appears that the shear applied in fluid gel production has caused the iota carrageenan to be entrapped within the same structure as the kappa carrageenan. When no shear is applied, the carrageenans preferentially phase separate resulting in the two peaks.

On cooling the kappa carrageenan sample, there was a single exothermic peak at approximately 23 ^{o}C. As expected, integration of the heating and cooling peaks (Table 4.2) shows that the transition enthalpy (within experimental error) is the same for the fluid gel and the quiescent gel and that there was no difference between heating and cooling enthalpies. This indicates that the helix structure and extent of helix formation are the same under shear as they are when carried out quiescently. As previously reported (Norton et al., 1983), the hysteresis

between melting and setting temperatures is due to the aggregates stabilising the helix form of kappa carrageenan.

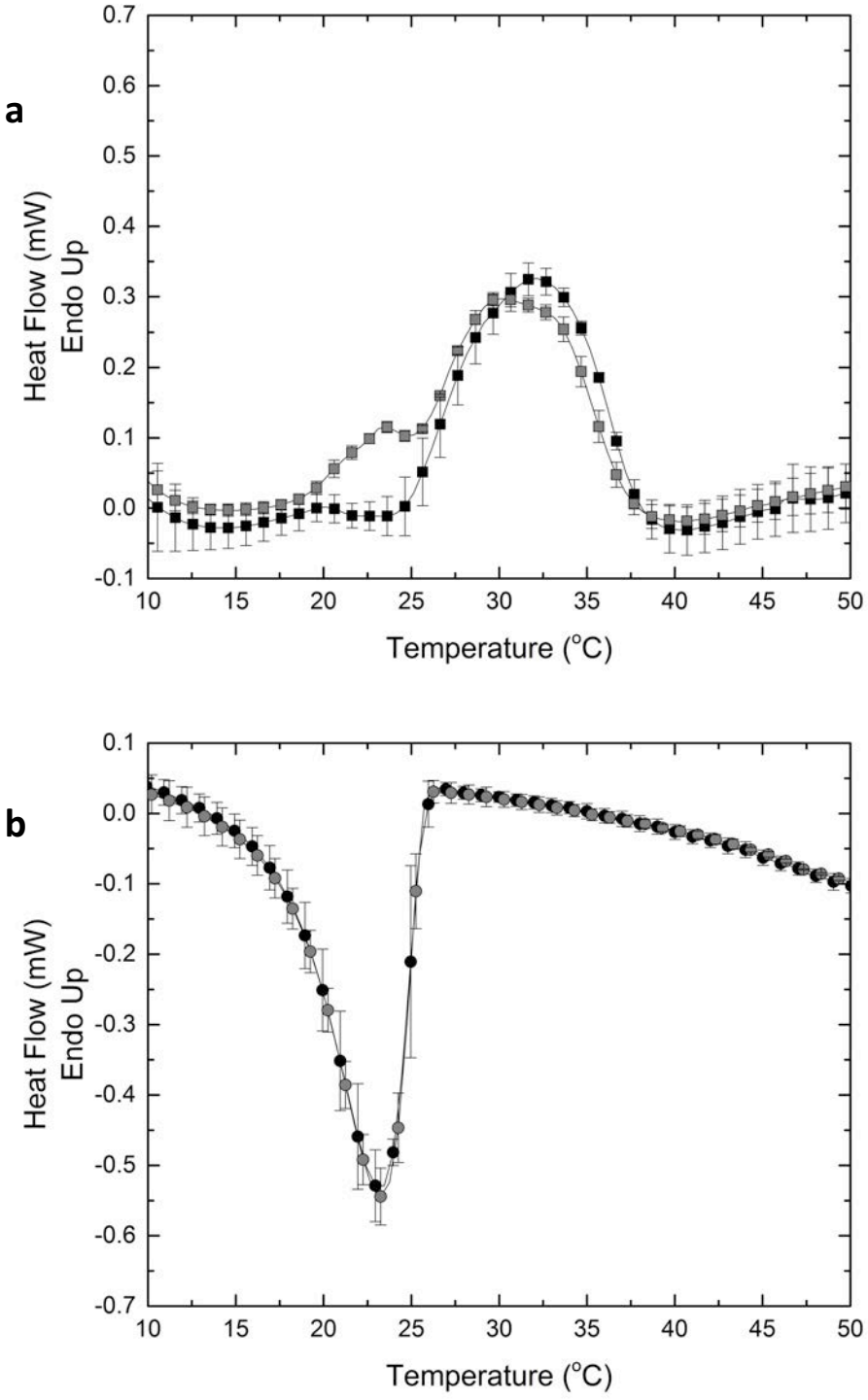

Figure 4.12 - DSC heating (a) and cooling (b) profiles of 1% κC. The first heating scan (step 1(■)) shows melting of a fluid gel; the second heating scan (step 3 (▣)) shows the melting of a quiescent gel; step 3 (●) and step 4 (◍) show formation of a quiescent gel and any hysteresis affects.

During cooling of gellan/kappa carrageenan mixtures, two distinct peaks were observed (Figure 4.13b). The smaller peak at 35 ^{o}C has an area which was consistent with the gellan peak observed in Figure 4.10b and the second larger peak at 27 ^{o}C has an area which was consistent with the gelation of kappa carrageenan. The temperatures of the peaks have shifted to slightly higher temperature, 35 ^{o}C compared with 27 ^{o}C for the gellan and 27 ^{o}C compared with 23 ^{o}C for the kappa carrageenan. This was expected as a consequence of the overall concentration of the polymers and ions in the mixed system. The size of the peaks confirms that the gelation temperatures were assigned correctly in the viscosity study and allowed the identification of the different processes in the viscosity profiles on cooling the mixtures (Figures 4.7 and 4.8). Integration of the cooling curves gives a combined enthalpy of ~ 40 J for the 2 g of sample present in the sample. This was somewhat higher than the addition of the peaks obtained for the gellan and kappa carrageenan obtained on their own (~ 34 J). As discussed earlier, there is an increase in the ordering temperatures as a consequence of the increased effective concentration of the polymers. This increase in enthalpy is also probably caused by the effective concentration of the hydrocolloids increasing in the mixed (phase separated) system.

On heating the gellan/ kappa carrageenan mixtures (Figure 4.13a), a broad peak is observed which shows multiple transitions. Again, as the lower temperature transition (the gellan melting) is occurring at temperatures close to the scan start temperature, the starting transient of the calorimeter is affecting the peak area and shape, resulting in smaller enthalpies than expected (Table 4.2). The overall

features of the peak, however, are consistent with the peaks observed for the single polymer systems. As can be seen, there was a smaller peak at about 32.5 ^{o}C, which is the melting of the low acyl gellan gel. This is then followed by a larger peak at about 41 ^{o}C, which is shifted to slightly lower temperatures, and has a lower maximum for the quiescent gel structure than for the fluid gel. On comparing the smaller peak (the shoulder), it seems as if the area of this peak is increased somewhat when compared with 1% gellan in a single system (Figure 4.11). As discussed earlier, the effective concentration of hydrocolloids have increased in the mixed system due to the phase separation, so the increased size of the peak is to be expected.

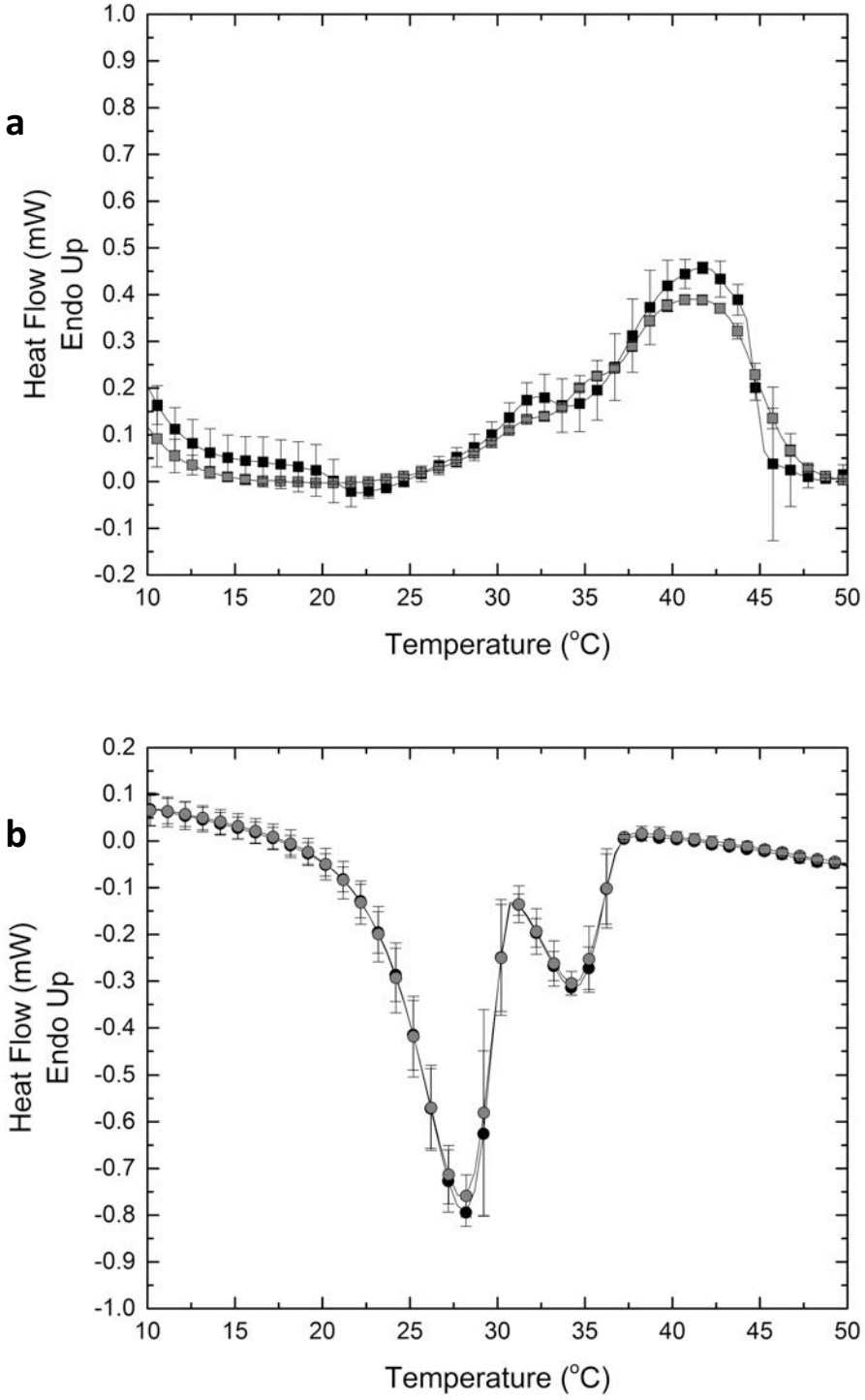

Figure 4.13 - DSC heating (a) and cooling (b) profiles of 1% low acyl gellan 1% κC. The first heating scan (step 1(■)) shows melting of a fluid gel; the second heating scan (step 3 (▣)) shows the melting of a quiescent gel; step 3 (●) and step 4 (◉) show formation of a quiescent gel and any hysteresis affects.

Table 4.3 - Enthalpies of melting and conformational ordering of 1% gellan, 1% κC and a mixture of 1% gellan with 1% Kappa carrageenan from the micro differential scanning calorimetry. All values are the mean from 3 repeats.

	Step 1 (Melting of Fluid gel)	Step 2 (Quiescent gel formation)	Step 3 (Melt of Quiescent gel)	Step 4 (Quiescent gel formation)
gellan	3.4 J/g	9.9 J/g	3.8 J/g	9.6 J/g
κC	22.9 J/g	25.4 J/g	25.4 J/g	23.7 J/g
gellan κC mixture	16.4 J/g (32.7 J/ 2g)	19.8J/g (39.6 J/ 2g)	15.4 J/g (30.7 J/ 2g)	20.0 J/g (40.0 J/ 2g)

4.4 Conclusions

Both gellan and kappa carrageenan produced fluid gels by applying shear during the setting with no additional crosslinking cations added to the system. These fluid gels had lower onset temperatures than previous reports in the literature due to the low concentrations of cations inducing gelation. Further ordering of the gellan fluid gels was found to occur after production, causing some crosslinking between the particles. This was not observed for the kappa carrageenan.

When the gellan and kappa carrageenan were mixed, fluid gels were formed with a two-step gelation profile. Differential scanning calorimetry (DSC) confirmed that the first polymer to form fluid gel particles was gellan, with the

second gelation attributing to the formation of kappa carrageenan particles. However, the phase volume, rather than the ratio of the two polymers determined the viscosity of the mixtures.

A small quantity of an iota carrageenan impurity was found to be trapped in the kappa carrageenan structure by the shear forces during gelation. These forms of carrageenan phase separate when quiescently cooled.

Finally, when the gelation of the two polymers occurred simultaneously, there is no evidence of the fluid gel particles being mixed, although further investigation would be interesting.

Chapter 5.

WARM (30 ^{O}C) HYDRATION OF POTASSIUM KAPPA CARRAGEENAN AND ITS INCLUSION IN EMULSIONS AND COMPLEX EMULSIONS

5.1 Background

As discussed in Chapter 4, fluid gels are of interest in the fields of bioengineering and wound healing because they can be structured to spread easily, but will then thicken once the spreading has ceased, giving protection to the area that they are applied to. However, fluid gels need to be produced from a solution of the polymer which is in a disordered state before shearing is carried out, as fluid gels are produced by disrupting gelation on ordering/cooling. Typical routes for forming fluid gels are not ideal for delivery of cells, because cells are both temperature and shear sensitive (Croughan et al., 1989, Smith et al., 1987) and drugs are often temperature sensitive (Qiu and Park, 2012). As such, alternative processing is needed if fluid gels are to be used for these applications.

This chapter explores an alternative method for structuring flowable materials. The alternative method requires the dispersion of potassium kappa carrageenan in warm water. The kappa carrageenan structure was then used within single and double emulsions, to determine how the hydrocolloid affected the structuring. The formation of duplex emulsions was studied as skin creams require a water continuous system.

5.2 Materials and Methods

5.2.1 Materials

Kappa carrageenan (Sigma-Aldrich Company Ltd., UK) with a 3.6% K^+ content, a 0.4% Na^+ content and a 0.005% Ca^{2+} content (of the dry powder) was used (data shown in Chapter 4). Distilled, deionised water, and 4-(2-Hydroxyethyl) piperazine-1-ethanesulfonic acid (HEPES) buffer (Sigma-Aldrich Company Ltd., UK) were used as the aqueous phases for dispersion and swelling of the kappa carrageenan, with no further ions added.

Dulbecco's Modified Eagle Medium (DMEM) buffer (Sigma-Aldrich Company Ltd., UK) was supplemented with 10% foetal bovine serum (FBS), 2.5% HEPES, 2.5% L-Glutamine and 1% penicillin streptomycin (pen strep). All samples of DMEM buffer were supplemented, and therefore will be known simply as DMEM for the rest of this chapter.

Paraffin oil (Sigma-Aldrich Company Ltd., UK) was used for the formation of emulsions. Span 80 (sorbitan monooleate) (Sigma-Aldrich Company Ltd., UK) and PGPR (polyglycerol polyricinoleate) (Palsgaard A/S, Denmark) were investigated for stabilising the initial water in oil emulsions (W_1/O), with Tween 20 (polyoxyethylene sorbitan monolaurate) and Tween 80 (Sigma-Aldrich Company Ltd., UK) used to stabilise the second interface when duplex ($W_1/O/W_2$) emulsions were investigated.

All concentrations were calculated by weight to weight (w/w). Unless otherwise stated, materials were used with no further purification.

5.2.2 Formation of kappa carrageenan samples

All samples were prepared using a Kinexus rheometer (Malvern Instruments, UK), with cup and vane geometry. The temperature for all stages of preparations were held at 30 ^{o}C, with a single shear rate of 500 s^{-1} used. All results shown are an average of three repeats, and error bars shown are one standard deviation.

5.2.2.1 Formation of Kappa carrageenan in water and buffers

For the formation of the gel phase, the appropriate amount of buffer was added to the rheometer cup. The kappa carrageenan powder was added directly into the cup, and the sequence of a single shear rate was started immediately, to try and avoid polymer clumping. Sequences were run for 30 minutes, or until a plateau in viscosity occurred. A range of kappa carrageenan concentrations (1% - 8%) in water, HEPES buffer and DMEM buffer were investigated.

5.2.2.2 Formation of primary emulsions

For the formation of the primary emulsion phase, the appropriate amount of paraffin oil and emulsifier was added to the rheometer cup. The appropriate amount of the gel phase was then added directly to the cup, and a single shear rate sequence was started immediately. The rheometer sequences were run for 30 minutes.

PGPR and Span 80 were investigated for the stabilisation of the primary emulsions.

5.2.2.3 Formation of secondary emulsions

For the formation of secondary emulsions, the appropriate amount of water and emulsifier was added to the rheometer cup. The appropriate amount of the primary emulsion was then added directly to the cup, and a single shear rate sequence was started immediately. Sequences were run for 30 minutes.

For secondary emulsions, two different emulsifiers, Tween 20 and Tween 80, were investigated.

5.2.3 Sample measurements

All samples were analysed between 24 hours and 36 hours after production.

5.2.3.1 Rheology

A Kinexus rheometer (Malvern Instruments, UK) was used to analyse the rheological properties of all samples produced. Using a cone and plate (4° cone angle, 40 mm diameter), oscillatory tests were carried out, using a stress controlled amplitude sweep (from 0.01% strain to 10% strain).

5.2.3.2 Differential Scanning Calorimetry (DSC)

Enthalpies and temperatures of thermal transitions were determined for the gel phase using a μDSC evo Dynamic Scanning Calorimeter (DSC) (Setaram Instrumentation, France). Screw-top 'closed batch cells' were used, and filled with 650 +/- 5 mg of a fluid gel. Reference cells were filled with an equal mass of deionised water. The samples were held isothermally at 5 ^{o}C for the first 30 minutes, followed by heating to 90 ^{o}C (step 1) and then cooling to 5 ^{o}C (step 2). All temperature transitions were at a rate of 1.2 ^{o}C / min. (Schematic representation is shown in Figure 5.1).

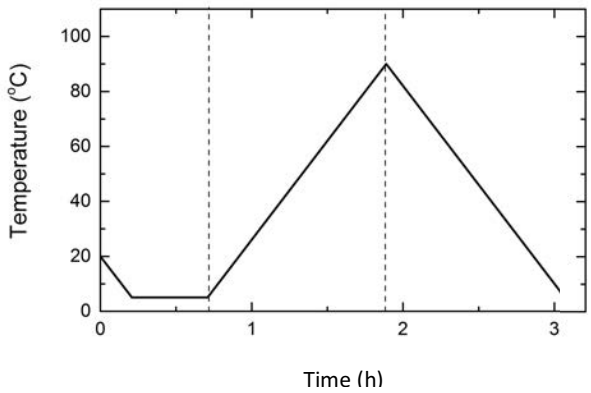

Figure 5.1 - Schematic representation of the Differential Scanning Calorimetry (DSC) temperature profile used. Temperature ramps were conducted at 1.2 °C/min

5.2.3.3 Mastersizer

Once the primary emulsion was formed, particle sizing was investigated using a mastersizer (Malvern Instruments Ltd., Worcestershire, England), with a Hydro SM manual small volume sample dispersion unit attached. The mastersizer was used to establish the diameter of the particles in micrometres. Paraffin oil was

used as the dispersed phase in the mastersizer, and the relevant refractive index for paraffin oil (1.475) was used. Values quoted in this chapter are of the peak maximum, or mode value, from the mastersizer, with the results an average of 6 readings.

5.2.3.4 Microscopy

Once the double emulsions were formed, light microscopy (Brunel SP300-fl, Brunel Microscopes Ltd.) was used for particle imaging. The size of double emulsions were determined by imaging immediately after production. Images were taken with a SLR camera (Canon EOS Rebel XS, DS126 191) fitted to the microscope. Images were processed using Image J.

5.3 Results and Discussion

5.3.1 Hydration and swelling of kappa carrageenan in water and HEPES and DMEM buffer

Dissolution of kappa carrageenan (1% κC in water) in water (with no added cations) resulted in a hydration curve (Figure 5.2), with an initial decrease in viscosity followed by a slow increase over the next 60 minutes. The initial reduction in viscosity was a consequence of the experiment protocol, whereby the carrageenan powder was added to the vane cup and then the vane was

switched on at a shear rate of 500 s^{-1}. Thus the powder initially started to hydrate and interact, but was rapidly disrupted by the applied shear once the vane was rotating. At a concentration of 2%, the kappa carrageenan powder added to the water was not dispersed properly as the initial structuring occurred rapidly; this resulted in the presence of residual unhydrated powder that remained in the bottom of the sample cup. This was thought to be as a consequence of too rapid hydration of the powder at the surface of the particles, which are then not disrupted by the shear applied. As the interest in this study was to investigate the formation of fluid gel-like properties from kappa carrageenan in the presence of buffers for cell cultures, attempts to investigate this problem further were not made.

Understanding the effect of buffer on the formation of kappa carrageenan hydrated particle gels was required, as both the HEPES and DMEM buffer contain ions which could affect swelling and hydration. Figure 5.2 compares the time dependent viscosity increase for kappa carrageenan in water at 2% kappa carrageenan in HEPES and DMEM buffers. It should be noted that the hydration and structuring are expected to be different, as potassium kappa carrageenan is unable to dissolve and form a gel without the temperature being increased to above the gel melting temperature (above 50 ^{o}C for the sample used here, see DSC curves reported later). The presence of ions in the buffers slow down the hydration of kappa carrageenan and potentially allow the swelling and hydration to occur more evenly, resulting in more consistent paste structures. Thus this approach may potentially be used as an alternative to high temperatures,

allowing the addition of cells or pharmaceutical ingredients, which would remain unaffected by the process.

As can be seen in Figure 5.2, when kappa carrageenan was dispersed in the buffers at 2% concentration, there was still an initial decrease in viscosity at the start of the application of shearing, but then there was no increase in viscosity over the 60 minute period. Unlike the results obtained for dispersion in water, no hydration or structuring was observed, and thus the resultant mixture could at this time be described as a thin viscous fluid, rather than a particulate/fluid gel. The presence of ions within the buffer is therefore hindering and slowing the hydration process of the kappa carrageenan. The presence of the ions could potentially reduce the ability of the powder to hydrate and so reduce the overall rheological properties. This was checked by DSC, as discussed later in the chapter.

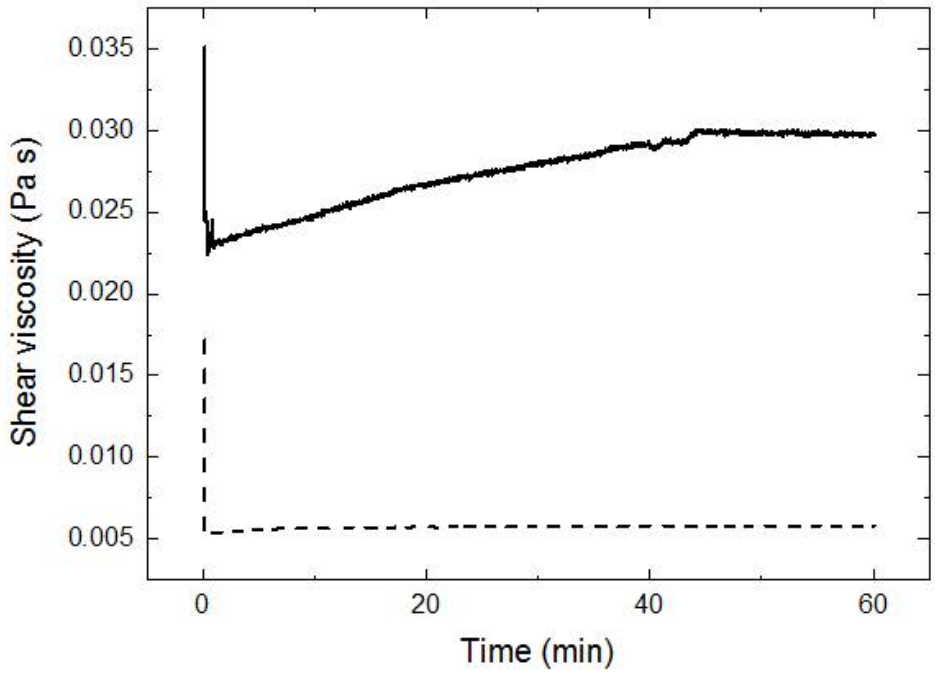

Figure 5.2 - Viscosity of 1% κC (solid line) dispersed in water versus 2% κC (dash line) dispersed in HEPES buffer. Dispersions formed at 500s^{-1}, with temperature held at 30 °C.

To determine whether hydration and structuring could be induced within the buffer systems, the concentration of kappa carrageenan in the buffers was increased (Figure 5.3 and 5.4). In DMEM buffer (Figure 5.3), with kappa carrageenan concentrations between 2% and 4%, very little increase in shear viscosity over time was observed (2% and 4% are not shown in Figure 5.3, as the shear viscosity was too low to distinguish from the x-axis). On increasing the kappa carrageenan concentration to 7%, an increase in viscosity with time was observed. At 8% kappa carrageenan in DMEM, there was an initial reduction in viscosity at the start of shearing in the vane. However, it appeared from the

profile that only partial breakup of the hydrated structure formed on initially adding the powder has occurred as a viscosity/ time profile is noisy at all times and the lowest viscosity is observed after about 5 minutes with a slight recovery of viscosity at longer times.

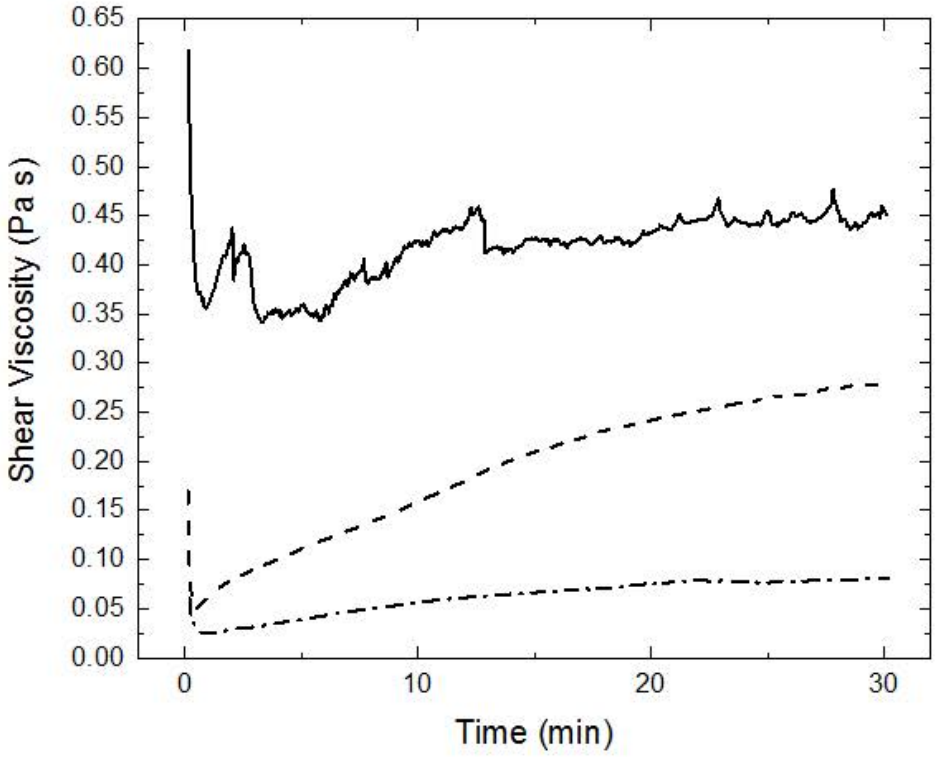

Figure 5.3 – Viscosity of κC dispersed in DMEM buffer over 30 min. 6% (dash dot), 7% (dash) and 8% (solid). The temperature was held at 30 °C.

In the HEPES buffer, as the kappa carrageenan concentration was increased up to 4%, little change in the viscosity/time profile was observed. However, on increasing the concentration to 5% and 6%, a significant change in the profile was observed, with the shear viscosity increasing by a factor of 10 or more. At higher concentrations than this, samples could not be made, since excess

unhydrated κC was observed in the bottom of the cup, in a similar manner to the results observed for 2% kappa carrageenan in water. As can be seen in Figure 5.4, at 6% kappa carrageenan, there was a rapid increase in viscosity after about 20 minutes followed by a plateau after 30 minutes. It appears that at this concentration the hydration and swelling occurs after 20 minutes so that the particles occupied the whole volume of the sample and started to interact. Above 20 minutes, the interactions continued to build, but the applied shear was breaking them down resulting in the noisy signal. This type of behaviour is often observed for fluid gel production when gel breakage occurs.

After 30 minutes the viscosity observed with 7% kappa carrageenan in DMEM buffer was about the same as that observed after 30 minutes for 5% kappa carrageenan in HEPES buffer. This difference shows that the rate of hydration of the kappa carrageenan is different for the two buffers, with a slower rate in DMEM than HEPES, although, as will be discussed later, the resulting gel like properties in the two buffers are very similar.

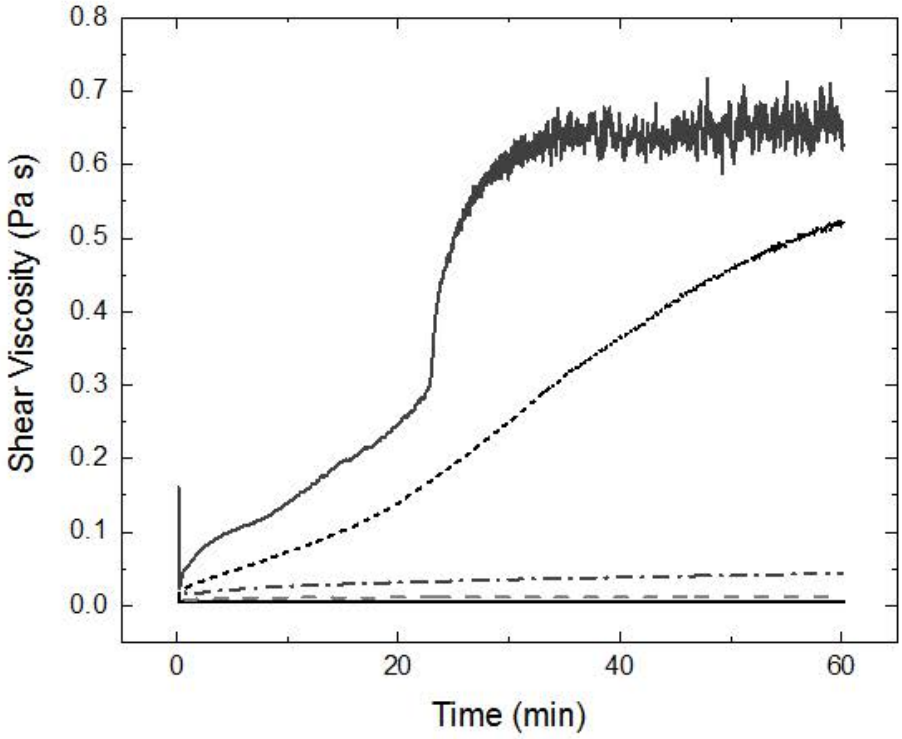

Figure 5.4 – Viscosity of κC dispersed in HEPES buffer for 1 hour (2% (solid line), 3% (dash line), 4% (dash dot line), 5% (dot line), and 6% (grey solid line)). The temperature was held at 30 °C.

Visual observation of the samples (Figure 5.5 and 5.6) showed that in DMEM the kappa carrageenan powder had hydrated at all concentrations and appears to have structured the liquid at all concentrations (Figure 5.5). However, at 8% kappa carrageenan in DMEM, the sample appeared to be a broken gel, although the rheological analysis of the sample does not support this. At kappa carrageenan concentrations between 2% and 5% when the sample vials were inverted, the samples flowed and the sample collected at the bottom of the vials. However, at concentrations of kappa carrageenan between 6% and 8% the flow

was reduced (Figure 5.6). In the case of 6% kappa carrageenan in DMEM, some of the sample has flowed to the bottom of the vial after being inverted for 3 hours. The 7% kappa carrageenan in DMEM sample shows that a lower amount of sample has moved and at 8% the whole sample has remained at the top of the vial.

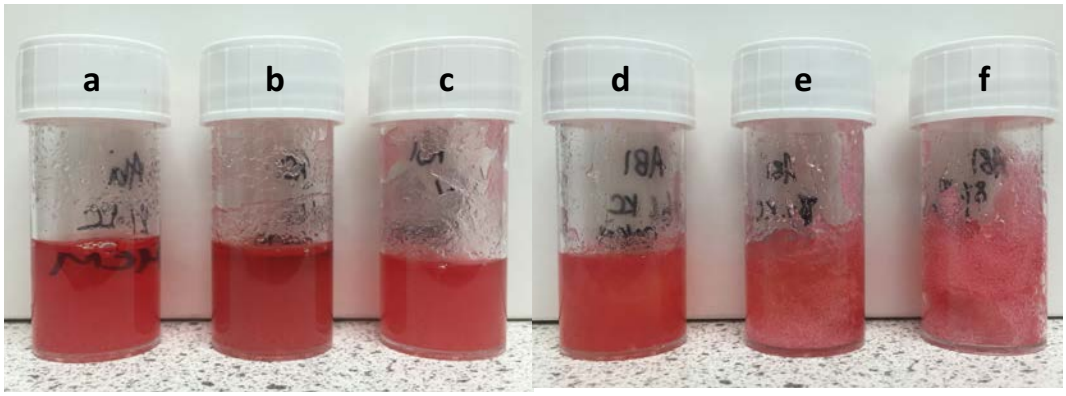

Figure 5.5 – Kappa carrageenan in DMEM at a range of concentrations (2% (a), 4% (b), 5% (c), 6% (d), 7% (e) and 8% (f)). Samples were formed at 30 ^{o}C, and sheared at 500 s^{-1} for 60 minutes, using a rheometer.

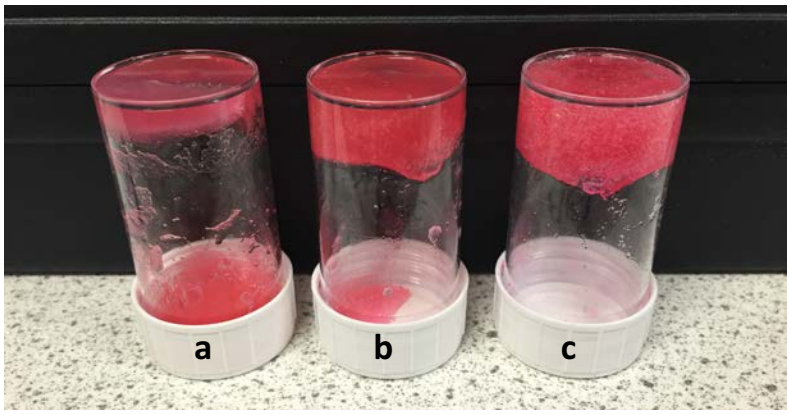

Figure 5.6 – Inverted vials of 6% (a), 7% (b) and 8% (c) kappa carrageenan in DMEM. Photographs were taken after vials had been inverted for 3 hours.

In HEPES buffer (Figure 5.7) very similar results were observed to DMEM, with swelling of the particles at all kappa carrageenan concentrations. Indications are that the swollen particles appear to occupy most of the water volume even at 2% kappa carrageenan (as indicated by the rheological measurements discussed in the next section). At 6% kappa carrageenan in HEPES, the broken structure suggested from the viscosity/ time profiles is apparent, suggesting that this is the limiting concentration for sample preparation.

The viscosity/ time data and the visual observations showed that DMEM and HEPES buffer allowed the hydration of kappa carrageenan to produce structures. They have not, however, resulted in the same gelation as would be observed by high temperature dissolution followed by cooling. As the shear has not been applied while cooling, a three dimensional structure of hydrated particles has been formed rather than a fluid gel, which could still potentially be used to structure products for application to human skin, housing water soluble actives, or potentially mammalian cells. These structures could be beneficial in the intended applications, as the active could potentially be trapped within the hydrated particle network, slowing down any movement and giving more control over their release.

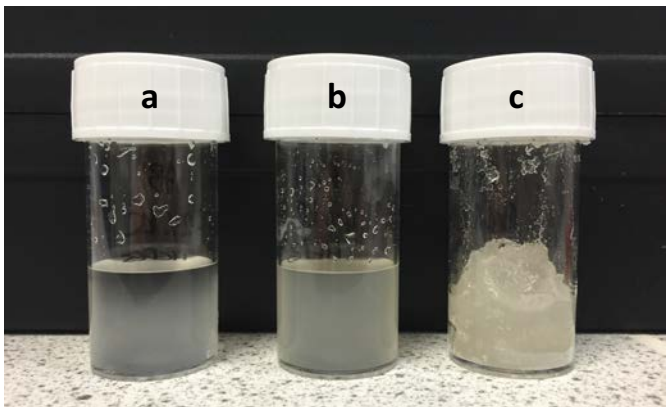

Figure 5.7 – Kappa carrageenan in HEPES at a range of concentrations (2% (a), 4% (b), and 6% (c)). Samples were formed at 30 °C, and sheared at 500 s^{-1} for 60 minutes, using a rheometer.

To further understand the structures that were produced, oscillation tests were carried out on the kappa carrageenan systems, between 24 hours and 36 hours after production using a Kinexus rheometer. Figure 5.8 shows the elastic and loss moduli obtained, as a function of strain, for kappa carrageenan (2% to 8%) in DMEM buffer. As can be seen, all concentrations exhibited a solid-like behaviour, with elastic (or storage) modulus (G') being larger than the viscous (or loss) modulus (G'') by a factor of about 10, for strains up about 1%. This data shows that even at low concentrations of kappa carrageenan hydrated at low temperatures (30 °C), gel-like structures have been formed. The elastic modulus obtained for 2% kappa carrageenan was 60 Pa which was lower than typically reported in the literature for samples produced by dissolution at high temperature (i.e. 80 °C) e.g. 1% kappa carrageenan G' of 100 Pa (Stading and Hermansson, 1993). However, it is still within the same order magnitude. As expected, the elastic modulus of the kappa carrageenan samples increased with

increasing concentration so that at 4% it was approximately 1000 Pa, at 5% it was approximately 15000 Pa and at 6%, 7% and 8% it was approximately 50000 Pa. The elastic and loss moduli in DMEM were plotted as a function of kappa carrageenan concentration in Figure 5.8. The elastic modulus increased by two orders of magnitude as the concentration of kappa carrageenan was increased from 2% to 5%, showing that a significant increase in the structuring had occurred (as can been seen in Figure 5.8). However, the loss modulus increases by about the same amount so that the difference at all carrageenan concentrations remained as a factor of approximately 10. In addition, as can be seen from Figure 5.8, the linear region was between 0.01% and 1% strain for all the samples. As expected for a structure that has been produced by hydrating a powder at low temperature, the data shows that all of the samples can best be described as particulate networks.

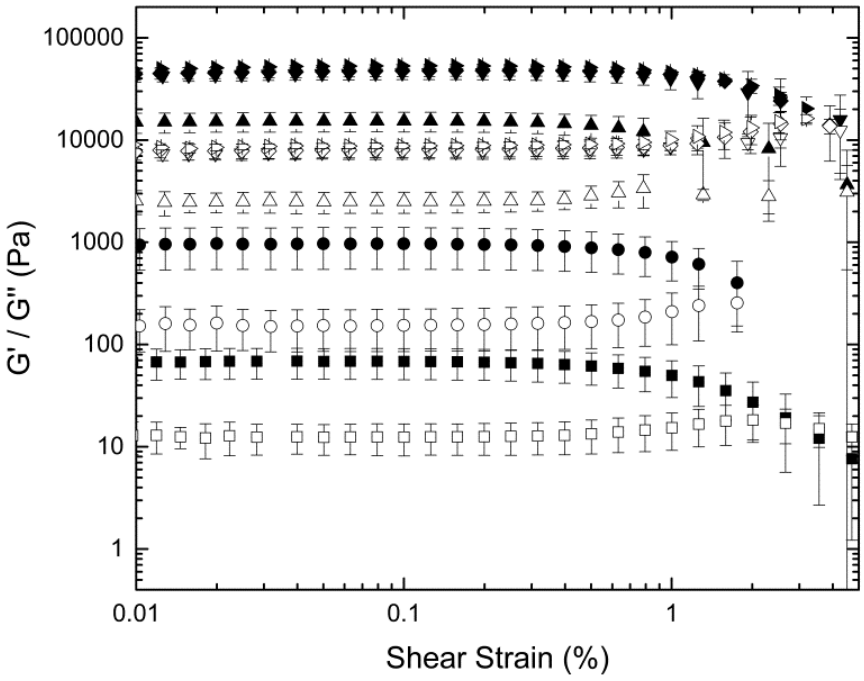

Figure 5.8 – Oscillation sweeps of κC DMEM gels, as a function of strain percentage. κC concentrations are 2% (□/■), 4% (○/●), 5% (△/▲), 6% (▽/▼), 7% (◇/◆) and 8% (▷/▶). Elastic modulus (G') is represented by closed symbols, with open symbols representing viscous modulus (G'').

The data obtained at 6%, 7% and 8% kappa carrageenan in DMEM showed that the solid like behaviour was no longer increasing with polymer content, but instead had plateaued (Figure 5.9). This suggested that over 6% polymer, the system is saturated with kappa carrageen so there was not enough liquid to allow further hydration of the polymer i.e. there was excess polymer so it was not properly dissolved, or the applied shear during production broke up the interactions between the particles as they swell, resulting in fluid gel like systems.

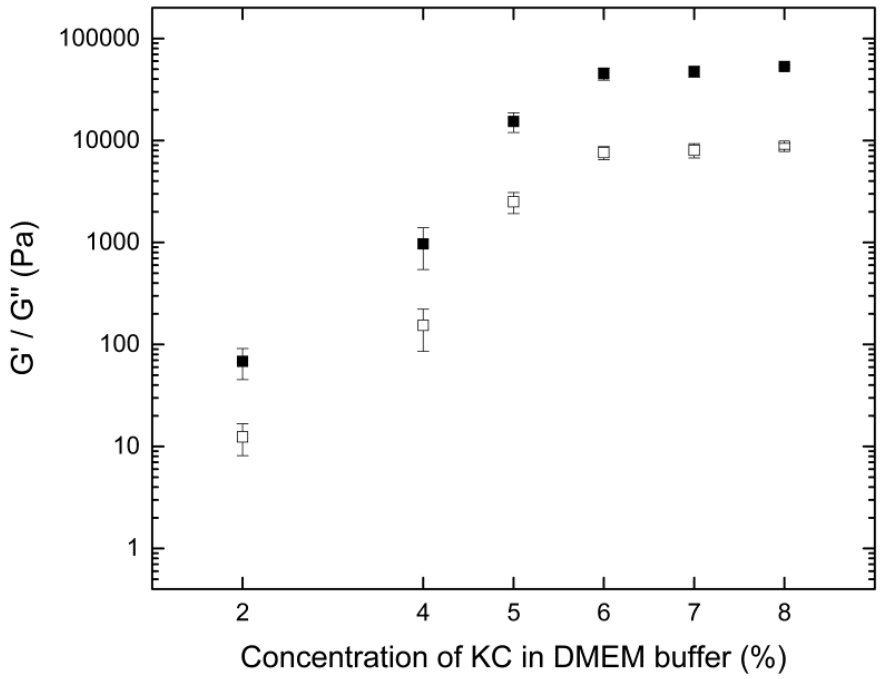

Figure 5.9 – Linear Visco Elastic Region value from the oscillation sweeps of a range of concentrations of κC dispersed in DMEM buffer. Elastic modulus (G') is represented by closed symbols, with open symbols representing viscous modulus (G'').

Similar behaviours were seen when kappa carrageenan was dispersed in HEPES buffer. Figure 5.10 shows the elastic and loss moduli obtained, as a function of strain percentage, for kappa carrageenan (2% to 6%). All concentrations exhibited a solid-like behaviour, with elastic (or storage) modulus (G') being larger than the viscous (or loss) modulus (G'') by a factor of 6 or 7, for strains up to 1%. Again, this data showed that even at low concentrations of kappa carrageenan, gel like structures were formed. The elastic modulus obtained for 2% kappa carrageenan was again approximately 60 Pa. As expected, the elastic modulus of the kappa carrageenan samples increased with increasing concentration, so that at 4% it was about 3000 Pa, at 5% it was approximately

5000 Pa and at 6% it was approximately 20000 Pa. The elastic and loss moduli in HEPES buffer are plotted as a function of kappa carrageenan concentration in Figure 5.11. As can be seen, the elastic modulus increased by almost 2 orders of magnitude as the concentration of kappa carrageenan was increased from 2% to 5%, again showing that a significant increase in the network has occurred. The loss modulus increased by about the same amount so that the difference at all carrageenan concentrations remained as a factor of approximately 6 or 7. In addition, there was no strain dependency for the elastic or loss moduli between 0.01% and 1% strain, for all the samples, and the data suggested that a particulate system was formed.

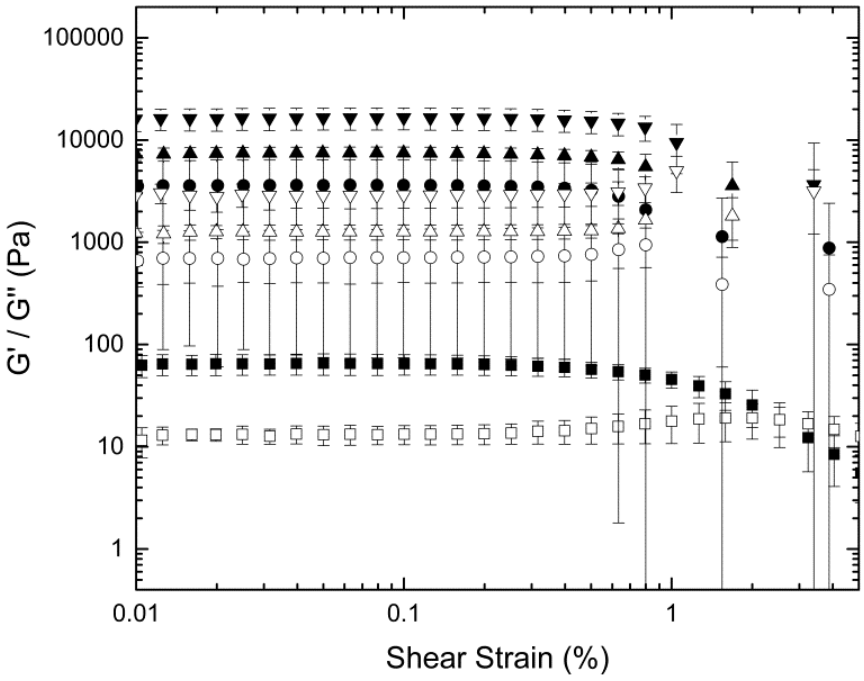

Figure 5.10 - Oscillation sweeps of κC HEPES gels, as a function of strain percentage. κC concentrations are 2% (□/■), 4% (○/●), 5% (△/▲) and 6% (▽/▼). Elastic modulus (G') is represented by closed symbols, with open symbols representing viscous modulus (G'').

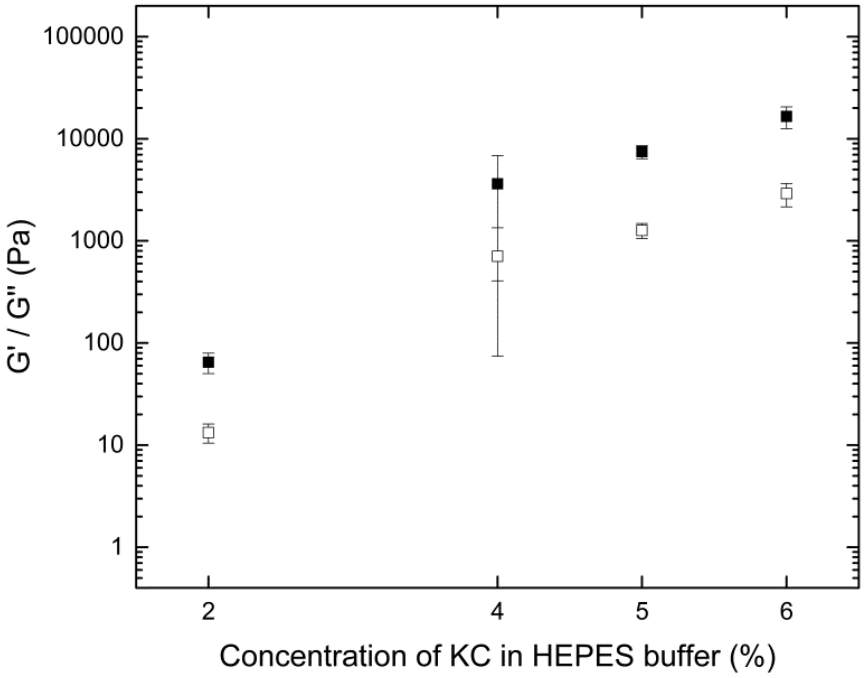

Figure 5.11 – Linear Visco Elastic Region value from the oscillation sweeps of a range of concentrations of κC dispersed in HEPES buffer. Elastic modulus (G') is represented by closed symbols, with open symbols representing viscous modulus (G'').

The rheological studies have shown that potassium kappa carrageenan can hydrate at 30 ^{o}C under shear to form particulate gel networks in DMEM and HEPES. In order to determine how these structures relate at the molecular level to kappa carrageenan gels formed by dissolution at high temperature, DSC measurements were carried out. Figure 5.12 shows the first heating and cooling scans for kappa carrageenan concentrations of 2%, 4%, 6%, 7% and 8% in DMEM, along with the results obtained for DMEM buffer alone. The data has been offset on the y-axis in order to allow visualisation of the individual scans. The DMEM buffer control, as expected, has no peaks between 10 ^{o}C and 90 ^{o}C, showing that

any transitions observed with the kappa carrageenan samples are a result of conformational changes occurring in the hydrocolloid (such as helix to coil on heating and the reverse on cooling) or of further solubilisation (if all of the carrageenan powder was not solubilised).

As can be seen from Figure 5.12, a single peak was observed for all samples on heating and cooling, and as the concentration of the kappa carrageenan was increased (from 2% to 7%) the peak areas increase, as do the peak temperatures. However, there seems to be little difference in the peak positions or peak areas on increasing the concentration from 7% to 8%. The temperatures of the peak maximum and peak areas are shown in Table 5.1. The increase in peak temperature was as a result of the increased polymer concentration and the increased potassium ion concentration introduced via the kappa carrageenan powder. The peak temperatures are in line with those reported in the literature (Morris et al., 1980, Norton et al., 1984) and the enthalpies are about the same as reported in Chapter 4. Therefore the enthalpy change is not affected to any great extent by the concentration of the carrageenan or ion concentrations. However, the transition temperatures are affected by the salt concentration.

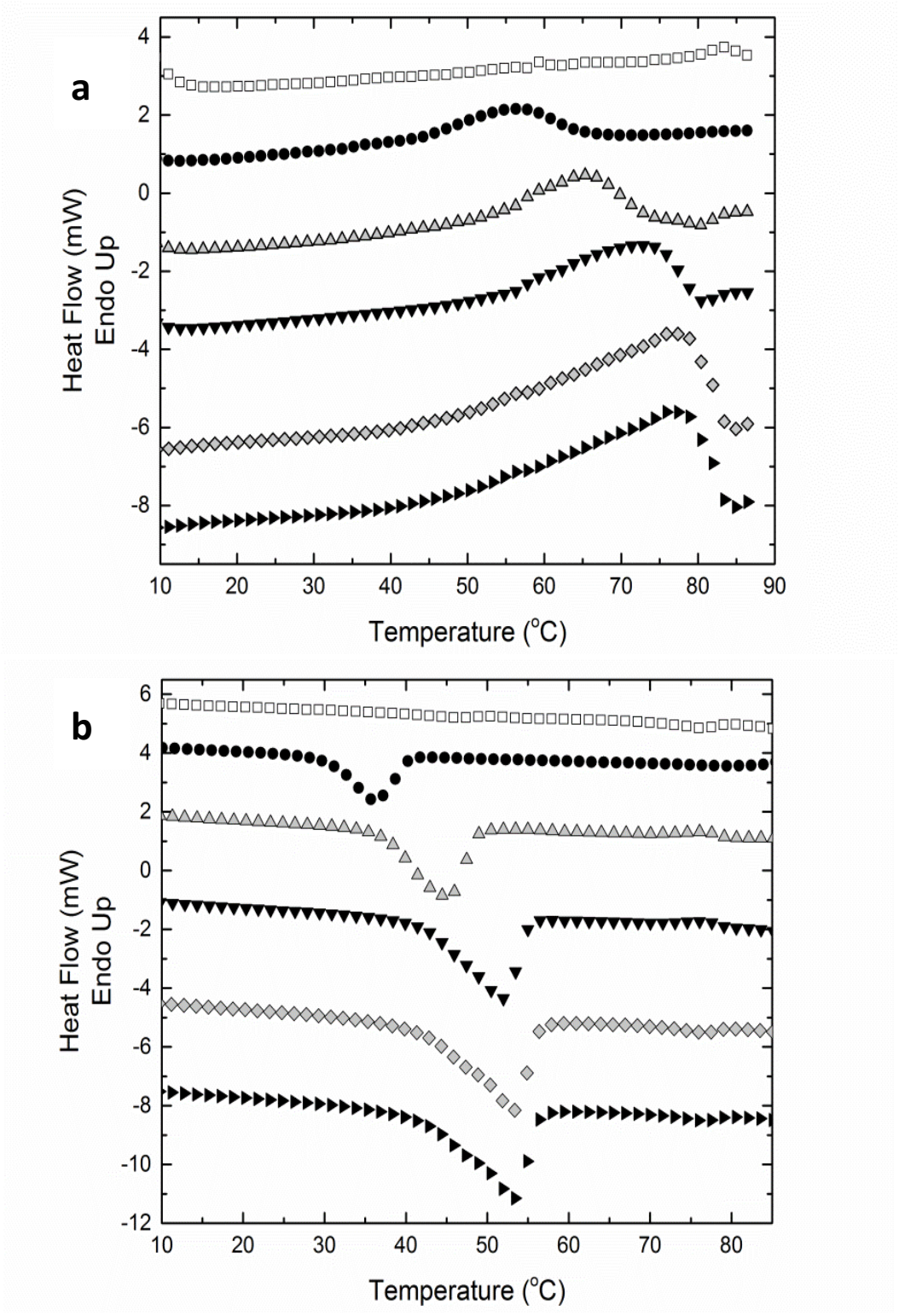

Figure 5.12 – DSC heating (a) and cooling (b) profiles for different concentrations of κC (0% (□), 2% (●), 4% (△), 6% (▼), 7% (◇), and 8% (▶)) dispersed in DMEM buffer.

Table 5.1 - Enthalpies and temperature maximums for Kappa carrageenan in DMEM buffer, determined by DSC.

Kappa Carrageenan (%)	Heating		Cooling	
	Enthalpy (J/g)	T_{max} (^{o}C)	Enthalpy (J/g)	T_{max}(^{o}C)
2	17.19	54	36.81	34
4	12.29	63	32.21	45
6	14.76	71	26.51	52
7	26.98	76	27.42	54
8	24.33	76	27.04	54

Figure 5.13 shows the heating and cooling scans for kappa carrageenan concentrations of 2%, 4%, 5% and 6% in HEPES, along with the results obtained for HEPES buffer alone. Similar to the DMEM buffer, the HEPES buffer control has no peaks between 10 ^{o}C and 90 ^{o}C, showing that any transitions observed with the kappa carrageenan samples are a result of conformational changes occurring in the hydrocolloid or of further solubilisation.

As can be seen from Figure 5.13, a single peak is observed for all samples on heating and cooling, and as the concentration of the kappa carrageenan is increased, the peak areas increase, as do the peak temperatures. The temperatures of the peak maximum and peak areas are shown in Table 5.2.

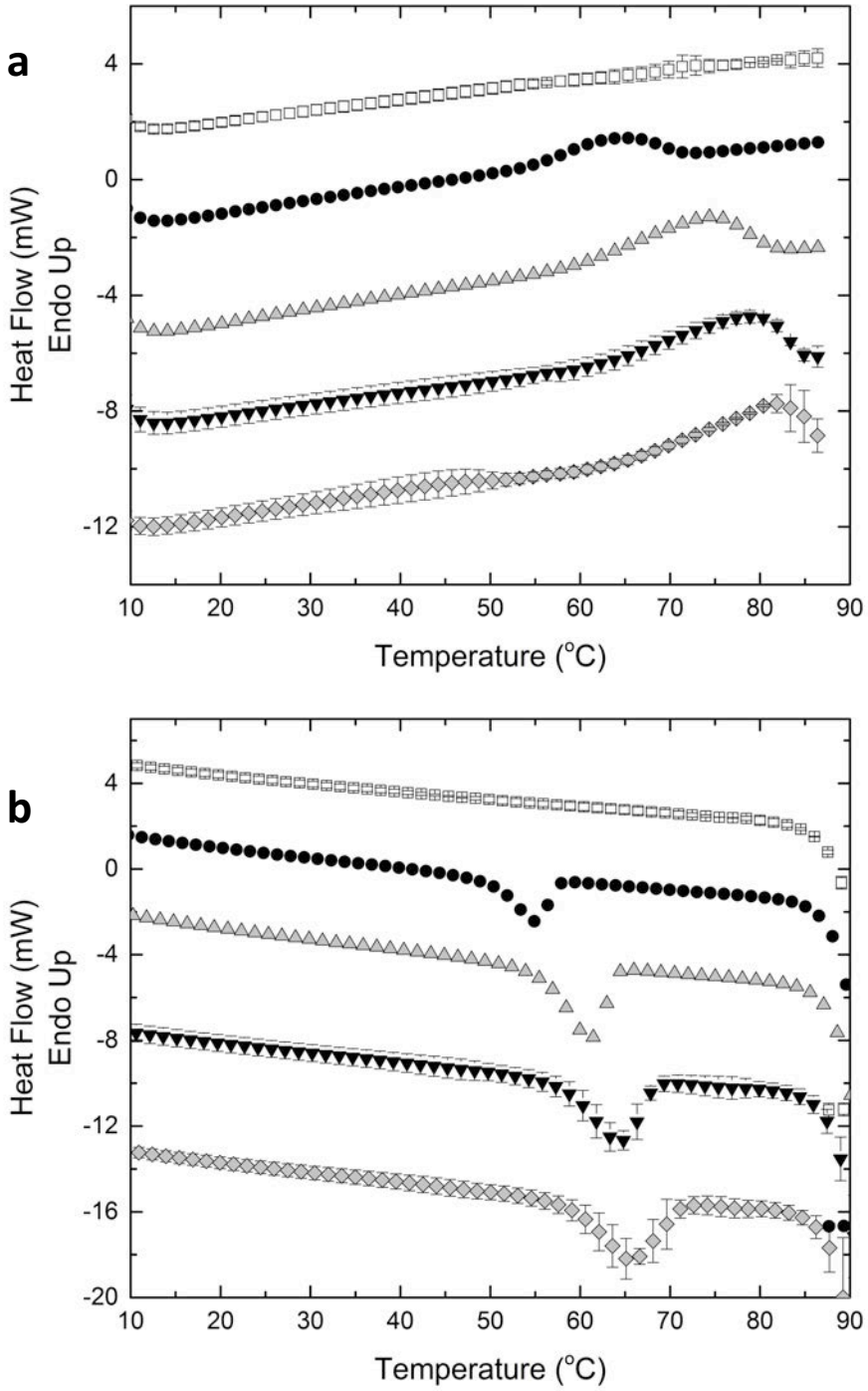

Figure 5.13 – DSC heating (a) and cooling (b) profiles for different concentrations of κC (0% (□), 2% (●), 4% (△), 5% (▼), and 6% (◇)) dispersed in HEPES buffer.

Table 5.2 – Enthalpies and temperature maximums for Kappa carrageenan in HEPES, using DSC. (The enthalpy of 6% κC is not stated, as the end of the transition did not occur).

Kappa Carrageenan (%)	Heating		Cooling	
	Enthalpy (J/g)	T_{max} (^{o}C)	Enthalpy (J/g)	T_{max} (^{o}C)
2	35.82	64	47.72	54
4	32.12	75	33.22	62
5	37.55	77	30.18	65
6		82	29.11	66

5.3.2 Inclusion of the kappa carrageenan low temperature hydrated gel networks within a water in oil emulsion

Different ratios of aqueous phase to oil, emulsified with 1% PGPR or 1% Span 80, were studied. Also the formation of simple water-in-paraffin oil emulsions was investigated. It was found that simple emulsions emulsified with 1% PGPR or 1% Span 80 did not form emulsions, with separation of the two phases occurring immediately. Furthermore it was found that if oil was in a concentration above 50% (with kappa carrageenan particulate aqueous phases were used), the emulsions were unstable, with creaming occurring.

Both PGPR and Span 80 are common emulsifiers for the stabilisation of water-in-oil emulsions. Therefore, the unsuccessful formation of stable emulsions could be either due to the oil used in this study, or the shear rate used for the emulsion formation process. The viscosity of paraffin oil (a common ingredient in skin creams) was lower than many other oils used for oil continuous emulsions (paraffin oil has a viscosity of 0.04 Pa s, compared with 0.075 Pa s for sunflower oil). The viscosity of paraffin oil is therefore closer to that of water/buffer than oils such as sunflower oil. Additionally, the formation of emulsions is typically done by applying a high shear to a pre emulsion mix, to produce small droplets, which in turn are slower at sedimentation and coalescing, and thus are more stable than emulsions with large droplets. The shear used in this study was selected to allow for the potential addition of shear sensitive actives, such as mammalian cells.

The addition of carrageenan to the aqueous phase was therefore investigated to determine whether changing the viscosity of the aqueous phase affects the emulsion stability. Figure 5.14 shows water in oil emulsions (with the two phases in a 50:50 ratio) after standing for 1 hour, with DMEM only and with increasing levels of low temperature hydrated kappa carrageenan from 2% to 8% when emulsified with PGPR. Samples produced with 2% and 4% kappa carrageenan were unstable and the emulsion had split after 1 hour (a free DMEM aqueous phase can be observed at the bottom of the vial) and the remaining water in oil emulsion and oil phase had creamed. At 5% kappa carrageenan, DMEM buffer is no longer observed; however, sedimentation has occurred with an oil layer

present (two layers are observed, as opposed to the three layers observed in the other samples on the top row of Figure 5.14). This suggests that the greater structuring in 5% κC, compared with 2% κC and 4% κC, is having a beneficial affect on the emulsion formation.

At kappa carrageenan concentrations between 6% and 8%, the emulsion is observed to be lighter in colour (as opposed to the dark red of the DMEM buffer), and have no visible sign of creaming or sedimentation, indicating that they are oil continuous emulsions with small (micron size) water droplets and they were stable for at least 1 hour.

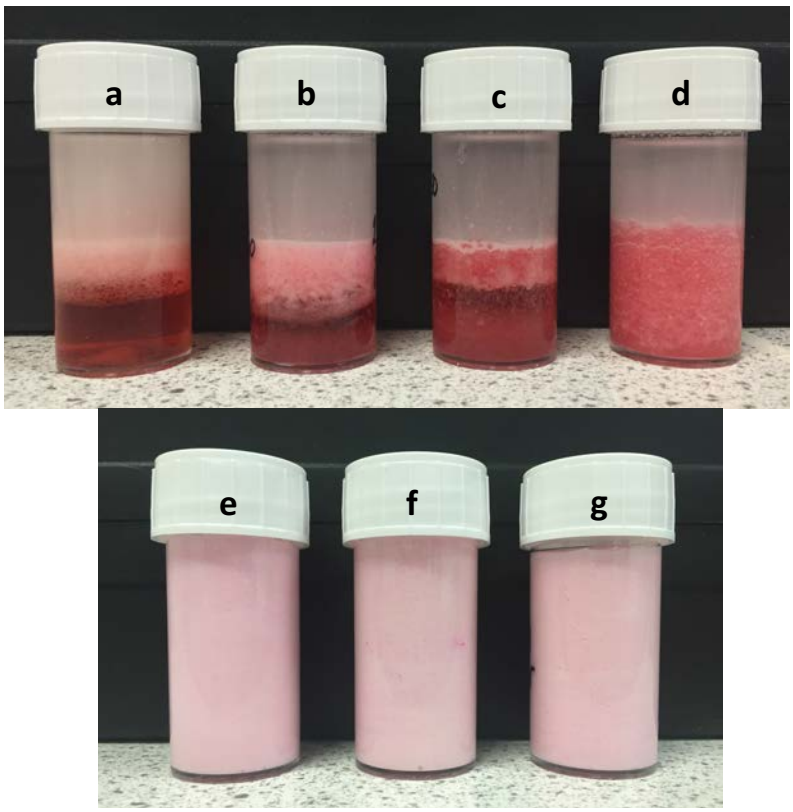

Figure 5.14 – Oil continuous emulsions with DMEM as the aqueous phase (a) and with warm (30°C) water hydrated kappa Carrageenan at 2% (b), 4% (c), 5% (d), 6% (e), 7% (f) and 8% (g) kappa carrageenan in DMEM (from top row second from the left to bottom right), emulsified with 1% PGPR.

The use of Span 80 as the emulsifier exhibited similar results to the PGPR emulsified emulsions. Samples produced with 2%, 4% and 5% kappa carrageenan (Figure 5.15) are unstable and the emulsions have separated into their component phases. At kappa carrageenan concentrations between 6 and 8%, the emulsions are lighter in colour and show no creaming or sedimentation, again indicating that they were oil continuous emulsions and they were stable for at least 1 hour.

Similar trends were observed for kappa carrageenan in HEPES buffer emulsions, when either PGPR or Span 80 was used (photographs are not shown). When carrageenan concentrations were 5% and 6% (the top κC concentrations investigated in HEPES), emulsions appeared to be stable for at least 1 hour. However, below 5% κC, emulsions separated into the different phases, in the same way the DMEM emulsions had done. The formation of stable emulsions correlates to the concentration of the particulate gel phases that had plateaued in their rheological behaviour (as shown in Figure 5.8 and Figure 5.10). This further suggests that the formation of stable water-in-paraffin oil emulsions is closely linked with the viscosity of the two phases being vastly different from one another.

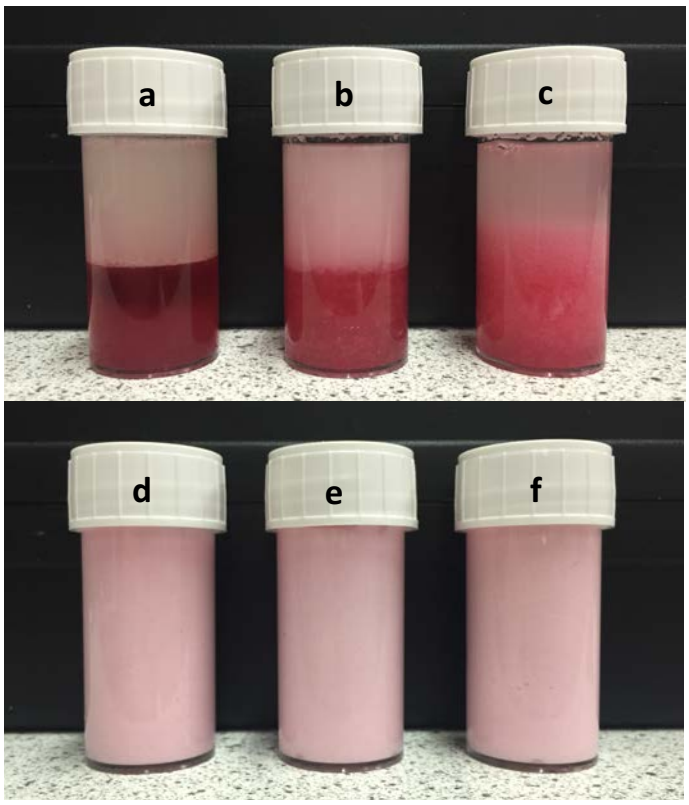

Figure 5.15 - Oil continuous emulsions with warm (30°C) water hydrated kappa Carrageenan at 2% (a), 4% (b), 5% (c), 6% (d), 7% (e) and 8% (f) kappa carrageenan in DMEM (from top row left hand picture to bottom right), stabilised with Span 80.

As ten formulations appeared to be stable after production, particle sizing was carried out to determine whether particle sizing was affected by the kappa carrageenan concentration. Table 5.3 shows the particle sizes for emulsions containing 6%, 7%, and 8% kappa carrageenan in DMEM buffer, and 5% and 6% kappa carrageenan in HEPES buffer.

When both PGPR and Span 80 were used to stabilise the emulsions, droplet sizes appeared to decrease as the kappa carrageenan concentration was increased. This trend was also observed for both DMEM buffer and HEPES buffer; however,

there is not a significant difference. The particle sizes were smaller when Span 80 was used compared with PGPR stabilised emulsions. However, once again these are not vastly different. As the differences between carrageenan concentrations are not significant, the hypothesis that the rheological properties of the aqueous phase (the particulate systems) determine emulsion stability would be further strengthened.

Table 5.3 – Droplet sizes for the stable emulsions, determined using a mastersizer. Values quoted are the peak maximum, or modal number.

Kappa Carrageenan (%)	DMEM		HEPES	
	1% PGPR	1% Span 80	1% PGPR	1% Span 80
5			5.4 μm ± 0.35	4.4 μm ± 0.2
6	6.2 μm ± 0.5	4.1 μm ± 0.35	4.7 μm ± 0.4	3.8 μm ± 0.55
7	4.4 μm ± 0.2	3.8 μm ± 0.2		
8	3.6 μm ± 0.7	3.8 μm ± 0.2		

Figure 5.16 shows the elastic (solid symbols) and loss (open symbols) modulii for the emulsions produced with 6%, 7% and 8% kappa carrageenan in DMEM using 1% PGPR or 1% Span 80. As can be seen, for all the samples the G' is above G'' with a difference of about a factor of 6. The linear region remains in the

amplitude sweep until about 0.1% to 0.2% strain. The samples therefore behave like weak particulate gels. The observed modulii were significantly lower than observed for the aqueous carrageenan phase alone. 50% included aqueous phase is considered as a high internal concentration, and therefore will result in some interaction between the droplets when an external force is applied. This would explain the observed modulii. The slight increase in G' observed on increasing the carrageenan concentration from 6% to 8% is a consequence of the increased hardness of the droplets as the amount of internal structuring increases. However, due to the size of the reduction in elastic modulus (approximately 100 Pa reduction for 6% κC, 200 Pa reduction for 7% κC, and 650 Pa reduction for 8% κC) (Figure 5.17), the observed weak gel behaviour is unlikely to be due to extensive aqueous phase continuity in the emulsions.

While no significant difference was observed in particle sizing between emulsions stabilised with PGPR and Span 80 (Table 5.3), there is a significant difference between the rheological behaviours of the emulsions. Span 80 emulsions had lower G' and G'' across all kappa carrageenan/DMEM concentrations investigated (Figure 5.17). This clearly indicates that there is less structuring within the Span 80 stabilised emulsions than seen in the PGPR emulsions.

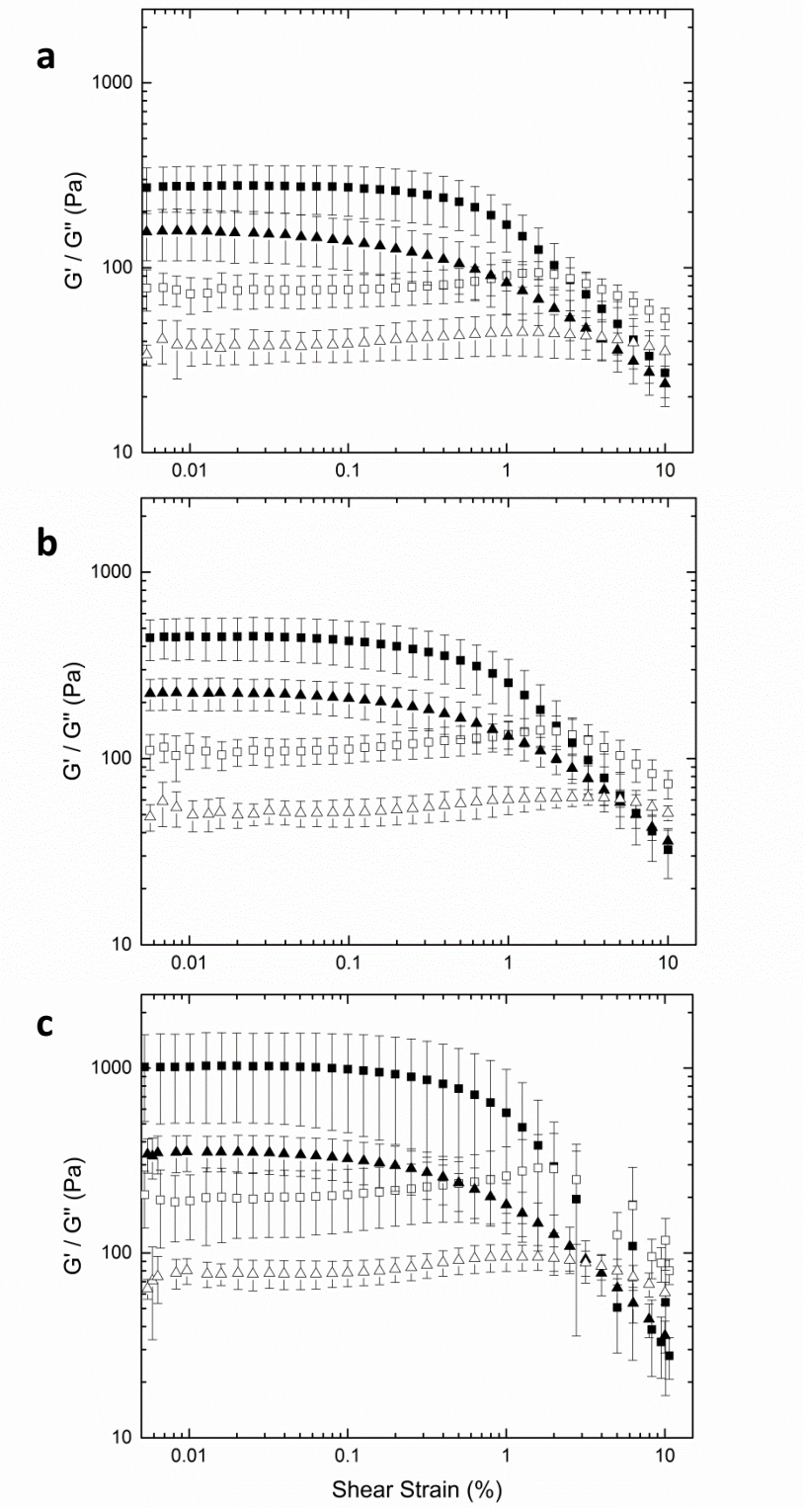

Figure 5.16 – Oscillation sweeps of κC DMEM-in-paraffin oil emulsions, stabilised with PGPR (□/■) and Span 80 (△/▲) (internal phase contains 6% κC DMEM (a), 7% κC DMEM (b) and 8% κC DMEM (c)). Elastic modulus (G') is represented by closed symbols, with open symbols representing viscous modulus (G'').

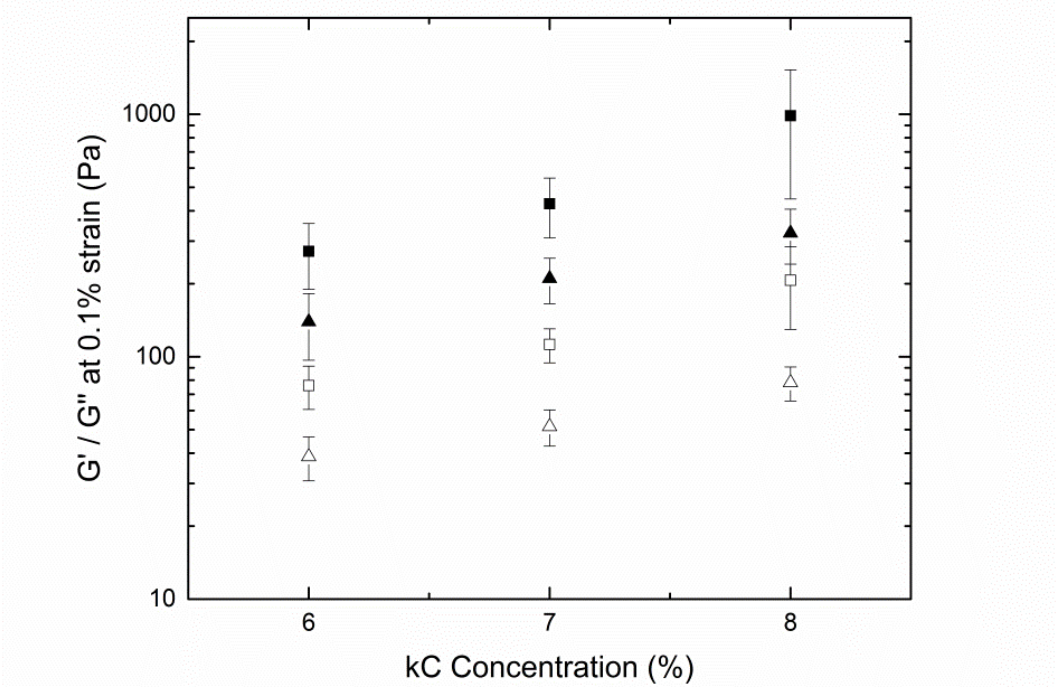

Figure 5.17 - Linear Visco Elastic Region value from the oscillation sweeps of primary emulsions with a range of concentrations of κC dispersed in DMEM buffer as the aqueous phase. Emulsions are stabilised with PGPR (□/■) or Span 80 (△/▲). G' is represented by closed symbols, and G'' is represented with open symbols.

Emulsions with carrageenan/HEPES internal phase show weak particulate gel properties, with the G' higher than G'', and a linear viscoelastic region, ending at 0.2% strain (Figure 5.18 a & b). The elastic modulus measured is in the same region as those observed for the DMEM samples and with 100 to 200 times lower than the measured values for the aqueous phase.

Similarly to emulsions formed with kappa carrageenan DMEM, emulsions formed with HEPES buffer had lower G' and G'' when stabilised with Span 80 than with PGPR. Once again, the use of Span 80 is showing less structuring within the

system, and therefore could be an indicator of less stable emulsions being formed.

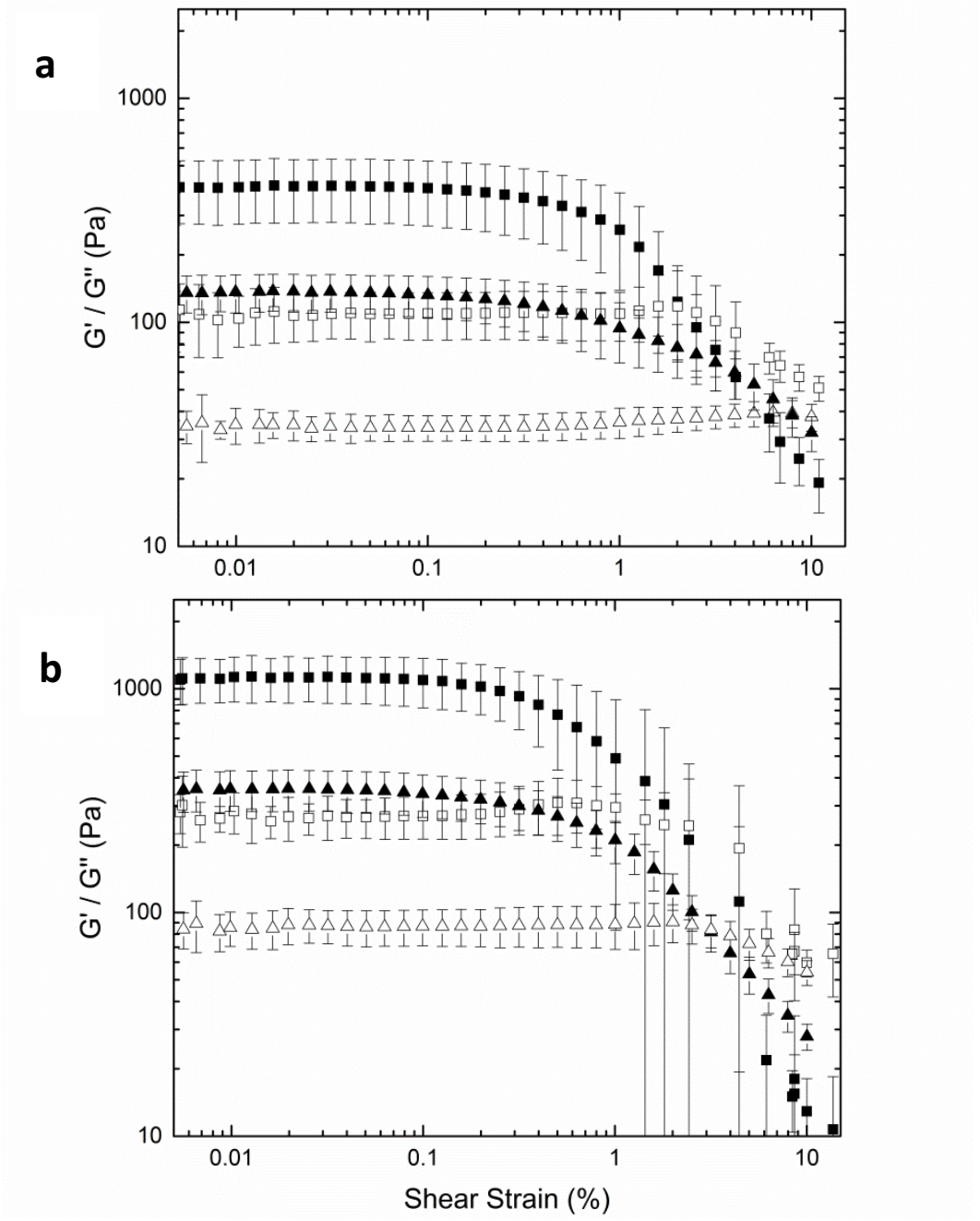

Figure 5.18 - Oscillation sweeps of κC HEPES-in-paraffin oil emulsions, stabilised with PGPR (□/■) and Span 80 (△/▲) (internal phase contains 5% κC HEPES (a), and 6% κC HEPES (b)). Elastic modulus (G') is represented by closed symbols, with open symbols representing viscous modulus (G'').

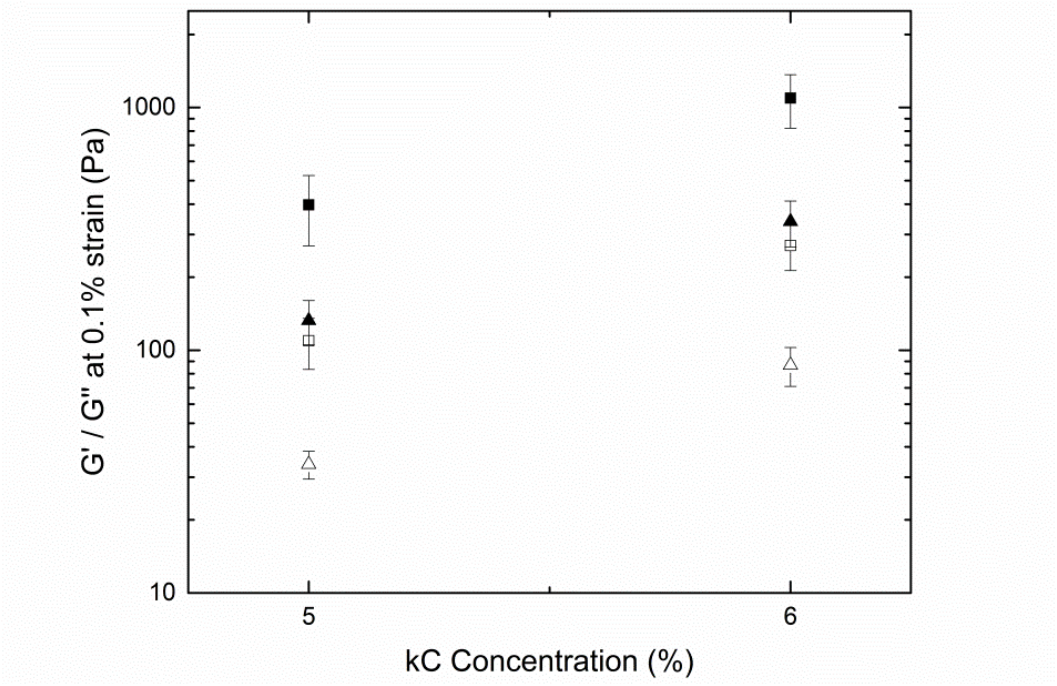

Figure 5.19 - Linear Visco Elastic Region value from the oscillation sweeps of primary emulsions with a range of concentrations of κC dispersed in HEPES buffer as the aqueous phase. Emulsions are stabilised with PGPR (□/■) or Span 80 (△/▲). G' is represented by closed symbols, and G'' is represented with open symbols.

5.3.3 Inclusion of kappa carrageenan stabilised primary emulsions for the production of duplex emulsions

The production and stability of duplex emulsions ($W_1/O/W_2$) were investigated with either 1% Tween 20 or 1% Tween 80. Duplex emulsions were produced using warm hydrated kappa carrageenan in both HEPES and DMEM buffer. A range of ratios of outer aqueous phase to primary emulsion phase was investigated: those produced with a 50:50 ratio of emulsion to secondary

aqueous phase were the most stable on storage and, as discussed later, resulted in emulsions with a cream like rheology.

When either tween 20 or tween 80 were used to emulsify PGPR stabilised single emulsions, the resultant duplex emulsions had similar structures (Figure 5.20 and Figure 5.21). Furthermore, the inclusion of DMEM or HEPES buffers appears to not greatly influence the structuring. When PGPR was used to stabilise the internal interface, multiple inner droplets were found within each secondary droplet. PGPR is a “sticky” emulsifier (Scherze et al., 2006), and thus this suggests that the primary droplets are able to stick together because the applied shear is too low to separate the droplets. Therefore, the secondary emulsion droplet is being forced to form around these aggregates of emulsion droplets.

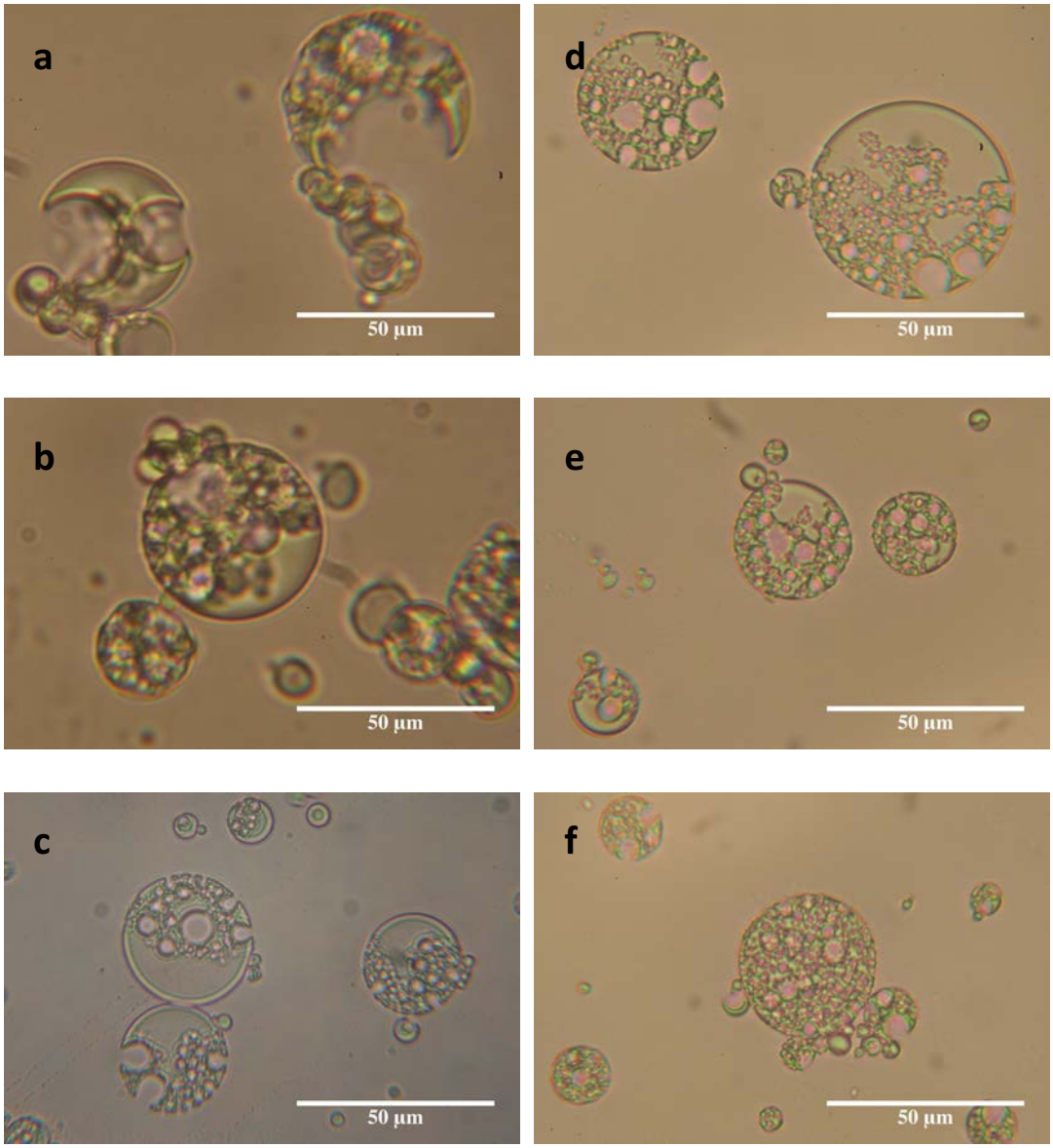

Figure 5.20 – Micrographs of duplex emulsions with the inclusion of 6% (a, d), 7% (b, e) and 8% (c, f) κC dispersed in DMEM buffer. Inner droplets were stabilised with PGPR, and outer droplets stabilised with Tween 20 (a, b, c) and Tween 80 (d, e, f). Micrographs were taken immediately after forming the duplex emulsion.

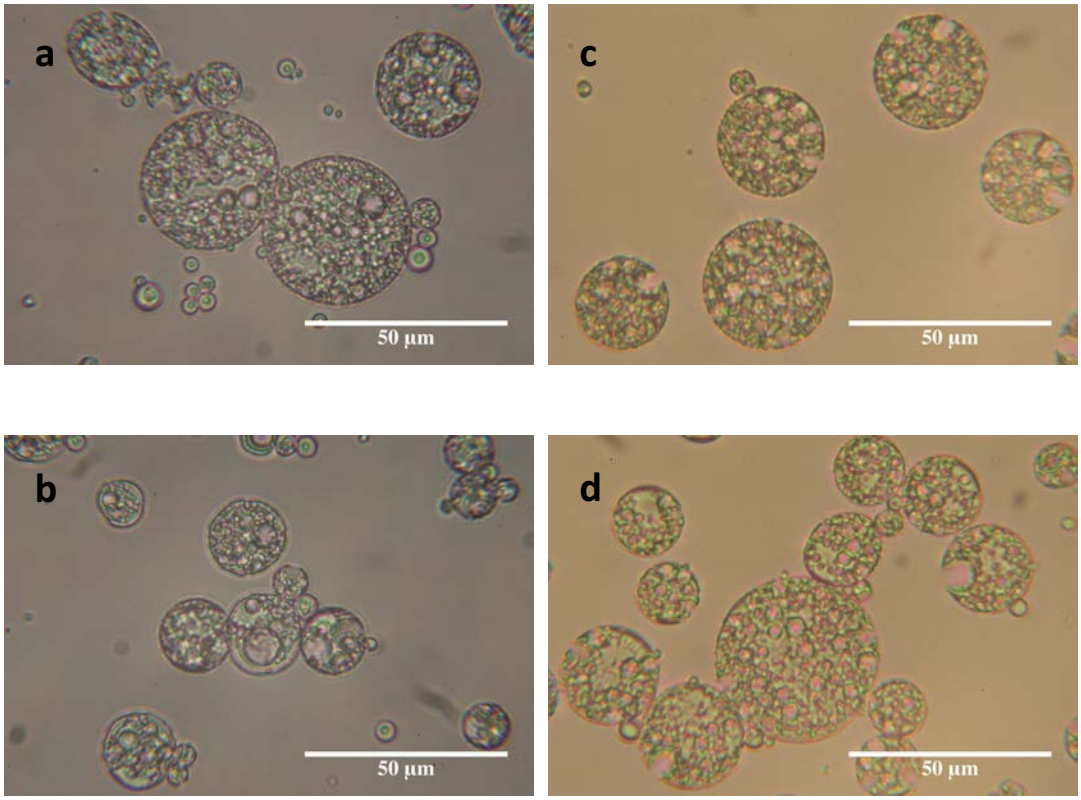

Figure 5.21 – Micrographs of duplex emulsions with the inclusion of 5% (a, c) and 6% (b, d) κC dispersed in HEPES buffer. Inner droplets were stabilised with PGPR, and outer droplets stabilised with Tween 20 (a, b) and Tween 80 (c, d). Micrographs were taken immediately after forming the duplex emulsion.

Conversely, when Span 80 was used as the internal emulsifier, the formation of duplex emulsions was less successful (Figure 5.22 and 5.23). Duplex emulsion droplets formed contain only one internal/ primary emulsion droplet. On day 1, primary emulsions can also be seen across all concentrations, showing that the formation of duplex emulsions has been largely unsuccessful. The difference between the PGPR duplex emulsions and the Span 80 duplex emulsions strongly suggests that PGPR, due to its large molecular size, is anchored into place (Benichou et al., 2007), while Span 80 is a smaller emulsifier, and thus has moved

from the interface, resulting in failure (smaller molecular weight surfactants need less energy to move from the interface, and are therefore more likely to move than larger molecules) (Frasch-Melnik et al., 2010). The instability of the Span 80 duplex emulsions (with lower levels of duplex structures formed on day 1 compared with PGPR) shows that this formulation would not be ideal for encapsulating environment sensitive actives.

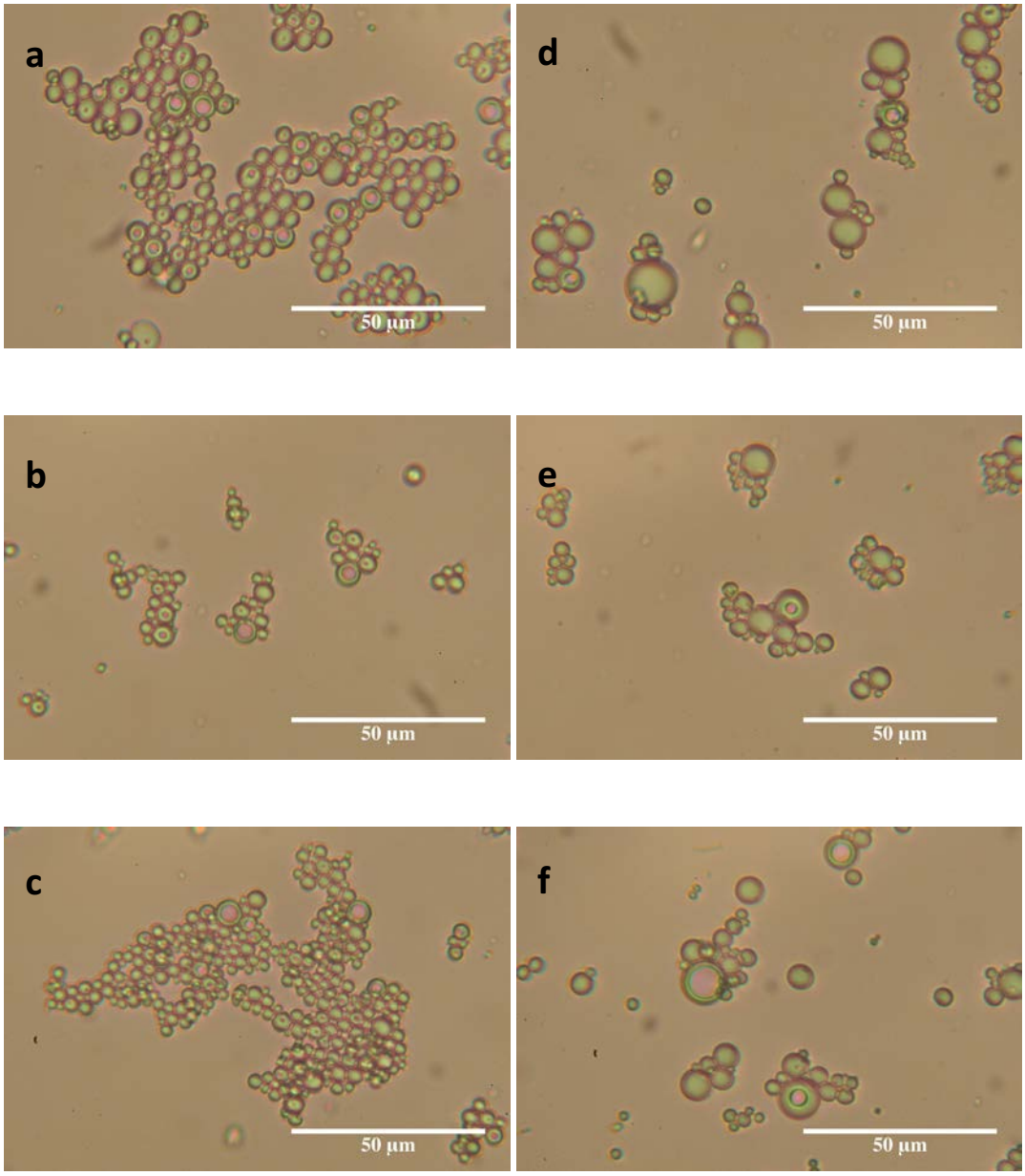

Figure 5.22 – Micrographs of duplex emulsions with the inclusion of 6% (a, d), 7% (b, e) and 8% (c, f) κC dispersed in DMEM buffer. Inner droplets were stabilised with Span 80, and outer droplets stabilised with Tween 20 (a, b, c) and Tween 80 (d, e, f). Micrographs were taken immediately after forming the duplex emulsion.

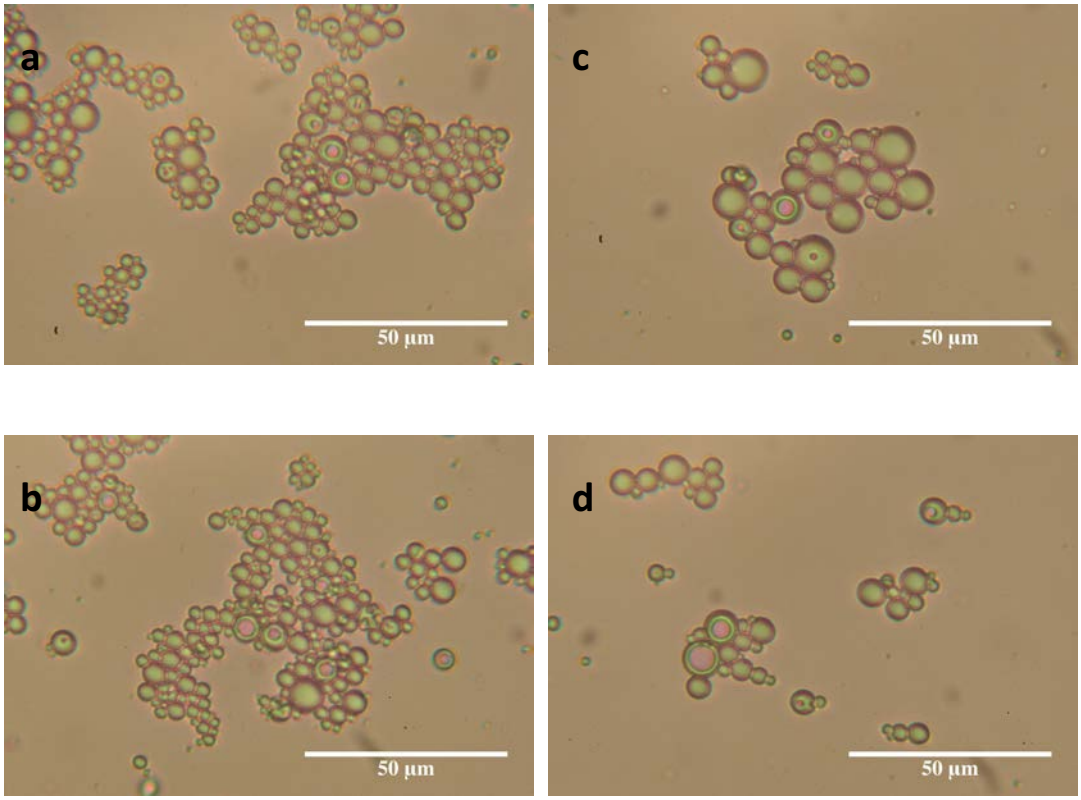

Figure 5.23 – Micrographs of duplex emulsions with the inclusion of 5% (a, c) and 6% (b, d) κC dispersed in HEPES buffer. Inner droplets were stabilised with Span 80, and outer droplets stabilised with Tween 20 (a, b) and Tween 80 (c, d). Micrographs were taken immediately after forming the duplex emulsion.

The rheological properties of the duplex emulsions were investigated: with the G' and G'' being very similar for the four combinations of emulsifier. The points at which the G' and G'' are no longer independent of the strain (up to about 0.4%) is also similar across all formulations where the aqueous phase includes κC in DMEM; but the values of G' and G'' are dependent on κC concentrations (Figure 5.24).

Thus the duplex emulsions containing warm water hydrated kappa carrageenan in DMEM have produced a solid-like response at low strains, with the elastic and loss modulii being very similar to those measured for the primary emulsion (comparing Figure 5.17 and 5.19). For the primary emulsion, the G' was measured in the range 100 Pa to 900 Pa on increasing the kappa carrageenan and the duplex emulsion is in the range 200 Pa to 800 Pa on increasing the kappa carrageenan concentration. The weak solid-like behaviour observed for the duplex emulsion is again a result of the high (50%) internal phase.

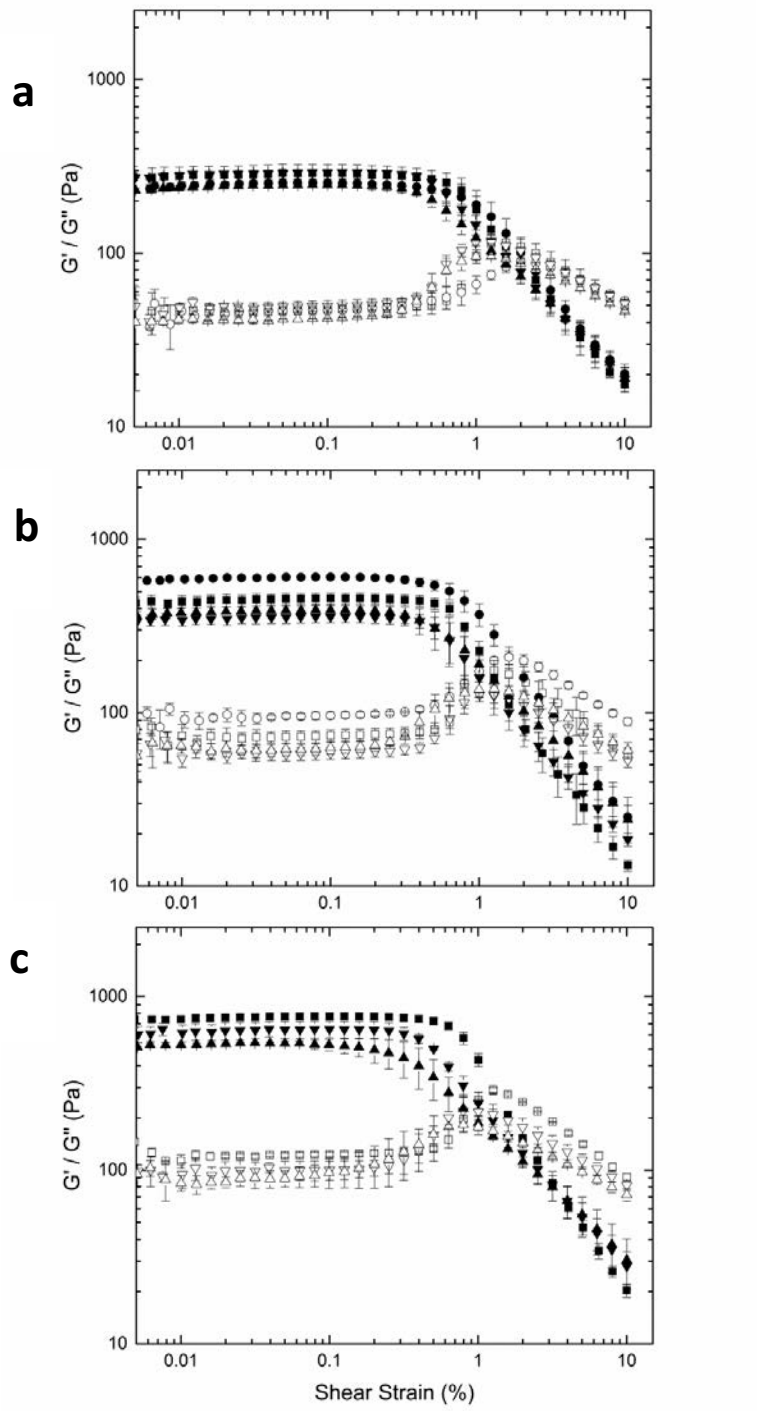

Figure 5.24 - Oscillation sweeps of κC DMEM-in-oil-in water duplex emulsions, stabilised with PGPR/ Tween 20 (□/■), PGPR/ Tween 80 (○/●), Span 80/ Tween 20 (△/▲) and Span 80/ Tween 80 (▽/▼) (the internal phase contains 6% κC DMEM (a), 7% κC DMEM (b), and 8% κC DMEM (c)). Elastic modulus (G') is represented by closed symbols, with open symbols representing viscous modulus (G'').

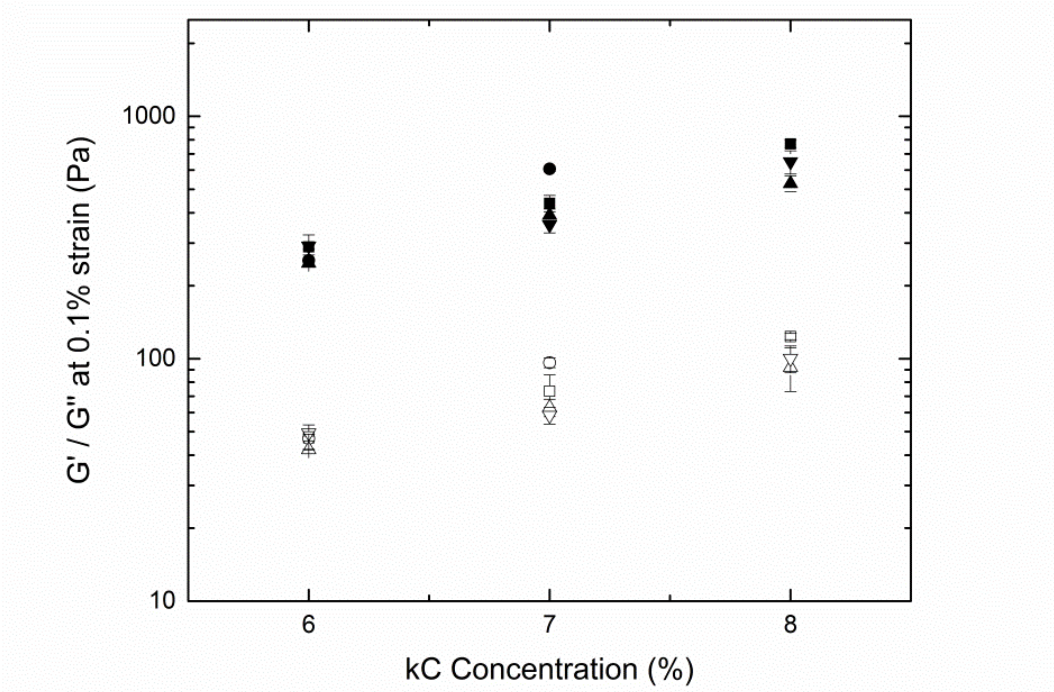

Figure 5.25 – G' and G'' in the Linear Visco Elastic Region from the oscillation sweeps of duplex emulsions with a range of concentrations of κC dispersed in DMEM buffer as internal aqueous phase. Emulsions are stabilised with PGPR/ Tween 20 (□/■), PGPR/ Tween 80 (○/●), Span 80/ Tween 20 (△/▲) and Span 80/ Tween 80 (▽/▼). G' is represented by closed symbols, and G'' is represented with open symbols.

Similar results were obtained for the duplex emulsions containing 5% and 6% kappa carrageenan in HEPES buffer (Figure 5.26), as shown for formulations with DMEM buffer. The point at which the G' and G'' are no longer independent of the strain (i.e. above about 0.7%) is approximately the same for all the samples and is very similar to the values observed for the duplex emulsions containing kappa carrageenan in DMEM. Again, as the kappa carrageenan concentration is increased, G' and G'' both increase (Figure 5.26), but this is not significant.

Thus the duplex emulsions containing kappa carrageenan in HEPES have produced structures with solid like response at low strains, with the elastic and loss moduli similar to those measured for the primary emulsion (comparing Figure 5.17 and 5.25). For the primary emulsion, the G' was measured in the range 100 Pa to 1000 Pa on increasing the kappa carrageenan from 5% to 6% and using these emulsions as the included phase in the duplex emulsion has resulted in G's in the range 200 Pa to 400 Pa. The weak solid like behaviour observed for the duplex emulsion is again a result of the high (50%) internal phase.

Span 80 was shown to form single emulsions with lower storage modulus than PGPR stabilised emulsions. However, when the double emulsions were formed (with DMEM buffer particulate systems), the emulsifier type had less of a significant impact on rheological properties (Figure 5.24 and Figure 5.25). While there is some indication of PGPR being higher across the concentrations of kappa carrageenan in DMEM buffer, the differences are not significant. This is unexpected, as the micrographs (shown in Figures 5.20 to 5.23) of the double emulsions containing PGPR demonstration better formation of the double emulsion structure, with less primary emulsion droplets present. When HEPES buffer is used within the aqueous phase, a greater difference is exhibited between emulsions containing PGPR and emulsions containing Span 80 (Figure 5.26 and Figure 5.27). However, once again this is unexpected, as the micrographs show little difference in the structure between emulsions containing DMEM buffer and emulsions containing HEPES buffer.

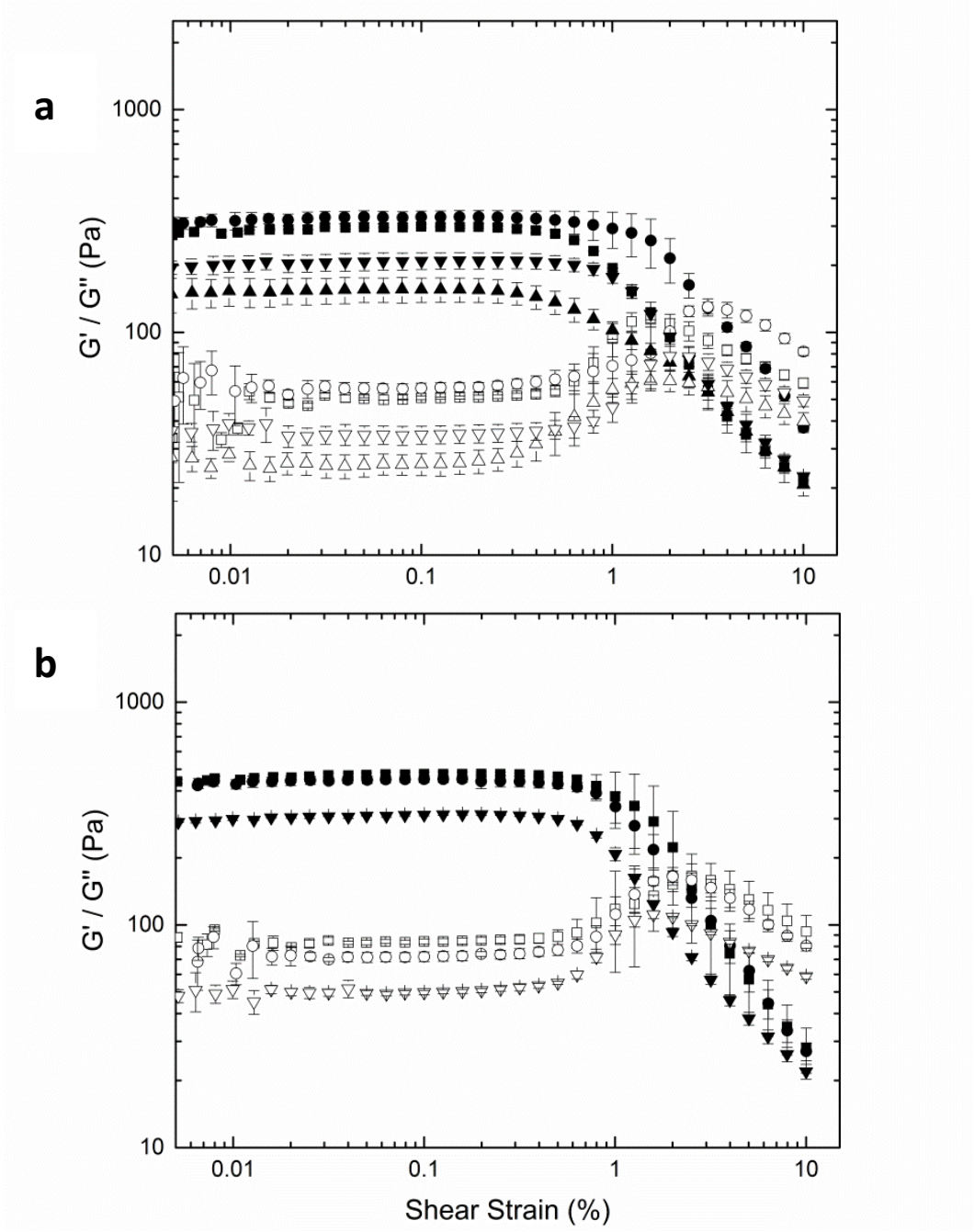

Figure 5.26 - Oscillation sweeps of κC HEPES in-oil-in water duplex emulsions, stabilised with PGPR/ Tween 20 (□/■), PGPR/ Tween 80 (○/●), Span 80/ Tween 20 (△/▲) and Span 80/ Tween 80 (▽/▼) (internal phase contains 5% κC HEPES (a), and 6% κC HEPES (b)). Elastic modulus (G') is represented by closed symbols, with open symbols representing viscous modulus (G'').

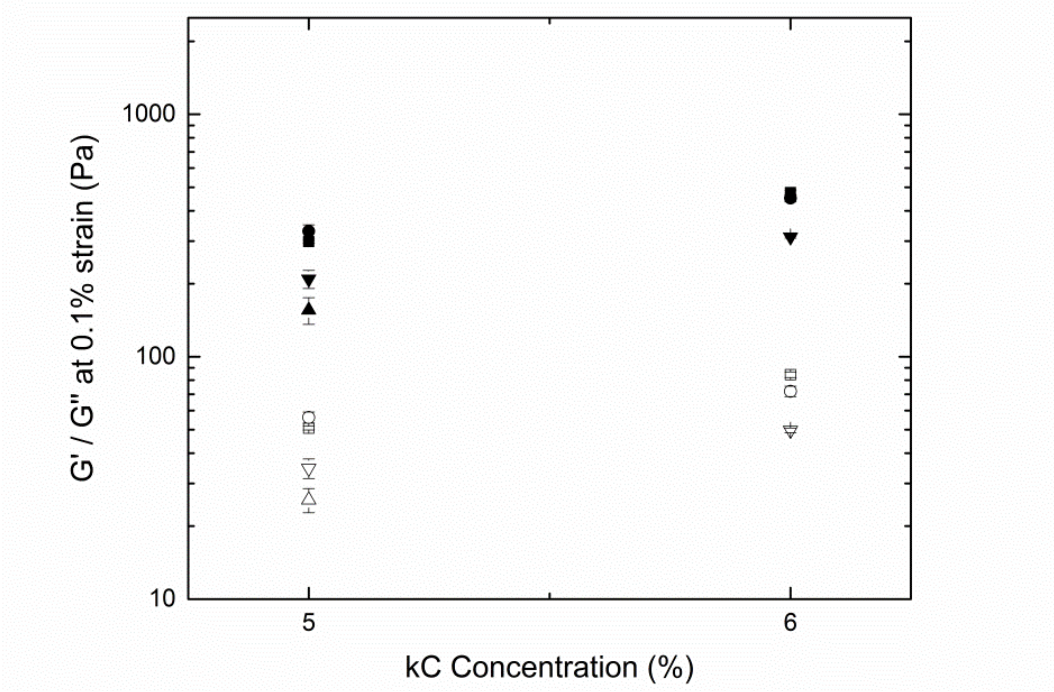

Figure 5.27 – G' and G'' in the Linear Visco Elastic Region value from the oscillation sweeps of secondary emulsions with a range of concentrations of κC dispersed in HEPES buffer as internal aqueous phase. Emulsions are stabilised with PGPR/ Tween 20 (□/■), PGPR/ Tween 80 (○/●), Span 80/ Tween 20 (△/▲) and Span 80/ Tween 80 (▽/▼). G' is represented by closed symbols, and G'' is represented with open symbols.

5.4 Conclusions

Hydration of potassium kappa carrageenan is possible at low temperatures under applied shear (500 s^{-1}), and results in a system which resembles a particulate, gel like, network which has properties similar to fluid gels produced from kappa carrageenan. The ionic nature of the aqueous phase (buffers) used at low temperature is important and controls the amount of kappa carrageenan which can be used before insoluble powder remains in the mixing vessel, at the applied shear rate. The presence of ions in the medium appears to slow down the rate of swelling allowing for more easily dispersion at the start of the process and then resulting in greater interaction and stronger gels once hydration as occurred. However, the kappa carrageenan helixes within the warm (30 ^{o}C) water hydrated structures are very similar to the helix contents of the high temperature solubilised gels (as determined from DSC enthalpies from Chapter 4 and Chapter 5).

Oil continuous emulsions have been formed at low shear rates (500 s^{-1}) with warm (30 ^{o}C) water hydrated and solubilised kappa carrageenan. At higher concentrations of kappa carrageenan aqueous phases (above 5% kappa carrageenan), stable single and double emulsions were formed. While carrageenan concentration and buffer type affected the gel properties and stability of the emulsions, they appear to have no significant effect on particle sizing.

Two emulsifiers were investigated for the stabilisation of single emulsions. While no significant difference was observed for the size and stability of the single emulsions, emulsifier type did have a significant effect on double emulsion formation and stability. The use of span 80 as an emulsifier resulted in instable double emulsions, with the emulsifier migrating from the interface, subsequently forming a majority single emulsion system, with very few double emulsion droplets. PGPR, a larger emulsifier, combined with either tween 20 or tween 80, was found to form stable single and then double emulsions. These structures could be highly beneficial for the medical and tissue regeneration fields, as stable and convenient methods of delivering bio-actives or cells topically to wounds.

Chapter 6.

CONCLUSIONS AND RECOMMENDATIONS FOR THE FUTURE

6.1 Hydrocolloid structuring for biomedical applications

The aim of this thesis was to investigate and advance the understanding of hydrocolloid structuring for uses in tissue regeneration and wound care applications. Whilst a significant amount of research had previously been carried out in the area of hydrocolloids, there had been less research in complex hydrocolloid systems, especially when two polymers are used within the same system. Processing of hydrocolloid gels have previously been defined as requiring high temperatures for dissolving the hydrocolloid, with gel formation occurring with a temperature decrease. This method of processing limits some of the applications, for instance, those which contain temperature sensitive drugs for health care. This thesis therefore also aimed to investigate new methods of processing in an attempt to widen the applications which could benefit from the inclusion of hydrocolloids.

The conclusions of this thesis will now be separated into four key areas, with future recommendations for each section.

6.2 Formation and characterisation of quiescent mixed gels

This study firstly looked at the role of a synthetic polymer, poly (vinyl alcohol) on the structure of the naturally occurring gellan polymer. Low acyl gellan was formed under quiescent conditions, with increasing PVA concentrations, with structural properties examined. As the concentration of PVA was increased, past the polymer overlap concentration for PVA, the system became PVA continuous

and thus failed with regard to gel strength. This change in structure as the PVA concentration was increased indicated a phase separation of the two polymers, with phase inversion occurring at the polymer overlap concentration of PVA. Three-dimensional gel structures (as shown in Chapter 3) were formed when the concentration of PVA was kept below the polymer overlap concentration.

With the formation of successful self-supporting structures, it would be of interest to determine whether these formulations could be used as a scaffold for mammalian cells. If the seeding of cells is possible, then the use of gellan/PVA mixed gels could form a new way of producing scaffolds, and thus replace the current gold standard methods in the field of tissue regeneration.

6.3 Visualisation of hydrocolloid microstructures

Understanding of hydrocolloid microstructures had previously been based on either mechanical properties, or inferring due to other components being present which could be visualised (such as proteins or oils).

If phase inversion was occurring in the gellan/ PVA system, it was of interest to visualise this occurring. Staining methods were therefore investigated. Simple, unbound stains were found to have no specificity, and thus there was no contrast between the polymers. The inclusion of the stain DTAF was examined, and was found to specifically bind to gellan, and thus gave contrast between the two polymers. This allowed for the visualisation of the phase inversion occurring at 14% PVA. However, further investigation showed that the inclusion of DTAF

resulted in mechanical changes to the gel structure. Furthermore, if staining gellan and unstained gellan were mixed, these two forms of gellan phase separated. This shows that the inclusion of DTAF changes the chemistry of the gellan and it behaves as a different polymer.

Further research is therefore required into the staining/visualisation of hydrocolloids. A future stain would need to have an insignificant effect on the hydrocolloid, on how the gelation is occurring, and on the consequent material properties. In this study, it was found that the large nature of DTAF, and the processing that had to be used (changing pH for a long period of time), was inappropriate. Therefore, a smaller stain, with a milder processing procedure, would be more ideal.

6.4 The formation and characterisation of multicomponent fluid gels

The processing of the gel systems was then investigated, with the formation of fluid gels being of interest. As spreadable systems, fluid gels give the potential of increasing the methods in which a patient can receive treatment. Multicomponent fluid gels were studied, with gellan mixed with the naturally occurring polymer, kappa carrageenan. It was found that when gellan and kappa carrageenan were mixed, phase separation occurred in the majority of samples. However, when 1.5% gellan was mixed with 0.5% kappa carrageenan, simultaneous gelation occurred, suggesting that a multicomponent fluid gel was formed. As gellan and kappa carrageenan would phase separate under quiescent

conditions, this strongly suggests that by shearing the optimal concentrations of both polymers, that the two polymers can be forced into the same system rather than separating (if the right conditions, such as gelation rates, were used).

In the future, mixing different thermally reversible hydrocolloids, such as pectin or xanthan, to determine whether a fluid gel with polymer polymers included in all the gel particles could be produced, could further develop the concept of having a multicomponent fluid gel. (Developing a visualisation method would then also be crucial, so that the structures produced could be more easily be concluded). This could then be further developed by looking at the mixing of a thermally reversible hydrocolloid, such as gellan, with a thermally irreversible hydrocolloid, such as alginate.

6.5 Warm hydration of kappa carrageenan

Whilst the previous systems are of great interest, applications within wound healing are more limited because bio actives, which may be required for the health of the patient/consumer, could be destroyed either by the high temperatures or by the processing (shear). Therefore, the use of low shear and low temperature was investigated for the formation of hydrocolloid systems. It was found that by mixing kappa carrageenan in warm buffers (DMEM and HEPES), hydration of the carrageenan powder could be achieved. This hydration method is not possible in deionised water, therefore showing that the success of this method is strongly related to the charged species present in the buffers.

Furthermore, the charged nature of the buffers allowed for a greater concentration of carrageenan to be included.

For wound healing applications, it was of interest to then look at single emulsions (so that any future active included would be protected from environmental factors) and double emulsions (for the interest of a water continuous product). The inclusion of kappa carrageenan allowed for stable single emulsions to be produced. However, the success of the double emulsions was found to be influenced by the emulsifier type and how likely the emulsifier was to migrate between the two interfaces.

Producing hydrated hydrocolloid gums, oil continuous single emulsions and water continuous double emulsions at low temperature and shear rates allows for a new low energy processing method, but also for the potential of including temperature sensitive actives in the future. This is an area which needs to be explored, with further studies regarding how a cell population or drug dose would be included.

Chapter 7.

REFERENCES

ABLETT, S., LILLFORD, P., BAGHDADI, S. & DERBYSHIRE, W. 1978. Nuclear magnetic resonance investigations of polysaccharide films, sols, and gels: I. Agarose. *Journal of Colloid and Interface Science,* 67**,** 355-377.

ALEXA, R. I., MOUNSEY, J. S., O'KENNEDY, B. T. & JACQUIER, J. C. 2010. Effect of κ-carrageenan on rheological properties, microstructure, texture and oxidative stability of water-in-oil spreads. *LWT-Food Science and Technology,* 43**,** 843-848.

AMMALA, A. 2013. Biodegradable polymers as encapsulation materials for cosmetics and personal care markets. *International journal of cosmetic science,* 35**,** 113-124.

ANDERSON, N., CAMPBELL, J., HARDING, M., REES, D. & SAMUEL, J. 1969. X-ray diffraction studies of polysaccharide sulphates: double helix models for κ- and ι-carrageenans. *Journal of molecular biology,* 45**,** 85IN589-8897.

ANDERSON, N., DOLAN, T., PENMAN, A., REES, D., MUELLER, G., STANCIOFF, D. & STANLEY, N. 1968. Carrageenans. Part IV. Variations in the structure and gel properties of κ-carrageenan, and the characterisation of sulphate esters by infrared spectroscopy. *Journal of the Chemical Society C: Organic***,** 602-606.

AUSTEN, K. R., GOODALL, D. M. & NORTON, I. T. 1988. Anion effects on equilibria and kinetics of the disorder‐order transition of κ‐carrageenan. *Biopolymers,* 27**,** 139-155.

BAINES, Z. V. & MORRIS, E. R. 1987. Flavour/taste perception in thickened systems: the effect of guar gum above and below c. *Food Hydrocolloids,* 1**,** 197-205.

BAKER, M. I., WALSH, S. P., SCHWARTZ, Z. & BOYAN, B. D. 2012. A review of polyvinyl alcohol and its uses in cartilage and orthopedic applications. *Journal of Biomedical Materials Research Part B: Applied Biomaterials,* 100**,** 1451-1457.

BARBANI, N., BERTONI, F., CIARDELLI, G., CRISTALLINI, C., SILVESTRI, D., COLUCCIO, M. & GIUSTI, P. 2005. Bioartificial materials based on blends of dextran and poly (vinyl alcohol-co-acrylic acid). *European polymer journal,* 41**,** 3004-3010.

BENICHOU, A., ASERIN, A. & GARTI, N. 2007. W/O/W double emulsions stabilized with WPI–polysaccharide complexes. *Colloids and Surfaces A: Physicochemical and Engineering Aspects,* 294**,** 20-32.

BERCEA, M., MORARIU, S. & RUSU, D. 2013. In situ gelation of aqueous solutions of entangled poly (vinyl alcohol). *Soft Matter,* 9**,** 1244-1253.

BIDARRA, S. J., BARRIAS, C. C. & GRANJA, P. L. 2014. Injectable alginate hydrogels for cell delivery in tissue engineering. *Acta Biomaterialia,* 10**,** 1646-1662.

BIRDI, G., BRIDSON, R. H., SMITH, A. M., MOHD BOHARI, S. P. & GROVER, L. M. 2012. Modification of alginate degradation properties using orthosilicic acid. *Journal of the Mechanical Behavior of Biomedical Materials,* 6**,** 181-187.

BOATENG, J. S., MATTHEWS, K. H., STEVENS, H. N. & ECCLESTON, G. M. 2008. Wound healing dressings and drug delivery systems: a review. *Journal of pharmaceutical sciences,* 97**,** 2892-2923.

BOSCHETTI, F., PENNATI, G., GERVASO, F., PERETTI, G. M. & DUBINI, G. 2004. Biomechanical properties of human articular cartilage under compressive loads. *Biorheology,* 41**,** 159-166.

BOUWSTRA, J. A., HONEYWELL-NGUYEN, P. L., GOORIS, G. S. & PONEC, M. 2003. Structure of the skin barrier and its modulation by vesicular formulations. *Progress in Lipid Research,* 42**,** 1-36.

BROWN, C., CUTLER, A. & NORTON, I. 1996. Liquid based composition comprising gelling polysaccharide capable of forming a reversible gel and a method for preparing such composition. *EP0355908*.

BUTLER, M. F. & HEPPENSTALL-BUTLER, M. 2003. Phase separation in gelatin/dextran and gelatin/maltodextrin mixtures. *Food Hydrocolloids,* 17**,** 815-830.

ÇAKIR, E. & FOEGEDING, E. A. 2011. Combining protein micro-phase separation and protein–polysaccharide segregative phase separation to produce gel structures. *Food Hydrocolloids,* 25**,** 1538-1546.

CARNEIRO, H. C. F., TONON, R. V., GROSSO, C. R. F. & HUBINGER, M. D. 2013. Encapsulation efficiency and oxidative stability of flaxseed oil microencapsulated by spray drying using different combinations of wall materials. *Journal of Food Engineering,* 115**,** 443-451.

CARVALHO, I., ESTEVINHO, B. & SANTOS, L. 2015. Application of microencapsulated essential oils in cosmetic and personal healthcare products–a review. *International journal of cosmetic science*.

CHENG, L., LIM, B., CHOW, K., CHONG, S. & CHANG, Y. 2008. Using fish gelatin and pectin to make a low-fat spread. *Food hydrocolloids,* 22**,** 1637-1640.

CRACKNELL, R. 2010. The Aging Population: Key issues for the 2010 Parliament.

CROUGHAN, M. S., SAYRE, E. S. & WANG, D. I. 1989. Viscous reduction of turbulent damage in animal cell culture. *Biotechnology and bioengineering,* 33**,** 862-872.

DAI, L., LIU, X. & TONG, Z. 2010. Critical behavior at sol–gel transition in gellan gum aqueous solutions with KCl and CaCl2 of different concentrations. *Carbohydrate Polymers,* 81**,** 207-212.

DIAS, A., BRAGA, M., SEABRA, I., FERREIRA, P., GIL, M. & DE SOUSA, H. 2011. Development of natural-based wound dressings impregnated with bioactive compounds and using supercritical carbon dioxide. *International journal of pharmaceutics,* 408**,** 9-19.

DICKINSON, E. 2003. Hydrocolloids at interfaces and the influence on the properties of dispersed systems. *Food Hydrocolloids,* 17**,** 25-39.

DICKINSON, E., PHILLIPS, G. & WILLIAMS, P. 2009. Hydrocolloids and emulsion stability. *Handbook of hydrocolloids***,** 23-49.

DRURY, J. L. & MOONEY, D. J. 2003. Hydrogels for tissue engineering: scaffold design variables and applications. *Biomaterials,* 24**,** 4337-4351.

DUNSTAN, D. E., SALVATORE, R., JONSSON, M. & LIAO, M.-L. 2000. Syneresis of k-carrageenan gels at different KCl and LBG concentrations. *Gums and Stabilisers for the Food Industry,* 10**,** 137.

EDWARDS, C. & MARKS, R. 1995. Evaluation of biomechanical properties of human skin. *Clinics in Dermatology,* 13**,** 375-380.

ELSNER, J. J. & ZILBERMAN, M. 2010. Novel antibiotic-eluting wound dressings: An in vitro study and engineering aspects in the dressing's design. *Journal of tissue viability,* 19**,** 54-66.

FERNANDES, P. B. 1995. Influence of galactomannan on the structure and thermal behaviour of xanthan/galactomannan mixtures. *Journal of Food Engineering,* 24**,** 269-283.

FIELD, C. K. & KERSTEIN, M. D. 1994. Overview of wound healing in a moist environment. *The American journal of surgery,* 167**,** S2-S6.

FRASCH-MELNIK, S., SPYROPOULOS, F. & NORTON, I. T. 2010. W1/O/W2 double emulsions stabilised by fat crystals – Formulation, stability and salt release. *Journal of Colloid and Interface Science,* 350**,** 178-185.

GABRIELE, A., SPYROPOULOS, F. & NORTON, I. 2009. Kinetic study of fluid gel formation and viscoelastic response with kappa-carrageenan. *Food Hydrocolloids,* 23**,** 2054-2061.

GARCÍA, M. C., ALFARO, M. C., CALERO, N. & MUÑOZ, J. 2011. Influence of gellan gum concentration on the dynamic viscoelasticity and transient flow of fluid gels. *Biochemical Engineering Journal,* 55**,** 73-81.

GARREC, D. A., GUTHRIE, B. & NORTON, I. T. 2013. Kappa carrageenan fluid gel material properties. Part 1: Rheology. *Food Hydrocolloids,* 33**,** 151-159.

GARREC, D. A. & NORTON, I. T. 2012. Understanding fluid gel formation and properties. *Journal of Food Engineering,* 112**,** 175-182.

GIACOMONI, P. U. 2005. Ageing, science and the cosmetics industry. *EMBO reports,* 6**,** S45-S48.

GIBSON, W. & SANDERSON, G. 1997. Gellan gum. *Thickening and gelling agents for food.* Springer.

GROEBER, F., HOLEITER, M., HAMPEL, M., HINDERER, S. & SCHENKE-LAYLAND, K. 2011. Skin tissue engineering — In vivo and in vitro applications. *Advanced Drug Delivery Reviews,* 63**,** 352-366.

GUNNING, A., MACKIE, A., WILDE, P. & MORRIS, V. 2004. Atomic force microscopy of emulsion droplets: Probing droplet-droplet interactions. *Langmuir,* 20**,** 116-122.

GUO, J.-H., SKINNER, G., HARCUM, W. & BARNUM, P. 1998. Pharmaceutical applications of naturally occurring water-soluble polymers. *Pharmaceutical science & technology today,* 1**,** 254-261.

GUPTA, S., GOSWAMI, S. & SINHA, A. 2012. A combined effect of freeze--thaw cycles and polymer concentration on the structure and mechanical properties of transparent PVA gelsPart of this work was presented at the international conference of BIO 2011-Biomaterials and Implants. Prospects and Possibilities in the New Millenium at the CGCRI, Kolkata, India, July 21–23, 2011. *Biomedical Materials,* 7**,** 015006.

HASSAN, C. M. & PEPPAS, N. A. 2000a. Structure and applications of poly (vinyl alcohol) hydrogels produced by conventional crosslinking or by freezing/thawing methods. *Biopolymers· PVA Hydrogels, Anionic Polymerisation Nanocomposites.* Springer.

HASSAN, C. M. & PEPPAS, N. A. 2000b. Structure and morphology of freeze/thawed PVA hydrogels. *Macromolecules,* 33**,** 2472-2479.

HERMANSSON, A.-M., ERIKSSON, E. & JORDANSSON, E. 1991. Effects of potassium, sodium and calcium on the microstructure and rheological behaviour of kappa-carrageenan gels. *Carbohydrate Polymers,* 16**,** 297-320.

HUNT, N. & GROVER, L. 2010. Cell encapsulation using biopolymer gels for regenerative medicine. *Biotechnology letters,* 32**,** 733-742.

HUNT, N. C., SHELTON, R. M. & GROVER, L. 2009. An alginate hydrogel matrix for the localised delivery of a fibroblast/keratinocyte co‐culture. *Biotechnology journal,* 4**,** 730-737.

HUNT, N. C., SMITH, A. M., GBURECK, U., SHELTON, R. M. & GROVER, L. M. 2010. Encapsulation of fibroblasts causes accelerated alginate hydrogel degradation. *Acta Biomaterialia,* 6**,** 3649-3656.

HUTMACHER, D. W. 2000. Scaffolds in tissue engineering bone and cartilage. *Biomaterials,* 21**,** 2529-2543.

IMESON, A., PHILLIPS, G. & WILLIAMS, P. 2000. Carrageenan. *Handbook of hydrocolloids***,** 87-102.

JANE, J. L. 1993. Mechanism of starch gelatinization in neutral salt solutions. *Starch ‐ Stärke,* 45**,** 161-166.

JANSSON, P.-E., LINDBERG, B. & SANDFORD, P. A. 1983. Structural studies of gellan gum, an extracellular polysaccharide elaborated by Pseudomonas elodea. *Carbohydrate Research,* 124**,** 135-139.

KANG, K. S. & VEEDER, G. T. 1982. Polysaccharide S-60 and bacterial fermentation process for its preparation. Google Patents.

KANG, K. S., VEEDER, G. T. & MIRRASOUL, P. J. 1982. Agar-like polysaccharide produced by a Pseudomonas species: production and basic properties. *Applied and Environmental Microbiology,* 43**,** 1086-1091.

KASAPIS, S., GIANNOULI, P., HEMBER, M. W., EVAGELIOU, V., POULARD, C., TORT-BOURGEOIS, B. & SWORN, G. 1999. Structural aspects and phase behaviour in deacylated and high acyl gellan systems. *Carbohydrate Polymers,* 38**,** 145-154.

KASAPIS, S., MORRIS, E. R., NORTON, I. T. & BROWN, C. R. T. 1993. Phase equilibria and gelation in gelatin/maltodextrin systems—Part III: Phase separation in mixed gels. *Carbohydrate polymers,* 21**,** 261-268.

KASHYAP, N., KUMAR, N. & KUMAR, M. R. 2005. Hydrogels for pharmaceutical and biomedical applications. *Critical Reviews™ in Therapeutic Drug Carrier Systems,* 22.

KIM, J. O., PARK, J. K., KIM, J. H., JIN, S. G., YONG, C. S., LI, D. X., CHOI, J. Y., WOO, J. S., YOO, B. K. & LYOO, W. S. 2008. Development of polyvinyl alcohol–sodium alginate gel-matrix-based wound dressing system containing nitrofurazone. *International journal of pharmaceutics,* 359**,** 79-86.

LEE, K. Y. & MOONEY, D. J. 2001. Hydrogels for tissue engineering. *Chemical reviews,* 101**,** 1869-1880.

LEE, K. Y. & MOONEY, D. J. 2012. Alginate: Properties and biomedical applications. *Progress in Polymer Science,* 37**,** 106-126.

LI, Y., DICK, W. A. & TUOVINEN, O. H. 2003. Evaluation of fluorochromes for imaging bacteria in soil. *Soil Biology and Biochemistry,* 35**,** 737-744.

LIN, C.-C. & METTERS, A. T. 2006. Hydrogels in controlled release formulations: Network design and mathematical modeling. *Advanced Drug Delivery Reviews,* 58**,** 1379-1408.

LIRA, A. A. M., ROSSETTI, F. C., NANCLARES, D. M., NETO, A. F., BENTLEY, M. V. L. & MARCHETTI, J. M. 2009. Preparation and characterization of chitosan-treated alginate microparticles incorporating all-trans retinoic acid. *Journal of microencapsulation,* 26**,** 243-250.

LISA, B. 1997. Biomaterials: Polymers in controlled drug delivery. *Med Device Link, Los Angeles, CA: Med Plastics Biomater. November edition*.

LOZINSKY, V. I., ZUBOV, A. L. & TITOVA, E. F. 1996. Swelling behavior of poly(vinyl alcohol) cryogels employed as matrices for cell immobilization. *Enzyme and Microbial Technology,* 18**,** 561-569.

LUBBE, A. & VERPOORTE, R. 2011. Cultivation of medicinal and aromatic plants for specialty industrial materials. *Industrial Crops and Products,* 34**,** 785-801.

LUNDIN, L. & GOLDING, M. 2009. Structure design for healthy food. *Australian Journal of Dairy Technology,* 64**,** 68.

LUNDIN, L. & HERMANSSON, A.-M. 1995. Supermolecular aspects of xanthan-locust bean gum gels based on rheology and electron microscopy. *Carbohydrate Polymers,* 26**,** 129-140.

MACNEIL, S. 2007. Progress and opportunities for tissue-engineered skin. *Nature,* 445**,** 874-880.

MAHDI, M. H., CONWAY, B. R. & SMITH, A. M. 2014a. Evaluation of gellan gum fluid gels as modified release oral liquids. *International Journal of Pharmaceutics*.

MAHDI, M. H., CONWAY, B. R. & SMITH, A. M. 2014b. Evaluation of gellan gum fluid gels as modified release oral liquids. *International Journal of Pharmaceutics,* 475**,** 335-343.

MALDA, J., KREIJVELD, E., TEMENOFF, J. S., VAN BLITTERSWIJK, C. A. & RIESLE, J. 2003. Expansion of human nasal chondrocytes on macroporous microcarriers enhances redifferentiation. *Biomaterials,* 24**,** 5153-5161.

MANGIONE, M. R., GIACOMAZZA, D., BULONE, D., MARTORANA, V., CAVALLARO, G. & SAN BIAGIO, P. L. 2005. K+ and Na+ effects on the gelation properties of κ-Carrageenan. *Biophysical Chemistry,* 113**,** 129-135.

MAO, R., TANG, J. & SWANSON, B. G. 2000. Texture properties of high and low acyl mixed gellan gels. *Carbohydrate Polymers,* 41**,** 331-338.

MATSUKAWA, S. & WATANABE, T. 2007. Gelation mechanism and network structure of mixed solution of low- and high-acyl gellan studied by dynamic viscoelasticity, CD and NMR measurements. *Food Hydrocolloids,* 21**,** 1355-1361.

MCCLEMENTS, D. J., DECKER, E. A., PARK, Y. & WEISS, J. 2009. Structural design principles for delivery of bioactive components in nutraceuticals and functional foods. *Critical Reviews in Food Science and Nutrition,* 49**,** 577-606.

MIYOSHI, E., TAKAYA, T. & NISHINARI, K. 1996. Rheological and thermal studies of gel-sol transition in gellan gum aqueous solutions. *Carbohydrate Polymers,* 30**,** 109-119.

MORRIS, E., CUTLER, A., ROSS-MURPHY, S., REES, D. & PRICE, J. 1981. Concentration and shear rate dependence of viscosity in random coil polysaccharide solutions. *Carbohydrate polymers,* 1**,** 5-21.

MORRIS, E. R. 1990. Mixed polymer gels. *Food gels.* Springer.

MORRIS, E. R., NISHINARI, K. & RINAUDO, M. 2012. Gelation of gellan–A review. *Food Hydrocolloids,* 28**,** 373-411.

MORRIS, E. R., REES, D. A. & ROBINSON, G. 1980. Cation-specific aggregation of carrageenan helices: domain model of polymer gel structure. *Journal of molecular biology,* 138**,** 349-362.

MORRIS, V. 1986. Multicomponent gels. *Gums and stabilisers for the food industry,* 3**,** 87-99.

MORRIS, V. & CHILVERS, G. 1983. Rheological studies of specific cation forms of kappa carrageenan gels. *Carbohydrate Polymers,* 3**,** 129-141.

MORRISON, N., CLARK, R., CHEN, Y., TALASHEK, T. & SWORN, G. 1999. Gelatin alternatives for the food industry. *Physical chemistry and industrial application of gellan gum.* Springer.

MUSCHIOLIK, G. 2007. Multiple emulsions for food use. *Current Opinion in Colloid & Interface Science,* 12**,** 213-220.

NAUTIYAL, O. H. 2012. Effect of Galactomannans and Low Esterified Pectin Combinations on Fruit Preparation Synersis, Rheology and Stability on Storage.

NICKERSON, M., PAULSON, A. & HALLETT, F. 2004. Dilute solution properties of κ-carrageenan polysaccharides: effect of potassium and calcium ions on chain conformation. *Carbohydrate polymers,* 58**,** 25-33.

NICKERSON, M. T., PAULSON, A. T. & SPEERS, R. A. 2003. Rheological properties of gellan solutions: effect of calcium ions and temperature on pre-gel formation. *Food Hydrocolloids,* 17**,** 577-583.

NISHINARI, K., MIYOSHI, E., TAKAYA, T. & WILLIAMS, P. A. 1996. Rheological and DSC studies on the interaction between gellan gum and konjac glucomannan. *Carbohydrate polymers,* 30**,** 193-207.

NISHINARI, K., ZHANG, H. & IKEDA, S. 2000a. Hydrocolloid gels of polysaccharides and proteins. *Current opinion in colloid & interface science,* 5**,** 195-201.

NISHINARI, K., ZHANG, H. & IKEDA, S. 2000b. Hydrocolloid gels of polysaccharides and proteins. *Current Opinion in Colloid & Interface Science,* 5**,** 195-201.

NORTON, A., HANCOCKS, R. & GROVER, L. 2014. Poly (vinyl alcohol) modification of low acyl gellan hydrogels for applications in tissue regeneration. *Food Hydrocolloids,* 42**,** 373-377.

NORTON, A. B., COX, P. W. & SPYROPOULOS, F. 2011. Acid gelation of low acyl gellan gum relevant to self-structuring in the human stomach. *Food Hydrocolloids,* 25**,** 1105-1111.

NORTON, I. & FOSTER, T. 2002. Hydrocolloids in real food systems. *Special Publications of the Royal Society of Chemistry,* 278**,** 187-200.

NORTON, I. & FRITH, W. 2001a. Microstructure design in mixed biopolymer composites. *Food Hydrocolloids,* 15**,** 543-553.

NORTON, I., FRYER, P. & MOORE, S. 2006. Product/process integration in food manufacture: engineering sustained health. *AIChE Journal,* 52**,** 1632-1640.

NORTON, I., MOORE, S. & FRYER, P. 2007. Understanding food structuring and breakdown: engineering approaches to obesity. *Obesity Reviews,* 8**,** 83-88.

NORTON, I. T. & FRITH, W. J. 2001b. Microstructure design in mixed biopolymer composites. *Food Hydrocolloids,* 15**,** 543-553.

NORTON, I. T., GOODALL, D. M., MORRIS, E. R. & REES, D. A. 1983. Equilibrium and dynamic studies of the disorder–order transition of kappa carrageenan. *Journal of the Chemical Society, Faraday Transactions 1: Physical Chemistry in Condensed Phases,* 79**,** 2489-2500.

NORTON, I. T., JARVIS, D. A. & FOSTER, T. J. 1999. A molecular model for the formation and properties of fluid gels. *International Journal of Biological Macromolecules,* 26**,** 255-261.

NORTON, I. T., MORRIS, E. R. & REES, D. A. 1984. Lyotropic effects of simple anions on the conformation and interactions of kappa-carrageenan. *Carbohydrate research,* 134**,** 89-101.

NUTTELMAN, C. R., HENRY, S. M. & ANSETH, K. S. 2002. Synthesis and characterization of photocrosslinkable, degradable poly(vinyl alcohol)-based tissue engineering scaffolds. *Biomaterials,* 23**,** 3617-3626.

O'BRIEN, F. J. 2011. Biomaterials & scaffolds for tissue engineering. *Materials Today,* 14**,** 88-95.

O'NEILL, M. A., SELVENDRAN, R. R. & MORRIS, V. J. 1983. Structure of the acidic extracellular gelling polysaccharide produced by Pseudomonas elodea. *Carbohydrate Research,* 124**,** 123-133.

OLIVEIRA, J. T., MARTINS, L., PICCIOCHI, R., MALAFAYA, P., SOUSA, R., NEVES, N., MANO, J. & REIS, R. 2010. Gellan gum: a new biomaterial for cartilage tissue engineering applications. *Journal of Biomedical Materials Research Part A,* 93**,** 852-863.

OSMAŁEK, T., FROELICH, A. & TASAREK, S. 2014. Application of gellan gum in pharmacy and medicine. *International journal of pharmaceutics,* 466**,** 328-340.

PADDLE-LEDINEK, J. E., NASA, Z. & CLELAND, H. J. 2006. Effect of different wound dressings on cell viability and proliferation. *Plastic and reconstructive surgery,* 117**,** 110S-118S.

PARKER, R. & RING, S. 2001. Aspects of the physical chemistry of starch. *Journal of Cereal Science,* 34**,** 1-17.

PATRICK, C. W., MIKOS, A. G. & MCINTIRE, L. V. 1998. *Frontiers in tissue engineering*, Elsevier.

PEPPAS, N. A. 1975. Turbidimetric studies of aqueous poly (vinyl alcohol) solutions. *Die Makromolekulare Chemie,* 176**,** 3433-3440.

PERCIVAL, N. J. 2002. Classification of wounds and their management. *Surgery (Oxford),* 20**,** 114-117.

PEREIRA, R. F., BARRIAS, C. C., GRANJA, P. L. & BARTOLO, P. J. 2013. Advanced biofabrication strategies for skin regeneration and repair. *Nanomedicine,* 8**,** 603-621.

PHILLIPS, G. O. & WILLIAMS, P. A. 2009. *Handbook of hydrocolloids*, Elsevier.

QIU, Y. & PARK, K. 2012. Environment-sensitive hydrogels for drug delivery. *Advanced Drug Delivery Reviews,* 64, Supplement**,** 49-60.

QUEEN, D., ORSTED, H., SANADA, H. & SUSSMAN, G. 2004. A dressing history. *International wound journal,* 1**,** 59-77.

RADHAKRISHNAN, J., KRISHNAN, U. M. & SETHURAMAN, S. 2014. Hydrogel based injectable scaffolds for cardiac tissue regeneration. *Biotechnology Advances,* 32**,** 449-461.

REES, D. 1977. Polysaccharide shapes.

ROBINSON, G., MORRIS, E. R. & REES, D. A. 1980. Role of double helices in carrageenan gelation: the domain model. *Journal of the Chemical Society, Chemical Communications***,** 152-153.

ROBINSON, G., ROSS-MURPHY, S. B. & MORRIS, E. R. 1982. Viscosity-molecular weight relationships, intrinsic chain flexibility, and dynamic solution properties of guar galactomannan. *Carbohydrate Research,* 107**,** 17-32.

ROCHAS, C. & RINAUDO, M. 1984. Mechanism of gel formation in κ - carrageenan. *Biopolymers,* 23**,** 735-745.

ROY, D., CAMBRE, J. N. & SUMERLIN, B. S. 2010. Future perspectives and recent advances in stimuli-responsive materials. *Progress in Polymer Science,* 35**,** 278-301.

RUPENTHAL, I. D., GREEN, C. R. & ALANY, R. G. 2011. Comparison of ion-activated in situ gelling systems for ocular drug delivery. Part 1: Physicochemical characterisation and in vitro release. *International Journal of Pharmaceutics,* 411**,** 69-77.

RUSS, N., ZIELBAUER, B. I., KOYNOV, K. & VILGIS, T. A. 2013. Influence of Nongelling Hydrocolloids on the Gelation of Agarose. *Biomacromolecules,* 14**,** 4116-4124.

SCHERZE, I., KNOTH, A. & MUSCHIOLIK, G. 2006. Effect of Emulsification Method on the Properties of Lecithin‐and PGPR‐Stabilized Water‐in‐Oil‐Emulsions. *Journal of dispersion science and technology,* 27**,** 427-434.

SHEVCHENKO, R. V., JAMES, S. L. & JAMES, S. E. 2010. A review of tissue-engineered skin bioconstructs available for skin reconstruction. *Journal of the Royal Society Interface,* 7**,** 229-258.

SLOOTMAEKERS, D., MANDEL, M. & REYNAERS, H. 1991. Dynamic light scattering by κ-and λ-carrageenan solutions. *International journal of biological macromolecules,* 13**,** 17-25.

SMIDSRØD, O., ANDRESEN, I.-L., GRASDALEN, H., LARSEN, B. & PAINTER, T. 1980. Evidence for a salt-promoted “freeze-out” of linkage conformations in carrageenans as a prerequisite for gel-formation. *Carbohydrate Research,* 80**,** C11-C16.

SMITH, A. M., SHELTON, R., PERRIE, Y. & HARRIS, J. J. 2007. An initial evaluation of gellan gum as a material for tissue engineering applications. *Journal of biomaterials applications*.

SMITH, C. G., GREENFIELD, P. F. & RANDERSON, D. H. 1987. A technique for determining the shear sensitivity of mammalian cells in suspension culture. *Biotechnology Techniques,* 1**,** 39-44.

STADING, M. & HERMANSSON, A.-M. 1993. Rheological behaviour of mixed gels of κ-carrageenan-locust bean gum. *Carbohydrate Polymers,* 22**,** 49-56.

SULLO, A., ARELLANO, M. & NORTON, I. T. 2014. Formulation engineering of water in cocoa–Butter emulsion. *Journal of Food Engineering,* 142**,** 100-110.

SURH, J., DECKER, E. A. & MCCLEMENTS, D. J. 2006. Properties and stability of oil-in-water emulsions stabilized by fish gelatin. *Food Hydrocolloids,* 20**,** 596-606.

SWORN, G., NORTON, I., SPYROPOULOS, F. & COX, P. 2010. Xanthan Gum–Functionality and Application. *Practical Food Rheology: An Interpretive Approach***,** 85.

SWORN, G., PHILLIPS, G. & WILLIAMS, P. 2009. Gellan gum. *Handbook of hydrocolloids***,** 204-227.

SWORN, G., SANDERSON, G. & GIBSON, W. 1995. Gellan gum fluid gels. *Food Hydrocolloids,* 9**,** 265-271.

TANG, J., LELIEVRE, J., TUNG, M. A. & ZENG, Y. 1994. Polymer and ion concentration effects on gellan gel strength and strain. *Journal of Food Science,* 59**,** 216-220.

WALPORT, S. M. 2014. The Future of an Ageing Population. *In:* SCIENCE, G. O. F. & DEPARTMENT FOR BUSINESS, I. S. (eds.). GOV.UK.

WANG, F.-Q., LI, P., ZHANG, J.-P., WANG, A.-Q. & WEI, Q. 2010. A novel pH-sensitive magnetic alginate–chitosan beads for albendazole delivery. *Drug development and industrial pharmacy,* 36**,** 867-877.

WANG, F.-Q., LI, P., ZHANG, J.-P., WANG, A.-Q. & WEI, Q. 2011. pH-sensitive magnetic alginate-chitosan beads for albendazole delivery. *Pharmaceutical development and technology,* 16**,** 228-236.

WATASE, M. & NISHINARI, K. 1988. The effect of monovalent cations and anions on the rheological properties of kappa‐carrageenan gels. *Journal of texture studies,* 19**,** 259-273.

WILDE, P. J. 2000. Interfaces: their role in foam and emulsion behaviour. *Current Opinion in Colloid & Interface Science,* 5**,** 176-181.

WINTER, G. D. 1962. Formation of the scab and the rate of epithelization of superficial wounds in the skin of the young domestic pig.

WOLF, B., SCIROCCO, R., FRITH, W. & NORTON, I. 2000. Shear-induced anisotropic microstructure in phase-separated biopolymer mixtures. *Food Hydrocolloids,* 14**,** 217-225.

ZASYPKIN, D., BRAUDO, E. & TOLSTOGUZOV, V. 1997. Multicomponent biopolymer gels. *Food Hydrocolloids,* 11**,** 159-170.

ZHU, J. & MARCHANT, R. E. 2011. Design properties of hydrogel tissue-engineering scaffolds. *Expert review of medical devices,* 8**,** 607-626.